Evolution of the Human Immunodeficiency Virus Type 1 Envelope Glycoprotein During Chronic Infection

William L. Ince

A dissertation submitted to the faculty of the University of North Carolina at Chapel Hill in partial fulfillment of the requirements for the degree of Doctor of Philosophy in the Curriculum in Genetics and Molecular Biology

Chapel Hill
2010

Approved by,

Advisor: Ronald Swanstrom

Christina Burch

Joseph Eron Jr.

Mark Heise

David Margolis

Lishan Su

ABSTRACT

William L. Ince: Evolution of the Human Immunodeficiency Virus Type 1 Envelope Glycoprotein During Chronic Infection
(under the direction of Ronald Swanstrom)

A hallmark of Human Immunodeficiency Virus Type 1 (HIV-1) chronic infection is the rapid and continual evolution and diversification of the viral Envelope glycoprotein (Env), which results in multiple co-existing *env* genetic variants. Env mediates virus entry into host cells by engaging the primary receptor CD4 and either of two coreceptors, CCR5 or CXCR4. CXCR4-tropic variants typically emerge in late stage disease, coincident very low CD4+ T cell counts and severe immunosuppression, and rarely establish infection. Over the course of infection, Env diversifies as a result of immune escape selection and selection for differential usage of CD4 and co-receptors, presumably in order to expand into new target cell types, although the selective forces driving Env evolution in late stage disease remain poorly understood. In the work present here, I examined how variation affects compartmentalization of genetic and phenotypic subpopulations and the likely forces driving some of this variation in late stages of infection. First, I used a heteroduplex tracking assay (HTA) to measure the lifespan of cells producing different genetic variants in the population by measuring the decay rates of variants when subjects were placed on suppressive therapy. I found that all variants, regardless of their co-receptor tropism phenotype, decayed at the same rate

indicating they are replicating in the same cell types or cell types with similar infected life spans. I further examined the relationship between CCR5 and emergent CXCR4 variants and found that they frequently recombine, further indicated an overlap in target cell type. I also examined the evolution of Env in a humanized mouse model. I found that, consistent with a lack of a strong humoral immune response, Env evolved a more open conformation and enhanced CD4 affinity. I also found that in this phenotypic background, CXCR4 –tropic variants emerged, and showed evidence of tissue compartmentalization. Finally I attempted to link the phenotypes conferred by a more open Env conformation, that evolved in the immunosuppressed environment in the mouse, to evolution of CXCR4 and provided evidence that the environmental constrains of imposed by humoral immunity select against the open Env conformation that potentiates evolution of CXCR4 tropism.

Acknowledgements

I would like to thank the UNC Center For AIDS Research and the UNC General Clinical Research Center for sample collection. I would also like to thank Dale Kempf from Abbott and the ACTG 359 study team for making samples available for these studies. Much of the sequence analysis carried out in these studies was facilitated by Los Alamos National Laboratories HIV Database group through helpful discussion. I would also like to thank Rachel Lovingood and Tom Denny of the CHAVI for the Western blot analysis of the mouse samples.

All of the work described in this dissertation benefited from both the intellectual and material input from many others who are not named here, but in particular from members of the Swanstrom Lab and Su Lab. I would especially like to thank my thesis committee members for their patience, enthusiasm and guidance.

Table of Contents

List of Tables

Table

List of Figures

Figures

Abbreviations

HIV-1	Human Immunodeficiency Virus Type 1
AIDS	Acquired Immunodeficiency Syndrome
CTL	Cytotoxic T Lymphocyte
PNGL	Potential N-linked glycosylation site
V	Variable loop
bp	Base pair
X4	CXCR4-tropic
R5	CCR5-tropic
PCR	Polymerase Chain Reaction
RT-PCR	Reverse Transcription-Polymerase Chain Reaction
HTA	Heteroduplex Tracking Assay
PSSM	Position Specific Scoring Matrix
LTR	Long Terminal Repeat
DKO	Rag2-/- gammaC-/- double knockout mouse
HSC	Hematopoietic stem cell

CHAPTER 1

INTRODUCTION

Human Immunodeficiency Virus type 1 (HIV-1) is a lentivirus, in the virus family Retroviridae. Lentiviruses are distinguished from their other family members by their ability to infect non-dividing cells. These viruses establish chronic infection with ongoing viral replication in primates (SIV, HIV-1, HIV-2) and non-primate mammals (FIV, BIV, EAIV, CAEV, VMV). A Key feature of HIV-1, and likely all retroviruses, is its ability to rapidly evolve (151, 167, 175). The high mutation (174), recombination (4, 41, 240) and replication rates (113, 304), allow HIV-1 to rapidly generate large amounts of diversity in order to adapt to a highly dynamic host environment and persist as a chronic infection. This is particularly evident in the HIV-1 *env* gene that encodes the viral envelope glycoprotein (Env), which is responsible for mediating viral entry into a range of target cell types and is the only surface-exposed antigen of HIV-1. The high level of variation observed during chronic infection in this gene is therefore mainly a result of antigenic escape mutations (87, 245), and adaptations to different CD4 receptor and co-receptor densities and co-receptor types on distinct target cell subsets (97). Whereas viral infection is established by one or a few variants that give rise to an initially homogeneous population, the continuously shifting selective forces operating on Env, from a co-

evolving and then diminishing immune response, to changes in access to different cell populations, result in continual Env diversification and functional evolution over the course of chronic infection (87, 267).

This introduction will describe the history of HIV-1 infection in the human population, natural course of infection in the individual and the viral and host processes that drive the evolution of HIV-1 Env throughout infection and in late stages of infection in particular.

1.1 HIV-1 Natural History

1.1.1 Origin of HIV-1

The major HIV-1 lineage, group M, responsible for the global pandemic, emerged as a zoonotic transmission from Chimpanzee *Pan troglodytes troglodytes* to humans in south-central Cameroon (135) in the early part of the 20th century (89). HIV-1 has since spread throughout the world leaving no continent un-affected (although unconfirmed in Antarctica) and infecting an estimated 0.8% of the world population (2009 AIDS Epidemic Update, UNAIDS and WHO 2009). Group M viruses have diversified into at least 9 genetically distinct subtypes (A, B, C, D, F, G, H, K) and recombinants thereof, with subtype B predominating in Europe and the Americas and C predominating in Africa and accounting for the largest share of the pandemic. The major modes of HIV-1 transmission include sexual contact (251), vertical transmission (55), and sharing of contaminated intravenous drug paraphernalia (66).

1.1.2 Viral Proteins and the Life-Cycle of HIV-1

The HIV-1 genome encodes 4 enzyme activities (reverse transcriptase (RT) with an associated RNase H activity, integrase (IN) and protease (PR)), 5 structural proteins encoded in the Gag polyprotein (matrix (MA), capsid (CA), nucleocapsid (NC), p6), and the Envelope glycoprotein (Env), and 6 accessory proteins (viral infectivity factor (Vif), Viral protein R (Vpr), Viral protein U (Vpu), Regulator of virion expression (Rev), Transactivator (Tat), and Negative factor (Nef)). The viral enzymes and structural proteins are required for replication and are shared among retroviruses. The ability to productively infect non-dividing cells, a defining feature of lentiviruses, is mediated by specific accessory protein activities, including nuclear import and cell-cycle manipulation activities of Vpr(108, 110, 263). Accessory proteins are also involved in subverting host innate defenses (Vif (269) and Vpu (201)) and adaptive immune responses (Nef (45)). Tat and Rev facilitate virus transcription (242) and nuclear export of un-spliced vRNA (170), respectively. Several of these accessory proteins, including Vpr, Vpu and Nef, have multiple activities, some of which are not fully understood.

The virus particle is composed of the core, made up of CA proteins surrounding the NC-bound dimeric, single-stranded, positive-sense RNA genome. The core is enveloped by a lipid bi-layer derived from the host cell membrane; embedded in the envelope is the Env protein, which mediates viral entry into the target cell. The particle also contains other viral proteins involved in replication processes through integration and viral gene expression in the newly infected cell, including the enzymes RT, IN and the accessory protein Vpr (47).

HIV-1 replicates in CD4+ T cells (54, 140), monocytes (329), and macrophages (90). Viral entry into the host cell is mediated by Env which binds the primary receptor CD4 and co-receptor, either of two 7-transmembrane G-protein-coupled chemokine receptors (GPCR), CXCR4 (18, 61, 79) or CCR5 (14, 71), inducing virion fusion with the host cell and deposition of the viral core into the cytoplasm. The need for CCR5 or CXCR4 is shared by several other lentiviruses such as FIV, BIV, and SIV, in some cases in the capacity as the primary receptor (75, 78, 307, 308), suggesting the co-receptor and perhaps CXCR4 specifically, represents a primary primordial receptor for lentiviruses. In addition to CXCR4 and CCR5, other chemokine-receptor family members have been implicated in HIV-1 entry in cell-culture assays (14, 71, 179), although their significance *in vivo* is unclear.

Once inside the cell, the viral RNA genome is reverse transcribed by RT, which also possesses DNA-dependant DNA polymerase activity in order to generate the plus-strand DNA to form a linear double-stranded (ds) DNA copy of the genome. The resulting viral dsDNA, in a pre-integration complex with RT, IN, and other viral proteins, is transported to the nucleus where integration into the host genome is mediated by the enzymatic activity of IN. Viral genes are then expressed from the integrated provirus by host-cell gene expression mechanisms. Initially, spliced mRNA coding for Tat, Rev and Nef are produced. This is followed by expression of partially- and un-spliced mRNA coding for the Gag and Gag-Pro-Pol polyproteins, Vif, Vpr, Vpu, and Env. Gag and Gag-Pro-Pol are transported to the cell membrane

where they are cleaved into their constituent proteins by PR and, along with Env, mediate budding of the nascent virus particle.

1.2 Envelope Structure and Function

HIV-1 Env is a type-1 heterodimeric membrane glycoprotein responsible for mediating viral entry into the target cell. Env is translated as gp160, which is then cleaved in a furin-dependant reaction to yield the gp41 transmembrane subunit and the gp120 surface subunit (102, 266). These subunits form heterodimers that are assembled on the cell surface to form Env trimers, which are ultimately incorporated in the membrane of the budding virus particle. The gp120 subunit contains the binding sites for the receptor and coreceptor, which mediate attachment of the virion to the cell surface, while the gp41 subunit contains the machinery that mediates fusion of the apposing viral and cellular membranes.

The gp120 subunit can be divided into several regions based on structure and function. The inner domain faces inward in the trimer and interacts directly with gp41. The outer domain is on the outer face of the trimer and contains both the CD4 binding site and components of the coreceptor binding site, which involves both the inner and outer domains (157). gp120 contains 5 variable loops V1-V5, and 5 interspersed conserved regions (C1-C5). The inner domain contains C1, V1, V2, a portion of C2, and C5; the outer domain contains a portion of C2, V3, C3, V4, C4 and V5.

The first step of entry involves binding of gp120 to the cellular membrane glycoprotein CD4, the primary receptor. Conformational changes in gp120 induced by this initial interaction enhance interactions with CD4 to stabilize the bound state

(67, 327). Conformational changes induced by CD4 binding also expose the coreceptor binding site on gp120, which is composed of the bridging sheet, a beta sheet involving C1 and C2 at the base of the V1 and V2 loops in the inner domain and C4 in the outer domain, and the V3 loop of the outer domain (120). The bridging sheet and the V3 base interact with the N-terminus of either of two 7-transmembrane G-protein-coupled receptors, CXCR4 or CCR5 (70, 119, 319). The specificity for the co-receptor is principally determined by the sequence of the V3 loop, which is also exposed upon CD4 binding and interacts in a sequence-specific manner with the second extracellular loop of the co-receptor (39, 50, 306). Binding of the co-receptor induces conformational changes in gp41 required for fusion, including exposure of the N-terminal hydrophobic fusion peptide that is inserted into the host cell membrane, and the folding of the six-helix bundle, processes which bring the apposing membranes into close proximity and trigger membrane fusion (187).

Many of the structural features of gp120, along with its requirement for CD4 binding, are thought to play a role in masking from antibody recognition and neutralization important invariant epitopes required for entry (156). These protective features include the variable loops on both the inner (V1 and V2) and outer (V4 and V5) domains, which are relatively unconstrained genetically. In it's unbound trimeric state, the highly antigenic structures of Env, such as V3, are likely buried beneath antigenically and conformationally unconstrained epitopes in the variable loops that can co-adapt with the host humoral response (156). In addition, highly conformational epitopes, such as the bridging sheet and the CD4 binding site are not readily available or are too unordered to be recognized by immune surveillance in

the un-liganded structure. The primary receptor, CD4, can therefore be thought of as the key that unlocks the door to the functional receptor binding sites for the GPCRs. Given the conformational changes that must take place in the process of receptor binding, a replication capacity cost must be associated with these structural armaments. Alterations in the variable loops and overall structure of gp120 can enhance CD4 and co-receptor binding, perhaps in a manner that is heavily constrained by the strong selective forces imposed by adaptive immunity (9, 192, 235).

Env is heavily glycosylated by the host cell, with nearly half of its mass attributed to asparagine (N)-linked high mannose, hybrid, and complex glycans (2, 162). Asparagines in the NX(T/S)X_2 context, where X is any amino acid but proline, are targeted by the host glycosylation machinery. The number of potential N-linked glycosylation sites (PNLGs) in an Env protein is variable with a range or 18 to 33 sites per gp120 molecule in group M HIV-1 isolates (146), with about 20 relatively conserved sites (198). Glycosylation is important for proper protein folding and also plays a role in immune evasion by creating a shield of poorly immunogenic and shifting branched glycans that sterically hinder antibody access to constrained epitopes (302). Most of the glycosylation sites on gp120 are located in the outer surface of the outer domain, consistent with their function as an antibody “glycan shield” (302). Specific PNLGs can also influence CD4 binding, presumably by altering access to the binding site (74). While many sites are conserved, glycosylation patterns can be diverse in the virus population; in particular, much of the length variability in the variable loops V1 and V4 result from insertions and

deletions of PNLGs (231). Consistent with their proposed functions in immune evasion, variable loops and glycosylation patterns are subject to diversifying selection both at the population level and through the course of infection (302).

1.3 The Course of HIV-1 infection

1.3.1 Transmission and Acute Infection

Transmission of HIV-1 is typically a rare event. In about 80% of transmissions, infection is established by only one variant (1, 134). Importantly, for subtype B, 98% of infections are established by CCR5-tropic viruses (134). Simian Immunodeficiency Virus (SIV) infection in Rhesus macaques closely resembles HIV-1 infection in humans and has therefore provided a useful model for studying the early events of infection. SIV (and by extension HIV-1) has been shown to first establish infection of local target cells at the site of mucosal transmission and then disseminate to draining lymph nodes where CD4+ T cells are in high enough density to sustain larger amounts of replication (185). This occurs within several days after transmission; however, plasma viremia remains undetectable. Within the first two weeks, virus spreads systemically to other lymphoid tissue including the gut-associated lymphoid tissues (GALT), which harbors large numbers of CD4+CCR5+ activated and resting memory T cells that support rapid exponential increases in viral replication resulting in profound CD4+ T cell depletion in this tissue (24, 98, 163, 295, 326). Evidence suggests that HIV-1 has evolved to home to this target-cell-rich compartment through specific interactions between Env and a CD4+ T cell-expressed GALT-homing receptor, alpha4beta7 integrin (5). GALT-replicating virus is the major contributor to peak viremia, which is reached by about 2-3 weeks post

infection in the peripheral blood with viral loads measuring 10^6-10^7 copies per ml of plasma. At peak viremia, the virus population is relatively homogenous as diversifying selective pressures have yet to act on the virus (134, 256), but viral diversification rapidly increases soon after the adaptive immune response emerges, and continues through the course of chronic infection as the virus population adapts to new cellular niches in a changing host environment, in addition to the adaptive immune response.

1.3.2 Sources of Genetic Variation

Selection acts on sequence diversity that is generated by multiple mechanisms during replication. Much of the mutational load of HIV-1 is generated by the low fidelity of RT when the viral genome is reverse transcribed. One study found an in vivo mutation rate for HIV-1 to be 3.4×10^{-5} per bp per round of replication (~2×10^{-5} per bp for point mutations), such that 1 in every 5 genomes would be expected to have a point mutation (174). In addition to point mutations, RT can introduce insertions and deletions, particularly in homopolymeric regions where these events are most common. However, many of these mutational events, in addition to those that lead to frame shifts and nonsense codons, render the protein product non-functional.

Another possible source of mutations is the activity of the antiviral factor APOBEC3G/F (A3G), a host cell-encoded cytidine deaminase. WhenA3G is not recognized by the viral countermeasure, it is incorporated into the virus particle where it lies in wait to act on the nascent minus-strand vDNA as it is exposed during reverse transcription in the newly infected cell (107, 172). Multiple cytidine

deaminations along the genome result in G to A substitutions in the plus strand that can render the provirus “hypermutated” in multiple genes. A3G represents a potent antiviral mechanism, and HIV-1 has therefore evolved a mechanism to neutralize this activity through the viral protein Vif, which binds and sequesters human A3G preventing its incorporation into the budding particle(205, 269). However, protection is incomplete and many proviruses are found to be hypermutated in human infection (134). Alternatively, A3G may introduce sub-lethal levels of G-to-A mutations that actually contribute diversity. Some evidence suggests that A3G-induced G-to-A mutations can contribute to drug resistance and that A3G plays and important role in generating viral diversity (130).

Genomic recombination also plays an important role in generating viral diversity. The high frequency of recombination of about 5 events per genome between different genetic variants (4, 41, 240), highlights the importance of this process in generating diversity. Recombination between different viruses occurs when two or more viruses infect the same cell. The genome dimer can then be formed from two different genomes, and during reverse transcription in the target cell template switching by RT between the two genomes generates a recombinant viral DNA product. Recombination has the effect of generating combinations of mutations in a single virus more rapidly than sequential mutation, thus increasing more quickly the genetic diversity upon which selective pressures can act. This is particularly important in cases where several mutations are required in combination to increase fitness, as is the case with drug resistance mutations in *pro* and *pol* (195).

1.3.3 Diversifying Evolution in Env: Adaptation to an Adaptive Immune Response

Within 3-4 weeks post infection, coincident with peak viremia, a virus-specific cytotoxic T lymphocite (CTL) response ensues that partially suppresses viremia to a "set point", a reduced but relatively stable viral load (22, 93, 149). The level of this suppression is variable between individuals and higher set points are linked to more rapid disease progression (21, 149, 182, 197). Around this time, in the relatively homogenous virus population of early infection, CTL escape variants are detected, which represent the first signs of diversifying selection in the virus population. The mechanism of escape from CTL involves selection for amino acid substitutions within HLA-restricted epitopes that affect antigen processing and antigen presentation (320). Epitopes are in all viral proteins including Env, which, as the only viral surface antigen, is also subjected to diversifying selection by the humoral immune response.

1.4 The Antibody Response to HIV-1 Env

1.4.1 Timing of the Initial Antibodies

The first antibodies to HIV-1 Env are detected within the first 3-4 weeks post infection, but their ability to neutralize virus at this stage is weak (80, 245, 284, 302). Neutralizing IgG antibodies are detected starting around 3 months post infection with escape mutations in the virus appearing soon after (302). The primary epitopes to which antibodies are directed are in the variable loops (V1-V5) and the receptor binding site surfaces, including epitopes that are induced by CD4 binding (214, 227, 314, 316). Importantly, sera does not generally neutralize contemporaneous virus,

and this, along with the observation that neutralization of early virus by sera collected later in infection wanes over time indicates that virus and the neutralizing antibody response are co-evolving (87, 302, 305). In Env, this results in a rapid expansion in diversity and divergence from the founder population that continues into the chronic phase then levels off in later stages of disease, where diversity can reach as high as 10% in the *env* gene (267).

1.4.2 Antibody-Driven Evolution

Consistent with the specificity of most antibodies, escape-associated variation is primarily identified in the variable loops, excluding V3 (298), an important exception that will be explored below. Diversification in the variable loops V1/V2 and V4/V5 during chronic infection is therefore attributed to adaptation to the polyclonal antibody response to these epitopes (87, 245, 253). Variation develops in the form of a variety of amino acid substitutions, and insertions and deletions, all of which can affect the pattern of N-linked glycosylation. Although the relative contribution that different types of mutations make to antibody escape remains unclear, all of these changes can affect neutralization sensitivity (238, 254, 270, 302, 310).

The most well characterized antibody-driven evolution in Env is that involving glycosylation patterns. Variability in glycosylation patterns is thought to play an important role in antibody escape by sterically hindering antibody access to neutralization sensitive epitopes (302). While glycans can themselves serve as antibody epitopes (34, 260), glycan-reactive antibodies like 2G12 are rarely found in HIV-infected people (12, 261). Changes in glycosylation patterns are affected by

both point mutations that produce or eliminate NX(S/T)X motifs or by insertions and deletions of NX(S/T)X motifs in the length variable regions of the variable loops (254). The involvement of base pair triplet repeats in this process is suggestive of a mechanism of glycosylation site addition similar to that observed for triplet repeat expansions implicated in some human genetic diseases (53). Evolution of glycosylation does not necessarily result in a net change in the number of glycosylation sites, instead a shifting pattern of both conserved and variable glycosylation sites is observed (87, 302), although conservation in number may be specific to subtype B (64, 86). Maintenance of this large number of glycosylation sites likely incurs a fitness cost in the absence of antibody pressure, a feature of Env that will be explored further in chapter 3.

1.4.3 Rare and Common Antibody Epitopes

While most antibodies are directed at epitopes in gp120 that are not neutralization-sensitive in contemporaneous virus, a small number antibodies have been identified in rare cases that target unusual epitopes and are considered broadly neutralizing, that is, are able to neutralize a broad spectrum of diverse primary isolates. These include 2F5 and 4E10 (213, 331, 332) which target the membrane-proximal region of gp41, 2G12 which is specific for a discontinuous epitope composed of glycans on the outer domain (34, 260), b12 which is specific for a discontinuous epitope that overlaps the CD4 binding site (33, 327), and more recently, the most broad and potent antibody identified to date, PG9 (and the related somatic variant PG16), which targets an epitope that includes the conserved V1/V2 base, conserved regions of the V2 loop and V3 but only binds trimeric gp120 (299).

While antibodies to most of these epitopes are rarely identified in infected individuals, CD4 binding site-specific antibodies represent a large proportion of antibodies identified in infections (51, 261), although these antibodies generally do not exhibit the relatively broad potency of b12. As discussed above, while the CD4 binding site is conserved, conformation and glycosylation at proximal sites play an important role in occlusion of the conserved epitopes. b12 possesses an unusually long heavy chain complementary-determining region 3 (CDR H3) that allows it to penetrate the deeply recessed CD4 binding site that is not accessible to most antibodies (327).

Other antibodies have been identified that target the highly antigenic and relatively conserved linear epitope at the tip of the V3 loop. This class of antibody, which include the well characterized antibodies 447-52D and 19b (46, 264, 330) neutralize only a subset of primary isolates (13), because of masking of the conserved V3 epitope by V1/V2 in Env in primary isolates (152, 315). These antibodies have broadened and more potent neutralizing activity when a CD4-bound conformation is induced (313). Moreover, antibodies directed at V3 are frequently identified in chronic infection (51, 191), indicating their potentially important role in neutralization or as a selective pressure.

Evolutionary pathways to antibody escape can be divided into two categories: Amino acid substitutions in the targeted epitope itself that directly limit antibody binding, or substitutions that alter either envelope protein conformation or glycan placement and thereby limit access to conserved targeted epitopes. Escape from both CD4 binding site and V3 antibodies appears to be accomplished by the latter

path in most cases. Because of the importance of conformation on neutralization sensitivity to V3 antibodies in particular, and because the tip of the V3 loop contains a conserved linear epitope relative to other antibody-targeted epitopes, these antibodies may play a role in selecting for Env conformations, rather than specific changes in the target epitope, that could impact changes in receptor and co-receptor binding, a hypothesis that will be further developed and addressed in Chapters 3 and 4.

1.5 Evolution of Env Function

While much of the diversity in Env observed over the course of chronic infection is attributed to antibody selective pressure, specific changes in CD4 and coreceptor usage also contribute to increased diversity in the population, though as alluded to above, antibody selective pressures may be linked to phenotypic changes in Env. Phenotypic variation in Env has been described for its affinity for the primary receptor CD4, which affects the ability of the virus to enter cell types with low levels of receptor, such as macrophage (178, 220, 283), and for its ability to use the coreceptor CXCR4 as an alternative to CCR5, which impacts it's ability to infect target cells that exclusively express CXCR4. The phenotype of the virus that predominates in early infection requires relatively high levels of CD4 and is exclusively CCR5-tropic (134), but over the course of infection, Envs emerge, with variable frequency, that can use low levels of CD4 (macrophage-tropic) and/or have gained the ability to use CXCR4 (X4 variants).

1.5.1 Macrophage Tropism

Changes that allow the virus to use low levels of CD4 typically involve conformational changes in Env. Increased CD4 binding and the ability to efficiently infect macrophages have been mapped to changes in V2 (125, 142, 300) and to the removal of a specific PNLGS at position 386 (74) (amino acid numbering here forward corresponds to the reference strain HXB2, Genebank accession number K03455), but not changes in the CD4 contact residues themselves (157), although exceptions have been found (73). This suggests that the primary mechanism of enhanced CD4 binding and thus macrophage tropism is through conformational changes in Env induced by amino acid changes outside of the binding site. These conformational changes may also enhance the ability to use lower levels of CCR5 expressed on macrophage perhaps by decreasing the dependence on CD4-triggered conformational change (95).

The selective pressures driving macrophage tropism are not well understood. Target cell availability could drive macrophage tropism if virus that replicates in these cells has a selective advantage, as may be the case for virus compartmentalized in the CNS where macrophage may support viral replication (73, 74, 283). Macrophage-tropic variants have also been identified in alveolar macrophage in the lung (90, 123) and Kupffer cells in the liver (36). Importantly, macrophage-tropic variants have not been found to predominate in the peripheral blood, particularly in early infection (97, 126, 221).

1.5.2 CXCR4 Tropism

Another feature of the vast majority of viruses that establish infection is their exclusive use of the CCR5 coreceptor (R5 variants), a phenotype that is maintained through the early course of disease and into the chronic phase. In about one-half of individuals, Env variants emerge that have gained the ability to use the CXCR4 co-receptor (X4 variants). This phenotypic switch almost invariably coincides with immunosuppression and progression to AIDS, suggesting that X4 viruses are more pathogenic (15, 49, 244, 282); however it is still not clear whether or not the emergence of CXCR4-tropic viruses is the result or the cause of immunosuppression, an issue that will be discussed below. CXCR4-tropic variants emerge as a clonal outgrowth from the R5 viral population and often retain the ability to use CCR5, i.e. they are dual tropic (126) although variants may be functionally CXCR4-tropic in vivo (318). The primary genetic determinant of CXCR4 tropism is the V3 loop in which only a few changes at specific positions are required to confer CXCR4 tropism (117, 127). Genetically, CXCR4 tropism can be defined by the presence of basic residues at positions 11 and/or 25 of the 35 amino acid V3 loop, or an increase in overall positive charge (117, 129, 184). Variability in the V3 loop is therefore indicative of a phenotypic switch in co-receptor tropism (184, 202, 203).

As with macrophage tropism, the selective pressures driving evolution of X4 virus are not well understood, although several hypotheses exist. CXCR4 is exclusively expressed on the large subset of naïve CD+ T cells, whereas both CCR5 and CXCR4 are expressed on the memory T cell subset. Emergence of CXCR4-tropic virus may be driven by selection for virus that can expand its host cell range

and infect naïve T cells (241). While this may be the case, naïve T cells are abundant at all stages of infection, which does not explain why X4 variants typically only emerge late in infection. Another hypothesis, that I begin to address in Chapters 3 and 4, is that evolution of CXCR4 tropism requires conformational changes that are selected against by specific antibody responses that are diminished in the late stage immunosuppressed environments when X4 viruses are usually detected.

The case has been made that CXCR4 tropism evolution results in increased pathogenesis, and that the increased cytopathicity often observed in CXCR4-tropic viruses leads to the increased rate of immune suppression that is associated with the CXCR4 tropism emergence (15, 244). Alternatively, CXCR4 emergence may be a consequence of severe immune suppression (114). However, it is also likely that both are true and that CXCR4 tropism emergence potentiates its persistence, perhaps by creating a ratchet effect; once immune selective pressures fall below a threshold, CXCR4-tropic virus can evolve and establish a critical mass in naïve T cells in particular, initiating an irreversible decline in immune competence. Chapter 2 explores the relationship between CXCR4- and CCR5-tropic virus populations and attempts to address the question of whether these populations are replicating independently of each other.

1.6 Compartmentalization

Central to the evolution of HIV during infection is the spread of virus systemically into different organ and cellular compartments (257, 311). Viral populations can replicate independently in different tissue locations or cell types and genetically diverge as a result. Establishment of divergent populations that are

replicating independently of each other in different niches, or compartments, can result from a specific adaptation to a particular niche, such as macrophage tropism, or as a result of stochastic founder effects (85). Given the diversity of HIV-1 genetic and phenotypic variants coexisting in an individual, it is likely that at least some subset of these variants are compartmentalized, because the relatively stable coexistence of these distinct genetic and phenotypic variants implies some degree of niche selection. Compartmentalization is a common feature in different tissues such as the CNS, genital tract, and lymphoid tissue (37, 59, 136, 247, 257, 283), and also in different cell types, as some data suggest (15, 88).

The multiple selective pressures that drive diversification of HIV-1, as discussed above, result in the multiple genetic and phenotypic variants that are found to coexist in the peripheral blood. It is possible that different pathways of neutralizing antibody escape are a result of differential antibody selection in compartmentalized populations. Different functional Env variants may be emerging from compartmentalized populations under different selective pressures. In addition, populations compartmentalized due to stochastic seeding may also be represented as distinct genetic variants in the periphery, but with no discernable selective advantage. Chapter 2 attempts to address the degree to which the variants in the periphery represent compartmentalized populations.

Chapter 2

Major co-existing human immunodeficiency virus type 1 *env* gene subpopulations in the peripheral blood are produced by cells with similar turnover rates and show little evidence of genetic compartmentalization

The following material was published as a manuscript in the *Journal of Virology* under the following citation:

William L. Ince, Patrick R. Harrington, Gretja L. Schnell, Milloni Patel-Chhabra, Christina L. Burch, Prema Menezes, Richard W. Price, Joseph J. Eron Jr. and Ronald I. Swanstrom. 2009. **Major co-existing human immunodeficiency virus type 1 *env* gene subpopulations in the peripheral blood are produced by cells with similar turnover rates and show little evidence of genetic compartmentalization**. J. Virol. 83(9):4068-80.

2.1 ABSTRACT

A distinctive feature of chronic human immunodeficiency virus type 1 (HIV-1) infection is the presence of multiple co-existing genetic variants, or subpopulations, that comprise the HIV-1 population detected in the peripheral blood. Analysis of HIV-1 RNA decay dynamics during the initiation of highly active antiretroviral therapy (HAART) has been a valuable tool for modeling the life span of infected cells that produce the bulk HIV-1 population. However, different HIV-1 target cells may have different turnover rates, and it is not clear whether the bulk HIV-1 RNA decay rate actually represents a composite of the decay rates of viral subpopulations compartmentalized in different cellular subsets with different life spans. Using heteroduplex tracking assays (HTAs) targeting the highly variable V3 or V4-V5 regions of the HIV-1 *env* gene in eight subjects, we found that all detectable co-existing HIV-1 variants in the peripheral blood generally decayed at similar rates during the initiation of HAART, suggesting that all of the variants were produced by cells with a similar life span. Furthermore, single genome amplification and coreceptor phenotyping revealed that, in two subjects, co-existing HIV-1 variants with distinct CXCR4 or CCR5 coreceptor phenotypes decayed with similar rates. Also, in nine additional subjects, recombination and a lack of genetic compartmentalization between X4 and R5 variants were observed, suggesting an overlap in host cell range. Our results suggest that the HIV-1 *env* subpopulations detectable in the peripheral blood are produced by cells with a similar life span and are not genetically isolated within particular cell types.

2.2 INTRODUCTION

Infection with human immunodeficiency virus type 1 (HIV-1) is typically established by one or a few variants that give rise to an initially homogeneous viral population (58, 86, 134, 159). As infection progresses into the chronic phase, sequence diversification occurs throughout the viral genome, most dramatically in the envelope gene (*env)*, as a result of selection of humoral and cytotoxic T lymphocyte (CTL) immune escape mutations (22, 87, 149, 249, 309). Sequence diversity is clustered in variable regions in the *env* gene, termed V1 through V5, which encode surface loops in the Env protein that are important targets of the host antibody response (87). Diversification of *env* results in the presence of multiple, co-existing *env* variants in the peripheral blood that continually evolve during the course of infection (106, 139).

Typically, the HIV-1 population early after infection uses CCR5 as the coreceptor (R5) (134, 292, 324, 328), and variants that can use CXCR4 (X4) arise later in the disease course in approximately one-half of individuals infected with subtype B virus (49, 144). A major determinant of coreceptor use is found in the V3 loop, and sequence evolution in this region is often linked to the virus's ability to use CXCR4 (81, 129, 202). After the emergence of X4 virus, *env* genes encoding both CCR5 and CXCR4 tropism can co-exist for extended periods of time, maintaining a diverse V3 population (49, 202, 274). Variation in R5 Env proteins can also influence the ability of a virus to utilize varying levels of CD4 and CCR5 found on different cell types, such as macrophage and T cells (95, 97, 220, 226, 283, 300).

Distinct biological characteristics encoded by different *env* variants, such as coreceptor use, cellular tropism and sensitivity to immune pressure, may drive, or result from, HIV-1 compartmentalization. Genetic compartmentalization of HIV-1 variants has been well documented in anatomical compartments, such as the spleen (42, 85, 96), central nervous system (30, 104, 105, 148, 206, 247) and genital tract (59, 136, 211, 222, 233), and in different cellular compartments, such as monocyte/macrophage and CD4+ T cells (88, 168). Divergent coreceptor tropism in particular may lead to compartmentalization of virus in different cellular subsets. For example, naïve and memory T lymphocytes both express CXCR4 but differentially express CCR5 and have been shown to harbor unequal proportions of CXCR4- and CCR5-tropic viral variants that are concordant with their distinct coreceptor expression patterns (15, 290).

While genetic compartmentalization of HIV-1 between anatomically or cellularly segregated sequences has been extensively explored, evidence is limited as to the extent to which the co-existing *env* subpopulations circulating in the peripheral blood represent virus emanating from compartmentalized populations replicating independently of each other and in different cellular subsets. Although this question is challenging to address in the context of an infected individual, one approach stems from the examination of the rate of decay of HIV-1 RNA during the initiation of highly active antiretroviral therapy (HAART). Effective HAART prevents new rounds of HIV-1 infection, but cells already infected by HIV-1 continue to produce virus, and therefore the rate of viral RNA decay during effective HAART reflects the life span of the HIV-1-producing cells. This strategy was initially used by

Ho *et al*. and Wei *et al*. (113, 303) to characterize the turnover rate of HIV-1-infected cells. These and subsequent studies (16, 176, 218, 219) suggested that the average life span of infected cells that produce 99% or more of the bulk HIV-1 population in the peripheral blood is short, with a half-life of 1-2 days, presumably reflecting the life span of activated T-cells, whereas cells producing 1% or less of the population have a half-life measured in weeks, illustrated by a bi-phasic decay curve. However, the bulk HIV-1 RNA decay rate of the first phase may oversimplify the dynamics of the underlying viral genetic subpopulations, because this rate may represent an average without accounting for possible moderate differences between decay rates of co-existing variants, as might be the case for variants infecting cellular subsets in different stages of maturation or activation (92, 209, 326). Based on this model, two or more co-existing viral populations with the same rates of decay during HAART could be presumed to be produced by the same cellular subset, or at minimum two or more subsets with the same turnover rate. Conversely, the observation of different rates of decay would suggest that different cellular subsets are contributing towards a complex mixture of compartmentalized viral subpopulations.

In this study we characterized the decay rates of co-existing HIV-1 *env* variants in the peripheral blood of eight subjects initiating HAART. In two of these subjects, who possessed both CCR5- and CXCR4-tropic Env variants, we analyzed the decay rates of each phenotypically divergent *env* subpopulation. Furthermore, in an additional nine subjects, we characterized the degree of recombination between the R5 and X4 subpopulations and the degree to which each subpopulation was genetically compartmentalized. We found that all detectible HIV-1 *env* variants in the

peripheral blood, regardless of coreceptor tropism phenotype, decayed with similar rates during the initiation of HAART. In addition, we provide evidence of recombination and a lack of compartmentalization between co-existing X4 and R5 subpopulations, consistent with overlap in their target host-cell populations. Our findings suggest that the detectable HIV-1 *env* variants that co-exist in the peripheral blood are produced by cells with a similar life span and, by this measure, are not compartmentalized to particular cell types.

2.3 MATERIALS AND METHODS

2.3.1 Study subjects and sampling.

Blood plasma samples used for the variant decay analysis were obtained from subjects initiating HAART who were recruited either through a previously described study carried out at the University of California, San Francisco, (subjects 4015, 4021, 4022, 4030, 5005) (276) or at the University of North Carolina, Chapel Hill, specifically for this study (subjects 101, 106, 108, 109). Sampling of blood plasma was carried out on the day of treatment initiation and at 1-7 day intervals post treatment initiation; the median time between samplings for all subjects was 3 days.

Additional blood plasma samples used for the analysis of recombination and compartmentalization in populations with mixed coreceptor use were excess tissue obtained from the baseline blood draw of subjects participating in the virology sub-study of a ritonavir efficacy trial described previously (35) (subjects 1314, 1077, 1551) or from baseline blood draws of subjects entering ACTG 359 described

elsewhere (subjects 432, 135, 139, 411, 413, 310) (100). In all cases, written, informed consent was obtained and all protocols were subject to IRB approval.

2.3.2 Heteroduplex tracking assay and decay analysis.

Viral RNA was extracted from virus particles pelleted from 1 mL of blood plasma (25,000 x g for 1.5 hours) using the QiaAMP Viral RNA Kit (Qiagen, Chatsworth, CA). Two, 5 μL aliquots of the 60 μL eluate were amplified in parallel using the OneStep RT-PCR kit (Qiagen, Chatsworth, CA). The PCR thermocycling procedures, the primers used to amplify the V3 and V4-V5 regions and the HTA analysis have been previously described (60, 106, 202). Briefly, PCR products were annealed to a radiolabeled probe to generate heteroduplexes, which were then separated in a polyacrylamide gel. Gel-separated heteroduplexes were visualized by autoradiography and quantitated on a Storm 840 phosphorimager using the ImageQuant software (Molecular Dynamics/GE, Pittsburgh, PA). The HTA analysis was modified for this study by using a biotin-radio-labeled probe to facilitate isolation and sequencing of HTA bands, as described elsewhere (262). All samples were analyzed in duplicate to verify sampling reproducibility. Samples and time-points that could not be reproducibly sampled were excluded from the analysis. Viral RNA loads of individual variants were calculated as a product of the total viral RNA load and the fractional abundance of each variant. Variant half-lives were calculated using the time points between which viral load was declining.

2.3.3 Single Genome Amplification.

Viral RNA was extracted as described above. RNA was reverse transcribed using Superscript III Reverse Transcriptase (RT) System (Invitrogen, CA) and oligo

dT. A region of the HIV-1 genome encompassing *env* through 3' U3 was amplified using a limiting dilution, semi-nested PCR approach initially described by Simmonds, *et al*. (271) and Edmonson and Mullins (76), then modified by Palmer, *et al*. (212) and Salazar-Gonzalez, *et al*. (255). Primers and thermocycling procedures for amplification and sequencing were used as previously described in Keele, *et al*. (134) but modified by replacing the downstream *env* amplification primer set with a primer that captures the U3, the sequence of which is 5'-AAGCACTCAAGGCAAGCTTTATTG-3'. Sequences will be submitted to GeneBank by the time of publication.

2.3.4 Coreceptor tropism analysis.

Coreceptor phenotype was predicted based on V3 sequences of extracted HTA bands and SGA amplicons using a Position Specific Scoring Matrix (PSSM) generated using a training set of V3 sequences from envelopes with known coreceptor phenotypes on indicator cells expressing CD4 and either CXCR4 or CCR5 (129). PSSM was implemented through the web portal http://ubik.microbiol.washington.edu/computing/pssm/.

Phenotypic analysis was carried out as previously described by Kirchherr, *et al*. (137), but with modification. Briefly, a CMV promoter containing a 3' tag matching the 5' SGA primer binding site was linked to *env* SGA amplicons using overlapping PCR. For the CMV-*env* linking PCR, the 5' primer sequence is specific for the start of the CMV promoter (5'-AGTAATCAATTACGGGGTCATTAGTTCAT-3'), and the downstream primer (5'-

TGGGTGGCTCTGAAAAGAGCCTTTGGGCTGCTGGCTCAGCTCGTCTCATTCTTT

C-3') is specific for a sequence just 3' of the end of *env* and contains a histone (H1e) mRNA 3' stem-loop tag (underlined) for increased transcript stability. CMV-*env* amplicons were co-transfected with the pNL4-3.Luc.R-E- plasmid, obtained from the NIH ARRRP (108), to generate a pseudotyped, single-cycle luciferase reporter virus. The coreceptor phenotype of pseudotyped virus was assessed on U87.CD4 indicator cell lines, expressing either CXCR4 or CCR5, obtained from the NIH ARRRP (14).

2.3.5 Compartmentalization and recombination analysis.

All sequence alignments were generated using MAFFT (Multiple Alignment using Fast Fourier Transform) (133). Maximum likelihood phylogenies were generated in PhyML using the HKY85 substitution rate model with the following parameters: use of four substitution rate categories and estimations of the transition/transversion rate ratio, proportion of invariant sites and the gamma distribution parameter (99). A version of the Slatkin-Maddison test for gene flow was implemented using HyPhy (230, 272) and measures of K_{ST}* were obtained using DNAsp (252). K_{ST}* is calculated as described by Hudson, Boos and Kaplan (122). Briefly, $K_{ST}^* = 1-(K_S^*/K_T)$ where K_S* is the weighted average of the log of the pairwise differences within each of the two potentially compartmentalized subpopulations. K_T is the average number of pairwise differences between sequences irrespective of their grouping. For both SM and K_{ST}* tests, comparison of the observed result to the distribution of 1000 random permutations of the data was used to obtain a *P*-value. Recombination between X4 and R5 variants was detected in sequence alignments using the bootscan/RECSCAN analysis implemented in the Recombination

Detection Program 3 (RDP3) (177, 258). Bootscanning was carried out using a 200 bp window with a 20 bp step and trees were constructed using the Jukes-Cantor model with 1000 bootstrap replicates.

2.4 RESULTS

2.4.1 Decay rates do not vary between detectable *env* variants that co-exist in the peripheral blood.

We examined the decay rates of V4-V5 or V3 *env* variants in chronically infected subjects initiating HAART to characterize the life span of infected cells that produce co-existing genetic variants in the peripheral blood. Blood plasma samples from 8 subjects were drawn every 1-7 days after the initiation of therapy, with a median interval of 3 days, for up to 3 weeks or over a 1–2 log(10) drop in total viral RNA load (VL). All subjects in this study achieved suppression of VL to below detectable levels. RNA was extracted from the plasma samples and then amplified by RT-PCR to generate amplicons of the variable regions V4-V5 or V3, which were then subjected to heteroduplex tracking assay (HTA) analysis to resolve the co-existing sequence variants. The relative abundance of V4-V5 or V3 variants, potentially comprising as little as 1-3% of the total population, was measured by phosphorimaging analysis of HTA bands (239, 262). Duplicate RT-PCR reactions were analyzed to ensure sampling reproducibility; the ability to analyze duplicate samples to validate the quality of sampling is a key feature of the HTA strategy as the HTA pattern of two identical, complex populations will appear different if they are not adequately sampled (111); however, the HTA pattern only represents variants whose sequence differences cause a shift in migration rate. While much of the diversity in these highly variable regions of the genome is captured using this technique, in this work, we are testing the hypothesis that these HTA variants are markers of potentially compartmentalized populations.

The decay curves of V4-V5 and V3 HTA variants from two representative subjects are depicted Figure 2.1. The Log(10) magnitude of the VL drop, the $T_{1/2}$ (days) of the bulk VL, and the maximum differences in $T_{1/2}$ for the *env* variants detected in each subject are shown in Table 2.1. In all but one subject, virus decay appeared mono-phasic over the first 1- 2 Log(10) decline in VL. In subject 106, the VL decay appeared more rapid between the first and second time points (days 0 and 1), which had an apparent $T_{1/2}$ of 0.28 days (based on a single time-point), compared to the VL decline between the second and fifth time-points, which had an apparent $T_{1/2}$ of 2.22 days (Figure 2.1a). The median bulk VL decay rates for these subjects was $T_{1/2}$ =1.7 days. The decay rates of either V3 or V4-V5 variants within each subject did not vary significantly; the median value for the greatest differences between any two variants within a subject was 1.6-fold and did not exceed 2-fold within any subject, likely within the margin of error of this assay. The minor variation in decay rates of variants did not correlate with their relative abundance, including for variants comprising as little as 2% of the detected population (Table 2.1). We conclude that for variants comprising as little as 2% of the detected population and representing the first phase of decay: i) variants are not compartmentalized in anatomical locations or cellular compartments that are differentially targeted by anti-viral activity; ii) the life spans of potentially different, virus-producing cellular subsets do not differ to a significant degree for those cells producing the major variants of *env*; and iii) variants are not otherwise compartmentalized in a manner that differentially affects their rates of decay.

2.4.2 Decay rates do not differ between X4 and R5 variants in the first phase of decay.

The ability of a virus to use CXCR4 efficiently may allow infection of a different subset of target cells and hence may result in compartmentalization of X4 and R5 variants in cell types that differentially express these coreceptors, such as memory and naïve T cell subsets (19). Many X4 variants retain the ability to enter cells using CCR5 (i.e. dual-tropic), although it is not clear this ability is utilized *in vivo* (171, 318). Furthermore, naïve and memory T cell subsets have been shown to be preferentially infected by CXCR4 or CCR5 variants, respectively (15, 290).

We identified two subjects from the analysis described above who had co-existing CXCR4- and CCR5-tropic populations, which allowed us to determine the relative rates of decay of X4 and R5 variants specifically. Coreceptor usage was assessed by first using PSSM, followed by phenotypic analysis of the encoded Env protein in a pseudotyped virus entry assay. One subject (109) had a viral population with both X4 and R5 variants identified by PSSM and confirmed in an entry assay. In the other subject (101), distinct V3 variants failed to meet the cut-off value for a CXCR4 tropism designation by PSSM, but exhibited strong CXCR4-tropic activity in the entry assay. In both of these subjects, X4 variants retained some ability to use CCR5.

HTA analysis of the V3 and V4-V5 regions of *env* of virus from subject 109 revealed 2 and 4 HTA variants, respectively (Figure 2.2a and b). Recovery and sequencing of HTA bands, along with single genome amplification (SGA) and phylogenetic and phenotypic analysis of full length *env* genes from the first time-

point allowed us to link *env* sequences, and their coreceptor usage phenotypes, to the specific V3 and V4-V5 HTA bands for this subject. For example, X4 and R5 V3 variants formed distinct phylogenetic lineages that were each represented by one of the two HTA variants (Figure 2.3a) and V4-V5 HTA variants were linked to X4 V3 sequences by the presence of a deletion in each variable loop (data not shown). The full-length *env* sequences also formed distinct phylogenetic lineages according to V3 genotype and coreceptor phenotype (Figure 2.3b). The decay of X4- and R5-linked V3 and V4-V5 HTA variants are depicted in Figure 2.2a and b, respectively. The decay rate of the total VL for subject 109 was $T_{1/2}$ = 2.3 days, and over the course of a 2-Log(10) drop in VL, there was no significant difference in the decay rates of HTA variants relative to each other in subject 109 (Figure 2.2a and b, Table 2.1).

HTA analysis of virus from subject 101 revealed 2 variants in the V4-V5 region that decayed with similar rates (Figure 2.2c, Table 2.1). However, we were not able to amplify the V3 region from this subject, presumably as a result of subsequently identified V3 primer binding site mismatches in this viral population. In an alternative approach taken for this subject, SGA was carried out on each time point in order to assess the change in the relative proportions of all SGA-amplified *env* variants as VL declined. *env* sequences that exhibited strong X4 usage in the entry assay clustered together in a phylogenetic tree, as did their V3 sequences, indicating linkage coreceptor use (Figure 2.4a and b). While not meeting the threshold value for X4 usage according to PSSM, these V3 variants had distinctly higher PSSM values and were more positively charged relative to the rest of the population. V4-V5 genotypes were only weakly linked to tropism (data not shown).

Weak X4 entry activity was detected in some envelopes whose sequences were intermingled with those of exclusively R5 envelopes (Figure 2.4a and b), although the biological significance of this low-level X4 activity is unclear.

The decay rate of the total VL for subject 101 was $T_{1/2}$ = 2.3 days, and over the course of a 2-Log(10) drop in VL, there was no significant difference in the decay rates of V4-V5 HTA variants relative to each other (Figure 2.2c and Table 2.1). In addition, we did not detect a significant change in the proportion of *env* sequence variants, sampled by SGA, that clustered with phenotypically identified X4 or R5 variants at the 2 time points following initiation of therapy. X4 variants constituted 26% of the amplicons in the first time point and 20% in the third time point, P=0.7 (Figure 2.4a). That we did not detect differential decay of X4 versus R5 variants in subjects 101 or 109 leads us to conclude that either i) the bulk of the tropism variants are not compartmentalized between different cellular subsets, or ii) while tropism variants may be compartmentalized in different cellular subsets, these infected cells have similar life spans when productively infected. Furthermore, any differential effects that X4 or R5 infection may have on the life span of the infected cell, or any difference in susceptibility of these tropic variants to anti-viral inhibition, are not apparent in these data.

2.4.3 CXCR4 and CCR5-tropic variants exhibit limited genetic compartmentalization in the peripheral blood.

We next examined the potential genetic compartmentalization of co-existing R5 and X4 variants using an alternative approach. Specifically, we were interested in determining the degree to which viral genomes with distinct coreceptor tropisms

exhibit signs of genetic compartmentalization. For this analysis, we included the entry samples of the two subjects identified above (101 and 109) and an additional nine subjects, obtained from studies described in the Methods section, with co-existing X4 and R5 subpopulations identified by PSSM analysis of V3 sequences. Using SGA, which eliminates confounding recombination during PCR, we generated amplicons containing *env*, *nef* and the U3 region of the viral genome and carried out PSSM and phenotypic analysis on a representative subset of *env* variants from each subject. Phenotypic analysis was consistent with the result of the PSSM analysis for every amplicon tested in all but subject 101, as described above. CXCR4-tropic variants from all but two subjects in this study (138 and 411) also exhibited CCR5-tropic activity in the reporter assay, but will be referred to as X4 variants. In many subjects, phylogenetic analysis of *env* sequences showed a deep branch point between the R5 sequences and a monophyletic group (i.e., a group that has descended from a single ancestral virus) of X4 sequences, suggesting that the outgrowth of X4 variants derives from a clonal event. Representative examples of phylogenies of sequences encompassing V1 of *env* through the 3' U3 from three subjects are depicted in Figure 2.5.

If these X4 and R5 variants exist in distinct compartments with no migration of viruses between compartments, then the independent evolution of these virus subpopulations will produce a number of evolutionary signatures in regions of the genome outside of V3. We looked for these signatures using two methods applied to sequences from three regions of the genome: the V4-V5 region of *env*, the gp41 region of *env*, and the U3 region of the LTR. First we used the Slatkin-Maddison

(SM) test (272) to investigate whether independent evolution of X4 and R5 variants in distinct compartments had produced similar phylogenetic patterns in all genome regions. Essentially, our use of the SM test examines the expectation that X4 viruses should form a monophyletic group regardless of the genome region used to build the tree, if this group is compartmentalized. Second, we used a distance-based metric, K_{ST}* (see Methods) (34, 74, 89), to investigate whether independent evolution of X4 and R5 variants was occurring in distinct compartments and producing genetic differentiation between the compartments in regions outside of V3. The K_{ST}* statistic is a measure of whether the genetic distance (number of nucleotide differences) between the X4 and R5 subpopulations is significantly greater than the genetic distance among viruses within the X4 or R5 subpopulations. Gene flow between compartments would erode both of these signatures of independent evolution, and gene flow is expected to have the strongest impact on genomic regions that are most distant from V3, due to the increased likelihood of recombination.

Observed SM and K_{ST} values were compared to the distribution of 1000 random permutations of branches or sequences to determine the level of significance of separation. Because X4 and R5 subgroups were essentially defined by their V3 genotype, which in most subjects were monophyletic groups with highly similar genotypes, recombination events were inferred when the sequences of the regions analyzed did not cluster according to their linked V3 genotype, indicated by migration events in the SM analysis. However, a lack of compartmentalization can result in increased sequence homogeneity in regions distal to V3, and detection of recombination between X4 and R5 sequences in these regions is only possible in

cases where there remain strong phylogenetic signals that result in a well-supported tree.

The analysis revealed statistical support, by both K_{ST} and SM measures, for compartmentalization of two genetic populations defined by coreceptor use for markers proximal to V3, such as V4-V5 (Figure 2.6a and b). This would be expected as mutations closer to the population-defining V3 sequence would likely persist in linkage disequilibrium for a longer period of time after the outgrowth of the X4 V3 mutations, especially if they are functionally linked to V3. However, in most subjects, SM migration events between the R5 and X4 populations were increased in regions more distal to V3, such as U3 (Figure 2.6a), indicating that these populations were replicating at least part of the time in a shared cell type, providing the opportunity for recombination. Representative examples of detected recombination between X4 and R5 sequences and the predicted location of breakpoints, in these cases outside of gp120, are illustrated in Figure 2.7. This result is consistent with previous observations of recombination between X4 and R5 viruses made using different methods (183, 257, 291). We also observed decreasing values of genetic differentiation between X4 and R5 groups, as measured by $K_{ST,}$ for regions farther from V3 (Figure 2.6b). However, in several subjects (135, 411, 432, 1314) a compartmentalization signal in the U3 remained statistically significant, if decreased, by both measures (Figure 2.6a and b, bottom panels). Taken together, these results show that while X4 and R5 *env* variants are genetically distinct, in many of our subjects there is little evidence of genetic compartmentalization between X4 and R5 variants in regions outside of *env*, such as in the U3.

2.5 DISCUSSION

There are several reasons to hypothesize that variants that appear in the blood are potentially compartmentalized. Previous studies have demonstrated compartmentalization of HIV-1 variants between different anatomical compartments, such as the central nervous system, genital tract, and different lymphoid tissues (59, 68, 96, 101, 136, 148, 233, 247, 257, 268, 289) as well as tissue microenvironments (96). The gut-associated lymphoid tissue in particular represents a major source of active replication of potentially compartmentalized CCR5-tropic virus populations (5, 228, 289, 295). It is possible that virus spatially compartmentalized in these anatomical sites may be represented as distinct variants in the peripheral blood. Because the initiation of HAART abruptly blocks new rounds of HIV-1 infection, presumably without impacting viral RNA production from cells already infected, different decay rates of compartmentalized variants following suppression of viral replication should reflect different life spans of the cells from which they are emerging. Viral populations compartmentalized in either cell types or tissues that experience differential drug exposure may also decay at different rates if viral replication continues at some level in the presence of suboptimal drug concentration. However, our observation that all detectable HIV-1 genetic variants declined at comparable rates suggests that the vast majority of the co-existing HIV-1 subpopulations in the peripheral blood are neither compartmentalized to cell types with different life spans nor to cells or tissues with varying degrees of antiretroviral drug bioavailability.

Our use of the HTA allowed for relatively sensitive detection of variants potentially comprising as little as 1-3% of the population (111, 262). However, one important limitation of this study is the sensitivity for detection of minority viral populations below this 1% threshold, which may be produced by cells with different life spans. Such viral populations almost certainly exist based on the biphasic decay kinetics of the bulk HIV-1 RNA load during HAART (16, 176, 218). It has been hypothesized that the second phase of decay of the bulk HIV-1 RNA load represents virus produced by cells with a longer life span, presumably cells of the monocyte lineage. Compartmentalization of viral DNA populations between CD4+ T cells and monocytes has been reported (88, 168, 329), and assuming monocytes have longer half-lives relative to activated CD4+ T cells, variants compartmentalized in these different cell types would be expected to exhibit different rates of decay during HAART (52, 113, 218, 303). However, the proportion of variants compartmentalized in productively infected monocytes may be too small to be detected in our assay (218, 219), and monocytes may not be productively infected and only produce virus upon differentiation and entry into tissue (243, 273). Furthermore, the decay characteristics of HIV-1 upon initiation of therapy that includes an integrase inhibitor suggest that much of the second phase of decay observed in conventional therapy represents cells that are slowly undergoing integration, and that the proportion of productively infected, long-lived cells is smaller than previously thought (196, 265). Another limitation of this study is that it depends on the assumption that compartmentalized subpopulations can be distinguished by their *env* genotypes, and in particular, genotypes that can be resolved by HTA. However, in addition to its

function in determining host cell tropism, the extreme genetic complexity of *env* within infected individuals makes it a highly sensitive target for the detection of co-existing viral subpopulations, and any other genomic region that may drive HIV-1 compartmentalization would likely be linked to distinct *env* variants as a result of founder effects, genetic isolation or compartment-specific evolution. Furthermore, any compartmentalized variants would have likely diverged enough to be resolved by HTA analysis (105). Thus, we can conservatively conclude that the lack of genetic compartmentalization and differential decay rates observed in this study applies to the bulk of the HIV-1 population in the peripheral blood that represents primarily the first phase of viral RNA decay during HAART.

Another potential opportunity for cellular compartmentalization is between naïve and memory CD4+ T cells. While naïve and memory T cells express similar levels of CXCR4, CCR5 is expressed only memory cells (19, 160, 204). Previous studies have found a wide range of preferential infection by, and potential compartmentalization of, X4 and R5 variants in these cell types, in a manner consistent with their coreceptor expression patterns (15, 207, 290). If X4 and R5 variants are compartmentalized in these two cell types to a significant degree, then similarity in decay rates would indicate that the life span of infected naïve and memory cells are similar when they become activated and produce virus. It is thought that the bulk of viral replication occurs in activated CD4+ memory T-cells (113, 176, 218, 275, 277, 326), in which case any potential compartmentalization of R5 and X4 variants observed in resting memory and naïve cells may represent only a small fraction of the total population. Also, activated and previously activated T

cells express both CCR5 and CXCR4 (19, 204, 208), providing a potential source of mixing of R5 and X4 variants. There is evidence to suggest that the pool of cells supporting the bulk of virus replication is not homogeneous in its susceptibility to infection by X4 and R5 variants (92) and that X4 and R5 variants may be differentially affected by antiretroviral therapy (92, 223). However, we found no difference in the decay rates of X4 and R5 variants upon initiation of therapy, and that the decay rates of these variants is within the range reported in other studies for the first phase of decay, presumably reflecting the life span of the activated memory cells supporting ~99% of the virus population (113, 176, 218, 219, 303). This finding is consistent with a model where virus is emerging from a homogeneous pool of cells that is sufficiently susceptible to infection by both X4 and R5 variants to account for most of the production of these variants found in the periphery. This is also further supported by the finding of a lack of genetic compartmentalization between X4 and R5 populations in both subjects 101 and 109, for regions outside of *env*, indicating some overlap of target-cell types. However, the lack of data indicating differential decay rates of variants does not allow a definitive conclusion to be drawn regarding the half-lives of infected cells in different cellular subsets until the degree of cellular compartmentalization of X4 and R5 variants can be more fully and directly accounted for in studies of this type.

The divergent X4 and R5 lineages indicate some degree of genetic compartmentalization between these variants. This could be due to physical isolation in different cell types or due to genetic linkage selected across *env* for the ability to use different coreceptors. However, we detected an overall lack of

compartmentalization and evidence of recombination between these populations in sequence regions increasingly distal 3' of V3, suggesting the potential for sequence mixing between R5 and X4 variants in a co-infected cell (Figure 2.6 and 2.7). This observation is consistent with previous reports which have identified X4/R5 recombinants both within *env* and between *env* and other regions of the genome (183, 257, 291). However, our use of the single genome amplification approach avoided the possibility of recombination during PCR, which may have created artificial recombinants in some previous studies. These data support the conclusion that while X4 and R5 variants may preferentially replicate in distinct cellular compartments, they are not genetically isolated and must with some frequency infect the same cell types. Still, the deep branch-points in the phylogenetic trees suggest the initial outgrowth of X4 variants is from a monoclonal genotype.

This study found little evidence for differential decay and compartmentalization of *env* variants comprising the bulk of the virus in the peripheral blood, even in the case of divergent coreceptor phenotypes, indicating that HAART is equally effective on all the detectible variants making up the bulk virus in the peripheral blood. However, new technologies are becoming available that will allow sampling to below 1% (186), and the application of these technologies may yet reveal minor populations that exhibit differential rates of decay upon initiation of therapy.

2.6 ACKNOWLEDGMENTS

This work was supported by NIH grant R37-AI44667 to R.S., an AmFAR award to P.H., NIH training grant support to W.I. (T32-GM07092), G.S. (T32-AI07001) M.P. (T32-AI07419), and P.H. (T32-CA09156), the UNC Center For AIDS Research (NIH award P30-AI50410) and the UNC General Clinical Research Center. We thank Dale Kempf from Abbott and the ACTG 359 study team for making samples available for this study.

TABLE 2.1. Subject characteristics and viral decay rates

Patient ID	HTA variant number		Starting VL LOG(10)	CD4 Count	LOG(10) viral load drop	$T_{1/2}$ (days) bulk	% least variant[C]	Max fold difference $T_{1/2}$[d]
	V3	V4/5						
101[a]	NA	2	4.5	201	1.9	2.30	19	1.09 (V4/5)
106	3	7	4.7	421	2.3	0.90[b]	5	1.14 (V3)
108	3	5	4.3	158	1.6	0.76	2	1.16 (V4/5)
109[a]	2	4	4.9	23	2.1	1.09	11	1.24 (V45)
4015	NA	2	5.1	na	1.4	2.14	9	1.73
4021	NA	9	5.0	na	1.0	1.20	2	2.0
4022	NA	4	4.6	na	1.9	2.09	3	1.58
5005	NA	4	5.3	na	1.5	2.27	2	1.60

[a]Subjects with mixed-tropic viral populations
[b]Calculated using the first and last time-points
[c]Percent relative abundance of the least abundant variant detected
[d]Largest fold difference in half-life between any two variants

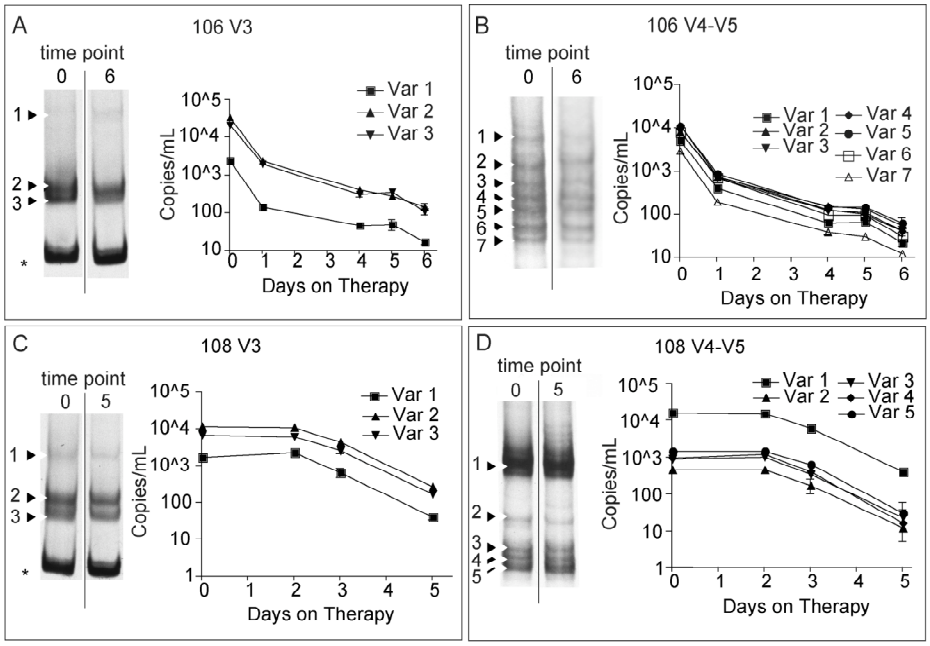

Figure 2.1. HTA and variant decay analysis of V3 and V4-V5 envelope regions for subjects 106 (a and b) and 108 (c and d). Left panels depict HTA gel lanes for the first and last time points. Numbered arrows designate reproducible HTA variants. Asterisks indicate single stranded probe bands. Right panels are plots of the viral loads for individual variants (Var) at each time point sampled. Error bars: standard deviation of 2 replicates. In subject 108 (c and d), a decline in viral load was not seen until after the second sampling time-point; therefore the decay rate was calculated from the second time-point in this subject.

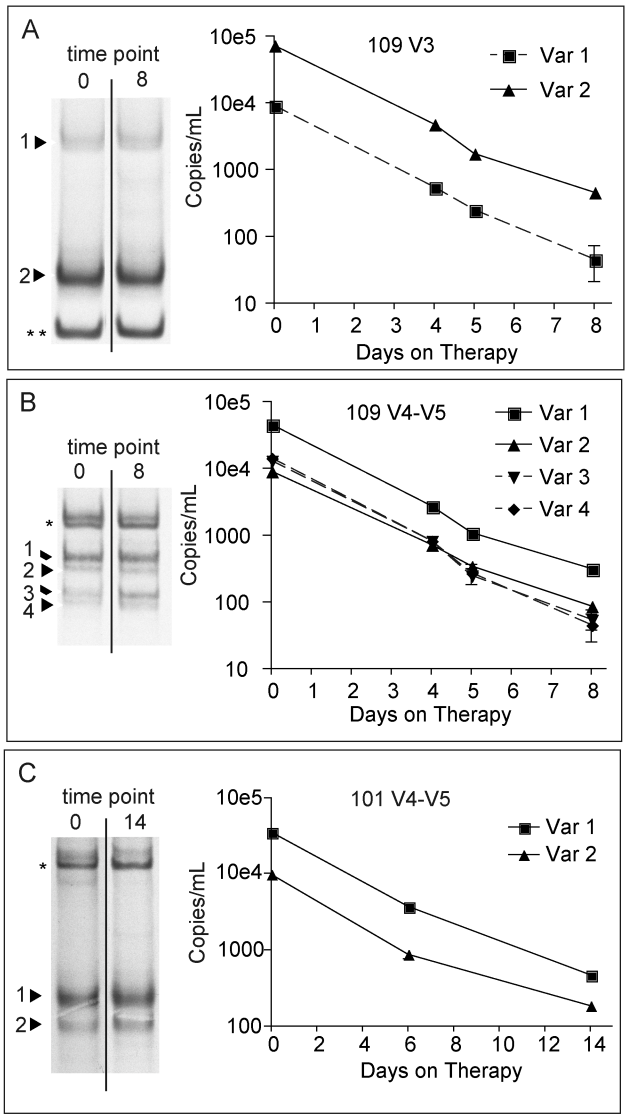

Figure 2.2. HTA variant decay analysis of V3 and V4-V5 envelope regions for subjects 109 (a and b) and 101 (c) (V4-V5 only). Left panels depict HTA gel lanes for the first and last time points. Numbered arrows designate reproducible HTA variants. Single and double asterisks indicate single stranded and double stranded probe bands. Right panels are plots of the viral loads for individual variants (Var) at each time-point sampled. Error bars: standard deviation of 2 replicates. Dashed lines indicate V3 and V4-V5 HTA variants linked to X4 usage.

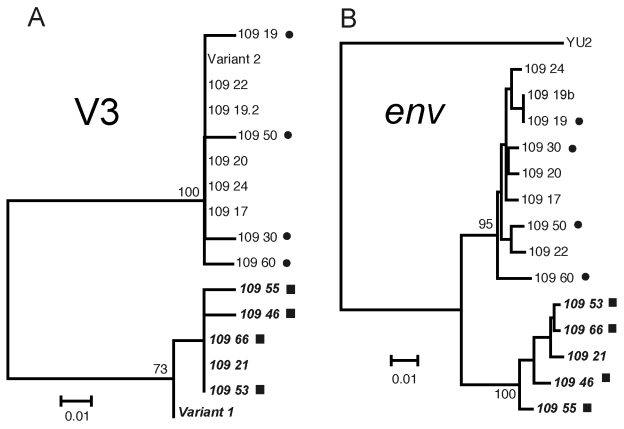

Figure 2.3. Maximum likelihood phylogenies of the V3 region (a) and full-length *env* (b) for subject 109. Node labels represent bootstrap values using 100 replicates. Italicized, bolded tip labels indicate *env* variants predicted to be X4 by PSSM. Circles indicate an entry assay R5 phenotype; squares indicate an entry assay X4 phenotype. The V3 tree (a) was rooted at the midpoint. The *env* tree (b) was rooted using the *env* sequence of the molecular clone YU2. V3 HTA variant sequences 1 and 2 correspond to variants in Figure 2.2a.

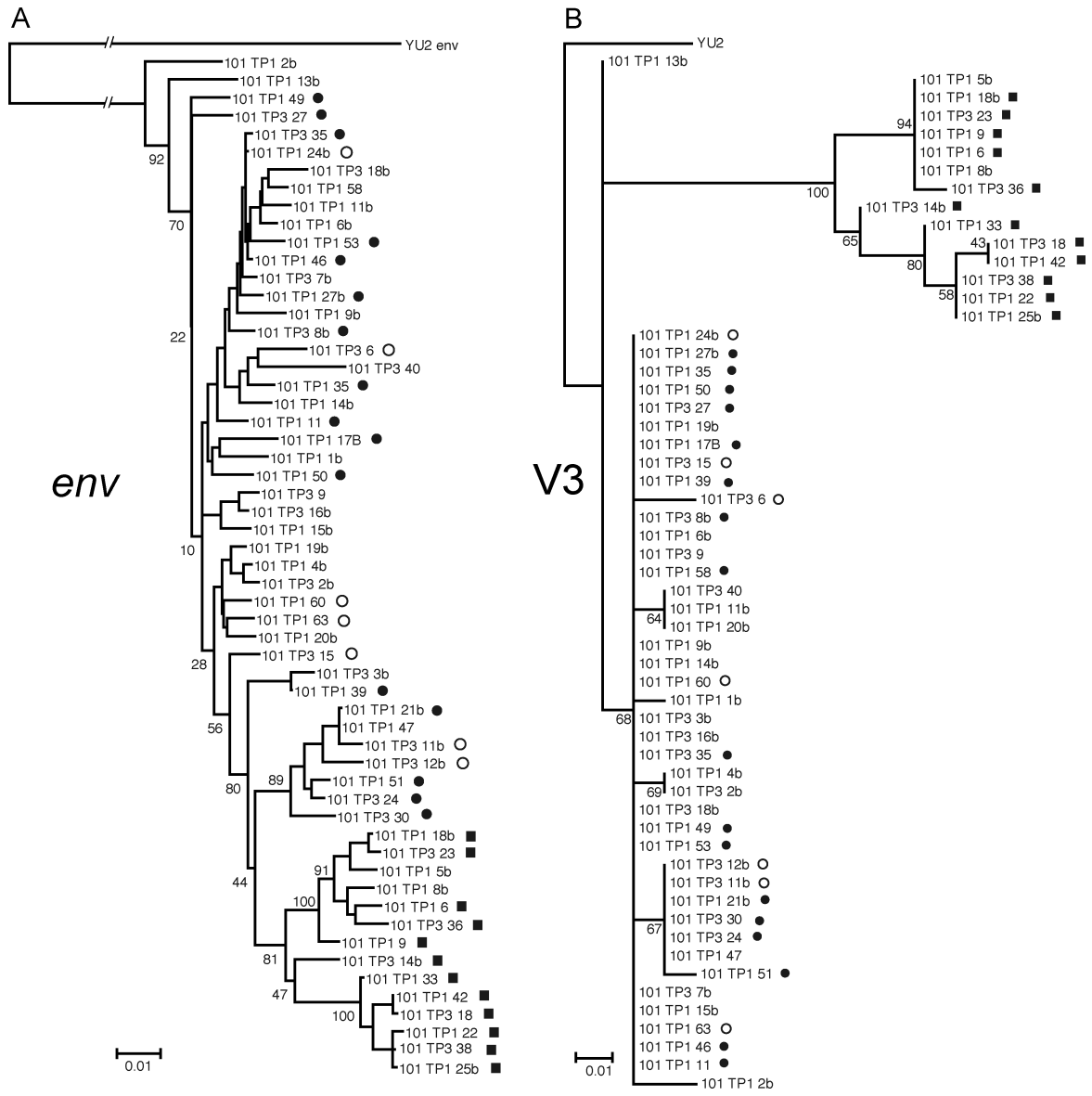

Figure 2.4. Maximum likelihood phylogenies of *env* (a) and V3 (b) sequences from the first and last time-points of subject 101. Node labels represent bootstrap values from 100 replicates. Trees were rooted using the molecular clone YU2. Closed circles indicate an entry assay R5 phenotype, squares indicate an entry assay X4 phenotype, and open circles indicate dual-tropic envelopes with weak X4 usage in an entry assay.

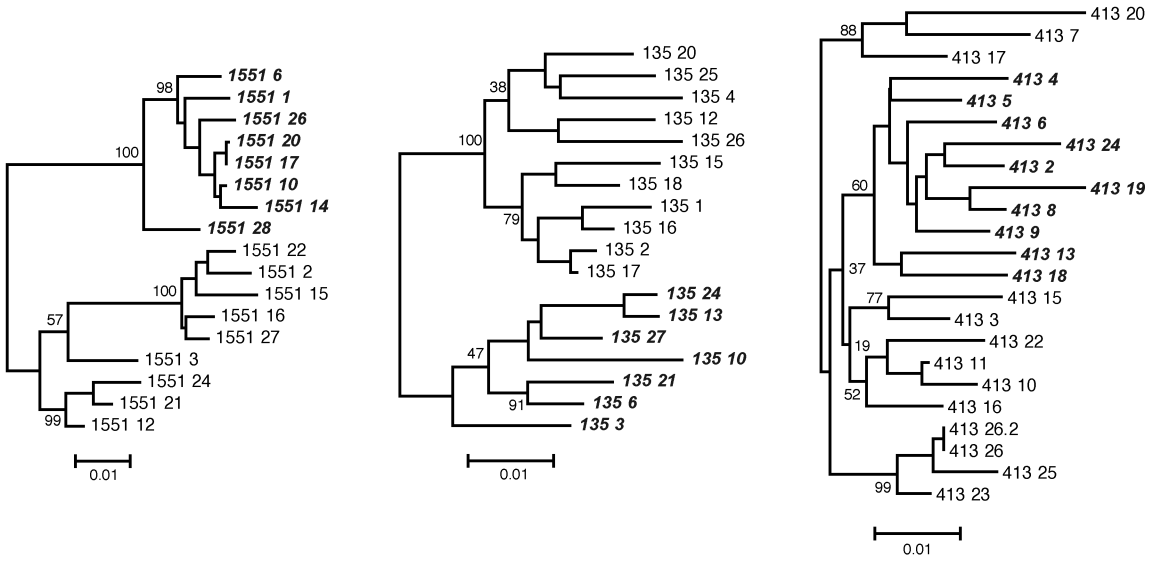

Figure 2.5. Maximum likelihood phylogenies of sequences encompassing *env,* (starting at V1), *nef* and U3 from three representative subjects with distinct X4/dual and R5 populations. Node labels represent bootstrap values from 100 replicates. Italicized, bolded tip labels indicate *env* variants predicted to be X4 by PSSM and confirmed in an entry assay.

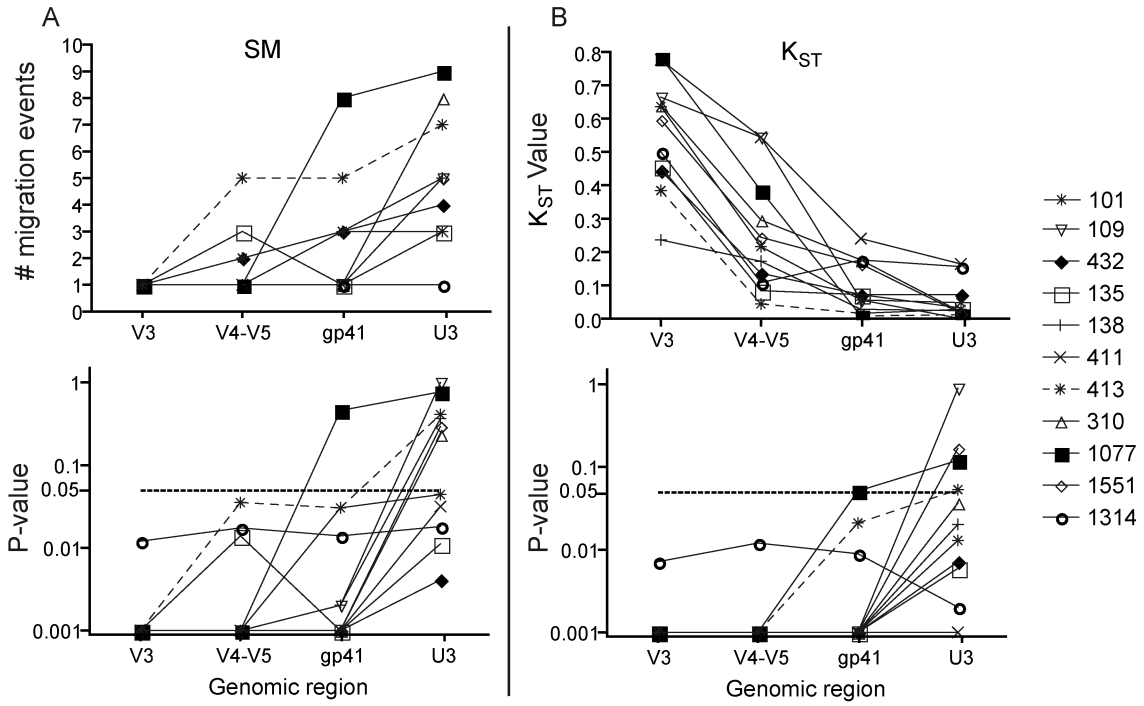

Figure 2.6. Analysis of compartmentalization of 4 genome regions between X4 and R5 variants. (a) Top panel: Slatkin-Maddison test branch migration events between X4 and R5 sequences; bottom panel: corresponding *P*-values for support of compartmentalization for each region as determined in the Slatkin-Maddison test. (b) Top panel: K_{ST}* values; bottom panel: corresponding P-values for support of compartmentalization between X4 and R5 variants for each genome region as determined by the K_{ST}* test. Dashed line indicates P=0.05.

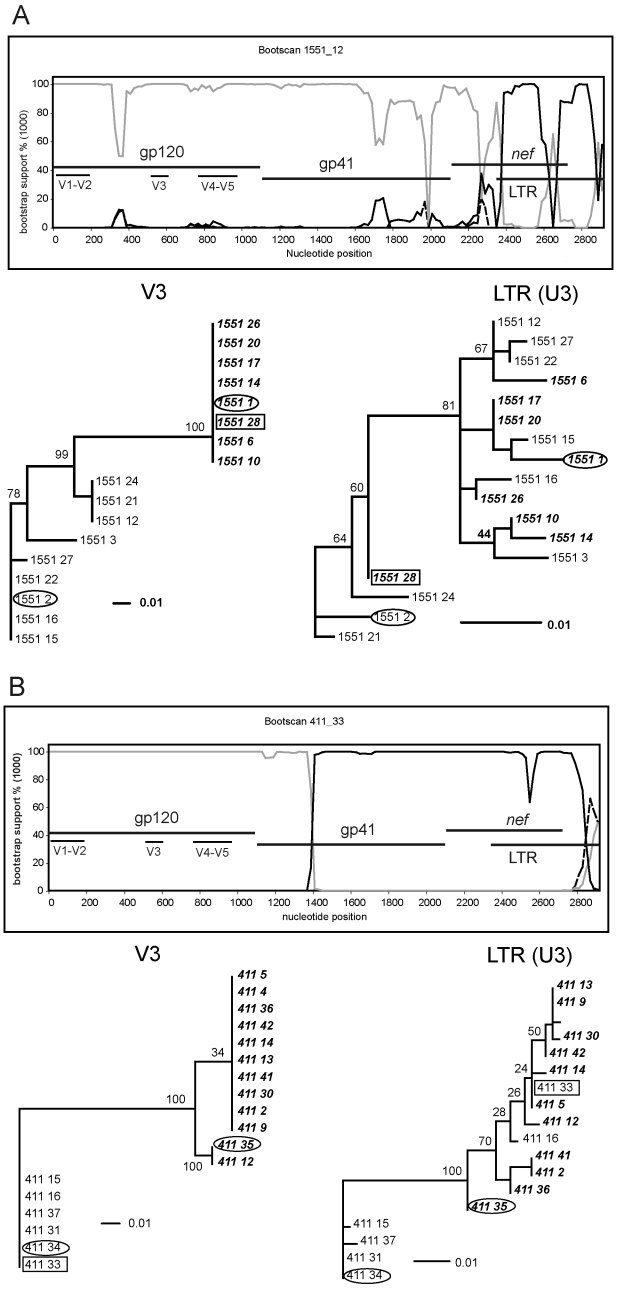

Figure 2.7. Representative examples of recombination between X4 and R5 variants in subjects 1551 (A) and 411 (B) Top panels: bootscanning plots identifying recombination break points. The horizontal axis indicates the nucleotide position in the putative recombinant (query sequence) and in the genomic regions mapped within the plot. The vertical axis is the % bootstrap support (1000 replicates) for clustering of the query sequence with either the R5 (grey) or X4 (black) putative parental sequences. Bottom: Maximum likelihood trees of V3 (left) and U3 (right) regions indicated in the bootscan plots. X4 variants are italicized and bolded. Recombinants are boxed and putative parents are circled

Chapter 3

Evolution of the HIV-1 *env* Gene in the Rag2$^{-/-}$γc$^{-/-}$ Humanized Mouse Model

The following material was published as a manuscript in the *Journal of Virology* under the following citation:

William L. Ince, Liguo Zhang, Qi Jiang, Kathryn Arrildt, Lishan Su and Ronald Swanstrom. 2010. **Evolution of the HIV-1 *env* Gene in the Rag2$^{-/-}$γc$^{-/-}$ Humanized Mouse Model.** J. Virol. 84(6):2740:52.

3.1 ABSTRACT

Rag2$^{-/-}$γ$_C^{-/-}$ mice transplanted with human hematopoietic stem cells (DKO-hu-HSC) mimic aspects of human infection with human immunodeficiency virus type 1 (HIV-1) including sustained viral replication and CD4$^+$ T cell decline. However, the extent of HIV-1 evolution in a long-term infection in these humanized mice, a key feature of the natural infection, has not been fully assessed. In this study, we examined the type of genotypic and phenotypic changes in the viral *env* gene that occur in the viral populations of DKO-hu-HSC mice infected with the CCR5-tropic isolate HIV-1$_{JRCSF}$ for up to 44 weeks. The mean rate of divergence of viral populations in mice was similar to that observed in a cohort of humans during a similar period of infection. Many amino acid substitutions were common across mice, including losses of N-linked glycosylation sites and substitutions in the CD4 binding site and in CD4-induced epitopes, indicating common selective pressures between mice. In addition, *env* variants evolved sensitivity to antibodies directed at V3, suggesting a more open conformation for Env. This phenotypic change was associated with increased CD4 binding efficiency and was attributed to specific amino acid substitutions. In one mouse, *env* variants emerged that exhibited a CXCR4-tropic phenotype. These sequences were compartmentalized in the mesenteric lymph node. In summary, viral populations in these mice exhibited a dynamic behavior that included sequence evolution, compartmentalization, and the appearance of distinct phenotypic changes. Thus, humanized mice offer a useful model for studying evolutionary processes of HIV-1 in a complex host environment.

3.2 INTRODUCTION

Animal models of HIV-1 infection are important tools for understanding transmission, replication, and pathogenesis, as well as therapeutic intervention, of HIV-1 infection. Non-human primates, such as Rhesus macaques infected with Simian or chimeric Simian/Human Immunodeficiency Viruses (SIV or SHIV), represent well-characterized and highly relevant models; however, key limitations include expense, genetic variability of the host animals, and the fact that SIV, while closely related, is distinct from HIV-1. Therefore, small animal models that support HIV-1 infection and recapitulate many aspects of the human infection have been sought using several approaches.

Recent approaches have involved the use of genetically immunodeficient mice that have been reconstituted using human-derived hematopoietic stem cells (HSC) (known as humanized mice). Several models have been developed based on this approach, including the Rag2$^{-/-}$$\gamma_C^{-/-}$ (DKO) and NOD/SCID/$\gamma_C^{-/-}$ (NOG or NSG) mice transplanted with human HSC (NOG-hu-HSC or DKO-hu-HSC) (128, 285) as well as the NOD/SCID mouse with transplanted human fetal thymus and liver tissue in addition to HSC (181). These models all support HIV-1 infection (3, 7, 11, 94, 279, 301, 323) (for a review of these models see Denton *et al*. (63)). The DKO-hu-HSC mouse lacks both recombination activating gene 2 (Rag2) and the cytokine receptor common gamma chain (γc) and as a result does not generate murine T, B and natural killer (NK) cells, but supports engraftment of HSCs and differentiation of human myeloid and lymphoid lineages. Immune reconstitution in this model likely involves education of human T cells in the mouse thymus, and dissemination of

differentiated human lymphoid subsets into the peripheral blood and to multiple lymphoid tissues including lymph nodes, spleen and bone marrow (285). The DKO-hu-HSC mouse along with the other humanized mouse models has been used in studies of transmission (10, 62), pathogenesis (131) and viral inhibition (43, 62, 154, 280, 288).

One important feature of HIV-1 infection is the diversification and evolution of the viral genome over the course of infection. Diversification occurs most prominently in the envelope (*env)* gene, which encodes the viral surface glycoprotein (Env). Env mediates viral entry into cells through attachment to the primary receptor CD4, which primes Env for engagement with a co-receptor, either CCR5 or CXCR4, triggering virion fusion with the cellular plasma membrane (155). HIV-1 infection is typically established by one or a few CCR5-tropic (R5) variants that give rise to an initially homogenous viral population, which then diversifies over the course of chronic infection (134, 267). Diversification of Env results from immune selective pressures (87), isolation in or adaptation to different cellular and anatomical compartments (59, 88, 104, 136, 148), and selection for altered CD4 affinity (226, 283, 300) and co-receptor tropism (81, 126). In many cases, during late stage infection, variants emerge from the R5 virus population that are CXCR4-tropic (X4), an event that is often associated with accelerated CD4 T cell loss and progression to AIDS (15, 48, 282). In an effort to determine if any of these aspects of HIV-1 evolution are exhibited in the humanized mouse model, we examined the extent of HIV-1 diversification and the types of evolutionary changes that occur in *env* in mice infected with a CCR5-tropic HIV-1 for up to 44 weeks.

Sampling of viral *env* variants from the peripheral blood plasma over the course of the infection revealed increasing diversity and divergence of the viral population at rates similar to those observed in natural infection. Mutations were identified that affected Env conformation and sensitivity to neutralizing antibodies, CXCR4 co-receptor use, and potential N-linked glycosylation sites. Other mutations potentially affecting the Env phenotype were identified in CD4 binding sites and CD4-induced epitopes. The patterns of substitutions indicated that certain sites were under selection, particularly in cases where the same substitution was identified in multiple mice.

This study demonstrates the potential for studying HIV-1 evolution in the DKO-hu-HSC model and also gives insight into the types of selective pressures driving HIV-1 *env* evolution in this host environment. These findings, while highlighting some of the limitations of this model, will help inform its appropriate use for studying different aspects of HIV-1 infection, such as the evolutionary constraints placed on HIV-1 during natural infection and in the face of pharmacological and immunological inhibition.

3.3 MATERIALS AND METHODS

3.3.1 Model generation.

Rag2$^{-/-}$$\gamma_C^{-/-}$ immunodeficient newborn mice were injected intrahepatically with human CD34$^+$ hematopoietic stem cells. Two separate CD34$^+$ cell donors were used to reconstitute mice 5-8, and mice 64 and 67, respectively (A and B in Table 1). After 8-12 weeks, immune system reconstitution was confirmed. HIV-1$_{JRCSF}$ (GenBank accession number: M38429.1) virus was generated by transfection of 293T cells with an infectious clone expression plasmid, pYK-JRCSF (150), obtained from the National Institutes of Health AIDS Research and Reference Reagent Program (ARRRP). Cell-free supernatant was used to intravenously infect reconstituted mice. Five mice from cohort A (4-8) and 4 mice from cohort B (63-67) were infected. Mice were analyzed from each cohort that were successfully engrafted, successfully infected and which were kept alive with active infection for at least 22 weeks. Viral load was monitored for 44 weeks in mice 5-8, and 22 weeks for mice 64 and 67.

As part of an additional study investigating the role of CD4$^+$CD25$^+$Foxp3$^+$ T regulatory cells (Treg cells) in HIV-1 infection, mice numbered 6-8 were treated at 43 weeks post-infection with denileukin diftitox (DAB$_{389}$IL-2, denileukin diftitox, or Ontak), which selectively depletes Tregs (131, 161). Tregs account for between 1-4% of all CD4$^+$ T cells in this model and Ontak treatment usually results in selective depletion of Tregs by as much as 90% (131). Treatment with Ontak correlated with increased immune activation as measured by CD38 expression, and Ontak-treated mice also exhibited a greater percentage of infected cells and greater CD4$^+$ T cell depletion. Ontak treatment may have increased viral replication perhaps as an effect

of global enhancement of $CD4^+$ T cell activation. While there were unique evolutionary events observed in individual mice, there was no clear distinction in the patterns of viral evolution between treated and untreated animals.

3.3.2 Sample collection.

Mice were monitored for peripheral blood viral load and CD4/CD8 ratios for up to 44 weeks. Peripheral blood samples were collected (~30 ul) at 3, 10, 22, 40, and 44 weeks post infection. Mice were sacrificed and tissue was harvested at 22 weeks (64 and 67) and 44 weeks (5-8) post infection.

3.3.3 Nucleic acid extraction.

Viral RNA was extracted from the available volume of blood plasma (~30 ul) using the QiaAmp Viral RNA kit (Qiagen, Valencia, CA), eluted in 60 ul diH_2O. Total DNA was extracted from tissue using the PicoPure DNA Extraction kit (Molecular Devices, Sunnyvale, CA). Pelleted cells extracted from collagenase-treated tissue (about 10^5–10^6 cells) were resuspended in 50 ul of PicoPure buffer containing Proteinase K. The extraction suspension was incubated at 65°C for 8 hours and used directly in PCR reactions as described below.

3.3.4 Viral RNA and DNA amplification and sequencing.

The 60 ul RNA eluate was reverse transcribed using the Superscript III Reverse Transcriptase (RT) System (Invitrogen, Carlsbad, CA) and an oligo dT primer. A region of the HIV-1 genome encompassing *env* through 3' U3 was amplified from cDNA using a limiting dilution PCR approach (single genome amplification - SGA) initially described by Simmonds *et al*. (271) and Edmonson and Mullins (76), then modified by Palmer *et al*. (212) and Salazar-Gonzalez *et al*. (255).

Primers and thermocycling procedures for amplification and sequencing were used as previously described in Keele *et al*. (134), but modified by replacing the downstream *env* amplification primer set with a primer that captures the U3, the sequence of which is 5'-AAGCACTCAAGGCAAGCTTTATTG-3'. The same procedure used for amplifying cDNA was used to amplify the envelope gene from viral DNA extracted from tissue samples. Automated sequencing followed by manual editing of sequences was carried out on SGA amplicons using the Big Dye Terminator system (Applied Biosystems, Foster City, CA). GenBank accession numbers for sequences generated in this study are: GQ412353-GQ412705.

3.3.5 HIV-1 sequencing data from human infections.

Sequences were from Shankarappa *et al.* 1999 (267) and Salazar-Gonzales *et al.* 2009 (256).

3.3.6 Sequence analysis.

Subtype B sequences used for assessment of sequence conservation at specific sites were accessed through the Los Alamos National Laboratories HIV Sequence Database (http://www.hiv.lanl.gov). Sequence alignments were generated using MAFFT (Multiple Alignment using Fast Fourier Transform) (133). The best fitting substitution rate model for each alignment was determined using FindModel, a variation of Modeltest (232), implemented through http://www.hiv.lanl.gov/content/sequence/findmodel/findmodel.html. Maximum likelihood phylogenies were generated in PhyML using the best fitting model (GTR or HKY85 in this study), 4 rates substitution categories and the PhyML-determined gamma shape parameter and number of invariant sites. Potential N-linked

glycosylation (PNLG) sites were identified using N-Glycosite (325) implemented through http://www.hiv.lanl.gov/content/sequence/GLYCOSITE/glycosite.html. Divergence was determined as the mean genetic distance of sequences at a given time point to the founder sequence. In the case of mouse viral populations, the founder sequence was that of HIV-1_{JRCSF}, and in the case of human viral populations, the "founder" sequence was taken to be the consensus of sequences sampled at a time 2-5 months post-seroconversion for the Shankarappa *et al.* 1999 sequence set, and an estimated 20-24 days post infection for the Salazar-Gonzales *et al.* 2009 sequence set. Distances were determined from ML tree branch lengths using Branchlength implemented through http://www.hiv.lanl.gov/content/sequence/BRANCHLENGTH/branchlength.html.

Selection analysis was carried out by determining the rates of synonymous and non-synonymous substitutions (200, 210). Rates were determined using SNAP (145) as implemented through: http://www.hiv.lanl.gov/content/sequence/SNAP/SNAP.html. A Wilcoxon signed rank test was used to compare rates of synonymous and non-synonymous base substitutions within mouse populations.

Linkage disequilibrium analysis was performed using DNAsp v5 (166). A Fisher's exact test was used to determine the significance of non-synonymous nucleotide substitution associations.

3.3.7 Env phenotype assays.

env gene expression vectors were generated from selected amplicons using the pcDNA3.1 Directional TOPO Expression kit (Invitrogen, Carlsbad, CA). 293T

cells were co-transfected with *env* expression vectors and the pNL4-3.Luc.R-E-luciferase reporter vector (108) (obtained from ARRRP) using the Fugene transfection reagent (Roche, Mannheim, Germany) according to the manufacturer's protocol to generate pseudovirus. Cells were washed with phosphate buffered saline 8-12 hours after transfection in order to reduce transfection complex carry-over and background luciferase expression in target cells, which was monitored with an Env-negative control. Virus supernatant was collected 48 hours after transfection. Co-receptor phenotype was determined based on detection of luciferase activity in U87.CD4$^+$ cells expressing either CCR5 or CXCR4 (14) (obtained from ARRRP) using the Luciferase Assay System kit (Promega, Madison, WI). Pseudovirus was incubated with U87.CD4.CXCR4/CCR5 cells for 36-48 hours prior to lysis of cells and measurement of luciferase activity. Co-receptor-dependent viral entry was confirmed using inhibitory concentrations of AMD3100 (112) (CXCR4 inhibitor) or TAK-779 (6) (CCR5 inhibitor) (both obtained from ARRRP). Sensitivity to neutralization by the anti-V3 antibodies 447-52D (46) (ARRRP) and 19b (20) (a gift from Dr. James E. Robinson) was assessed on TZM-BL cells (obtained from ARRRP), which are permissive to X4 and R5 viruses and contain an integrated, Tat-responsive luciferase cassette (226). Sensitivity to the anti-CD4 antibody Leu3a (CD4 Pure) (BD Biosciences, San Jose, CA) was assessed on U87.CD4.CCR5 cells.

Viral fusion kinetics were measured on U87.CD4.CCR5 cells in a 96-well format in triplicate. Pseudotyped virus supernatant and cells were cooled to 4°C and spinoculated for 2 hours at this temperature to synchronize entry. Immediately after

spinoculation, the medium was removed from cells and replaced with medium pre-warmed to 37°C. The fusion inhibitor T20 (obtained from ARRRP) was added at the inhibitory concentration of 200 nM at time 0 to the first well and at 5 minute intervals to successive wells for up to 70 minutes. Time to one-half maximal entry was used to compare viruses.

3.4 RESULTS

3.4.1 Diversification and divergence of HIV-1_{JRCSF} over the course of infection in a mouse model with sustained viral infection.

Six DKO-hu-HSC mice with stable human leukocyte reconstitution were infected intravenously with HIV-1_{JRCSF}, a CCR5-tropic isolate of HIV-1 generated from an infectious molecular clone. Viral infection persisted in all mice over the period of observation: 44 weeks for mice 5, 6, 7 and 8, and 22 weeks for mice 64 and 67 which received HSCs from a different donor (Table 1).The viral RNA load in the blood exhibited a slow decay of about 1 $\log_{10}$ over the course of 44 weeks in mice 5-8 (Figure 1), consistent with other reports using this model and different HIV-1 isolates (7), although the reason for this drop is not known. A relative decline in CD4 T cells was also observed (Table 1).

Given that these mice were able to support infection for 22- 44 weeks, we wanted to know if, and to what extent, the viral population had diversified, as is observed in human infections over a similar period of time. Viral RNA was extracted from the peripheral blood plasma and subjected to single genome amplification (SGA) for the entire *env* gene, a limiting dilution RT-PCR technique designed to facilitate direct sampling of viral genomes and to avoid PCR-generated mutations and recombination. Sequence diversification and divergence of HIV-1_{JRCSF} in the peripheral blood was assessed for a region of *env* that encodes variable loops 1 (V1) though 5 (V5) of gp120 and at multiple time points: weeks 10, 40 and 44 post infection for mice 5 and 6; weeks 3, 40 and 44 for mouse 8; and weeks 4 and 22 for

mice 64 and 67. The median number of sequences sampled from each time point was 16.5 and ranged between 11 and 39.

A maximum likelihood phylogeny of sequences from the last time points (week 22 for mice 64 and 67 and week 44 for mice 5-8) from each mouse is presented in Figure 2. Sequences were generally clustered by mouse, indicating distinct evolutionary paths that could distinguish mouse viral populations.

For a region of *env* encompassing C2-V5, the rate of divergence from the founder virus in the mice was compared to that observed in two datasets from infected humans initially sampled either prior to seroconversion and at time points 3-19 months later (Salazar-Gonzales *et al*. 2009) (256) or after seroconversion and at time points 9-24 months later (Shankarappa *et al*. 1999) (267). In the former study, viral populations from three subjects were initially sampled prior to seroconversion at an estimated 20-24 days post infection and 9-16 days prior to seroconversion. In the latter study, viral populations from 7 subjects were initially sampled within 2-5 months after seroconversion. In both datasets, the viral populations at the first time points sampled were relatively homogeneous, and these populations were compared to those present in the later time points. Divergence was determined as the mean distance (branch length) of sequences in a population at a given time-point from the "founder" virus sequence, which was either the consensus of sequences sampled at the first time point in the human infections, or HIV-1_{JRCSF} (accession number M38429.1) for the mouse infections. The rate of divergence was calculated by using the mean divergence from the founder of a population at the last time point measured divided by the time post infection. The mean rate of divergence in mice

and in the post-seroconversion human data sets was 0.0175%/week (range=0.034-0.0043%/week) and 0.018%/week (range=0.007-0.030%/week), respectively, which were statistically indistinguishable (P=0.96) (Figure 3A). The mean rate of divergence in the pre-to-post-seroconversion dataset was also similar (0.015%/week range=0.004-0.026%/week, P=0.706) although slightly lower than that observed in mice. The mean diversity (Figure 3B) in viral populations in humans, extrapolated to 44 weeks, was greater than, but still not statistically different from, that observed in mice (P=1 for the comparison to the pre-to-post-seroconversion human dataset and P=0.5338 for the comparison to the post-seroconversion dataset). The rates of divergence and diversification of HIV-1 in mice fell within the distribution of the rates measured in the two different human cohorts sampled starting at different points around the time of seroconversion. These similarities are in spite of the likely absence of an HIV-1-specific antibody response in the mouse, which is low to undetectable in this model throughout infection, a selective pressure that plays a major role in Env divergence and diversification in human infection, post-seroconversion (87). In this regard, Western blot analyses of plasma from the mice used in this study, taken early and late after infection, were uniformly negative for reactivity to HIV-1 antigens (data not shown). We conclude that there is no major difference in the evolutionary rate of HIV-1 within *env* in this mouse model over the first 44 weeks from the time of infection compared to an analogous early stage of human infection, although the selective pressures in these two settings likely differ (see below).

3.4.2 Features of *env* sequence evolution in mice.

We next wanted to examine the types and patterns of nucleotide substitutions that contribute to diversity. One distinctive mechanism that may contribute to sequence diversity during natural infection is the activity of the anti-viral factor APOBEC3G (A3G) (130), which, in spite of the A3G antagonist activity of the viral Vif protein, can give rise to disproportionate numbers of G-to-A transitions in the plus strand sequence in natural infection, indicating hypermutation of the nascent minus strand DNA by A3G (172, 248, 322). Examining *env* sequences from mice revealed a subset (1-4%) of hypermutated sequences exhibiting a disproportionate number of G-to-A transitions in A3G target motifs in each mouse, indicating that this mechanism is at work in this model. This observation also suggests that A3G may be contributing some proportion of G-A transitions observed at A3G recognition sites in sequences that were not overtly hypermutated.

A key feature of this model is the isogenicity of the hosts, when reconstituted with the same donor. We were interested to see if any common amino acid substitution patterns had emerged in different mice. Common amino acid substitutions represented in viral populations of multiple mice likely represent selected changes rather than mutations that have grown out due to genetic drift, as might be the case for substitutions represented in only one mouse.

Substitutions that grew out (i.e. were seen in more than one sequence either within or between mice) in each mouse viral population are depicted in Figure 4 and are categorized by their potential functional effects, along with the number of mice in which they were detected. Within a 380 amino acid long region encompassing V1

through V5 and much of the conserved region 5 (C5), substitutions at a total of 45 positions grew out. These mutations were concentrated in the variable loop regions compared to the constant regions of Env (p=0.0001, Fisher's exact test). However, no insertions or deletions were observed. Of the substitutions that grew out in mouse viral populations, 19 were detected in more than one mouse, and each of the four substitutions that were detected in three or more mice (D167N, N386K/S, N411D/S, and E482K) were represented in both donor sets (Figure 4).

Evidence of positive selection can also be obtained by determining the ratio of non-synonymous and synonymous base substitution rates (dN/dS). Ratios greater than or less than 1 indicate positive or negative selection, respectively. For the *env* region encompassing V1-C5, the dN/dS ratio was greater than 1 for viral populations in mice 6 (1.48) and 8 (1.32), which also showed the highest levels of divergence (Figure 3), nearly 1 in mouse 67 (1.03) and less than 1 in mice 5 (0.79), 7 (0.82), and 64 (0.57), although the differences between rates of synonymous and non-synonymous mutations were only significant in mice 6 (P=0.0126, dN/dS=1.48) and 64 (P=0.0001, dN/dS=0.57). We interpret these results with caution, because this analysis is limited in its sensitivity when there are too few substitutions to provide statistical power or when only a few sites are under positive selection, which is often the case in Env early in infection.

3.4.3 Substitutions identified at multiple potential N-linked glycosylation sites.

Glycosylation of Env at numerous sites has been shown to play a role in proper protein folding, receptor and coreceptor engagement (165, 229), and in escape from neutralizing antibodies (40, 141, 302). We identified one substitution,

S142N in mouse 6, that added a potential N-linked glycosylation (PNLG) sequon [$NX_1(S/T)X_2$, where X represents any amino acid other than proline (91)] in V1 and adjacent to a preexisting PNGS in HIV-1_{JRCSF}, which remained intact (Figure 4). In contrast, substitutions that disrupted PNLG sequons were observed at 7 positions and included (mean frequencies indicated in parentheses) N160K (8%), N187D (36%), N230S (43%), N241D (5%), N339K/D (8%), N386K/S (86%), N411D/S (40%) and T413I (36%) (Figure 4). All substitutions, except N160K and N241D, were detected by week 10. Substitutions N339K/D, N386K/S, N411D/S and T413I were identified in more than one mouse suggesting that loss of glycosylation at these sites was under some level of selection, although the low frequency of the N339K/D substitution at no more than 12% suggests that selection at this site was weak. The substitutions N386K/S, which rose to the highest frequency in the 3 mice in which it was detected (mean 86%), and N339K/D are located in V4 and C3 regions, respectively, and are part of the neutralizing antibody 2G12 epitope. Loss of these PNLG sites individually and in combination has been shown to confer resistance to this antibody (173, 287). The PNLG sequon composed of N411 and T413, located in V4, has been shown to co-vary with a number of other PNLG sequons and likely plays a role in the glycosylation of Env as a means of antibody escape (231, 302). The net loss of PNLG sites was widely distributed across Env, indicating that the heavy glycosylation of Env observed in natural infection may not be required for viral persistence in this model and may reflect the lack of a strong humoral immune response. Conversely, maintenance of these glycosylation sites likely has a fitness cost for replication.

3.4.4 HIV-1$_{JRCSF}$ evolves to become sensitive to specific anti-V3 antibodies.

Previous studies using the DKO-hu-HSC model have found the humoral immune response to HIV-1 to be weak (7) or undetectable (3, 94, 323), and we did not detect any HIV-specific antibodies in the mice in this study. Primary isolates of HIV-1 passaged in cell culture, in the absence of neutralizing antibody pressure, evolve to become sensitive to a spectrum of heterologous neutralizing antibodies (9, 192, 312). The antibody 447-52D is specific for a conserved epitope at the tip of the Env V3 loop and neutralizes viral isolates that are known to have a history of cell-culture passage, while primary isolates can encode the epitope but remain largely resistant (13, 46, 264). Sensitivity of cell-culture passaged virus to this and other V3 antibodies, such as 19b, is attributed to a loss of the Env conformation that masks the V3 epitope (180, 313). We were therefore interested in assessing the extent to which HIV-1$_{JRCSF}$, which encodes these V3 epitopes but is resistant to 447-52D, had evolved sensitivity to this antibody. *env* clones that included a broad spectrum of substitutions were generated from the amplicons from 5 mouse populations at the last time point (week 44 for mice 5-8 and week 22 for mouse 64). Screening of the *env* clones generated from these mice for expression of an Env protein with sensitivity to 447-52D (as tested in a pseudovirus assay) revealed a subset of clones in 4 of the 5 mice that encoded Env proteins that were neutralization sensitive compared to the input virus Env (Figure 5A). Two mutually exclusive mutations near the base of the V2 loop appeared to be linked to neutralization sensitivity, N165R/K and D167N, as one or the other was present in all neutralization sensitive Envs and

absent in those that remained resistant (Figure 5A and B). These mutations were detected early in infection. D167N was detected at week 10 in mice 5 and 6 and both N165K/R and D167N were present in mice 5 and 6 at week 44. Mice 8 and 64 exhibited only D167N, which was detected in these mice at 22 and 44 weeks post-infection, respectively. The frequency of these mutations in a population was on average 36% and 52% for N165R/K and D167N, respectively. Neither mutation was detected in mouse 7 or 67. When these mutations were reintroduced into the HIV-1_{JRCSF} *env* individually, they rendered the virus relatively neutralization sensitive (Figure 5C). We also tested these mutants, along with several of the 447-52D-sensitive clones, for sensitivity to another V3-specific antibody, 19b, and obtained similar results (data not shown). The frequency with which these substitutions were detected suggests that viruses replicating in these mice, as with virus passaged in cell culture, were not under strong selection by HIV-1-specific antibodies, and that these mutations may otherwise confer a selective advantage for an Env function possibly involving increased CD4 binding affinity, CD4 independence, or more rapid fusion (118, 143, 188, 193, 235).

In order to determine if increased neutralization sensitivity was linked to CD4 binding affinity, clones were selected that represented a range of sensitivities to the anti-V3 antibody, from relatively resistant to highly sensitive. Sensitivity to competitive inhibition by an anti-CD4 antibody, Leu3a, was used to evaluate CD4 binding efficiency. Table 2 shows the relative sensitivities of viruses pseudotyped with selected Env proteins to inhibition of entry by Leu3a. Env proteins that were highly sensitive to the anti-V3 antibody, those derived from mouse 6, showed a small

but significant decrease in sensitivity to Leu3a, while the JRCSF mutants I165K and D167N, which exhibited intermediate sensitivities to the anti-V3 antibody, exhibited only a marginal decrease in Leu3a sensitivity. This indicates that these Env proteins have enhanced CD4 binding. When viral fusion kinetics were measured in a time-of-addition experiment using T20, we failed to measure an increase in the rate of entry for any of these clones (data not shown). Although the mutations at positions 165 and 167 conferred only a slight increase in CD4 binding affinity, indicating that other mutations are likely involved in conferring a stronger phenotype, they are linked to anti-V3 antibody sensitivity and likely contribute to a more open Env conformation that potentiates CD4 binding and an increase in replication capacity. This is consistent with the observation that Envs with these mutations become fixed in multiple mouse viral populations.

When linkage analysis was performed, two sets of mutations were found to be in high linkage disequilibrium with each other in multiple mouse viral populations. Substitutions at positions 165 and 167 exhibited mutual exclusivity in the two mice in which both substitutions were present (mice 5 and 6), and each was linked to a different position in the same PNLG sequon occupying position 411-413. In mouse 6 substitutions at position 165 and 167 were linked to PNLG site-disrupting substitutions at position 413 and 411, respectively ($p<0.0001$ for both). In mouse 5, changes at position 165 and 413 were also strongly linked ($p<0.001$) although linkage between 167 and 411 was weak. In two other mice (mice 8 and 64) only substitutions at positions 167 and 411 were present, and in mouse 8, were largely coincident in the subset of genomes where they appeared ($p<0.01$). In mouse 64,

while a substitution at position 167 appeared in 30% of genomes, changes at position 411 appeared in all genomes. Weak linkage between positions in V3 and either position in the 411 sequon were also observed in mice 6 and 8. In summary, the substitutions at positions 165 and 167, themselves implicated in alterations of envelope structure, showed linkage to mutations that disrupted the same distant PNLG site, but the linkage was to different positions within the PNLG sequon. It seems likely that the specific amino acid that removes the carbohydrate attachment at position 411 has a context-dependent effect based on the substitution at position 165 or 167.

3.4.5 Evolution of co-receptor usage.

HIV-1 infection is primarily established by variants that utilize CCR5 as their co-receptor for entry into target cells (R5 viruses), but in about half of subtype B chronic infections, viral variants emerge that can use CXCR4 as their co-receptor (termed X4 viruses) (49, 144). The sequence of the V3 loop is a strong genetic determinant of, and can be used to predict, HIV-1 co-receptor phenotype (81, 129, 202). Because HIV-1_{JRCSF} utilized CCR5 exclusively, we were interested in determining if this virus had evolved to use CXCR4 in any of these animals. Six of 39 (15%) sequences from mouse 6 exhibited an X4-associated genotype with amino acid substitutions S11G and E25K in V3 (Figure 6B), sites at which variability is linked to co-receptor switching (184). In addition, nearly all V3 sequences from mouse 6 (92%) also had a S5N substitution, which represented a reversion to the subtype B consensus (Figure 6B). A serine at this position has been linked to CCR5 usage (184), indicating that this reversion may be linked to evolution of an X4

phenotype. These and additional selected clones from mice 5-8 were tested for their ability to enter indicator cell lines expressing CD4 and either CXCR4 or CCR5. Consistent with their sequence prediction, the clones from mouse 6 that exhibited the genetic features of X4 usage were able to infect a $CD4^+/CXCR4^+$ indicator cell line and were therefore classified has having an X4 phenotype (Figure 6A and B). Re-introduction of the X4-associated V3 sequence into the original HIV-1_{JRCSF} *env* was sufficient to confer CXCR4 tropism in the entry assay (data not shown). X4 variants emerged in the peripheral blood late in infection; they were not detected at week 40 (0 of 29 sequences) but were detected at week 43 in 3 of 13 sequences (23%). Thus, HIV-1 has the potential to evolve to use CXCR4 in this model, following an evolutionary path similar to what is observed in natural infections.

3.4.6 Compartmentalization of phenotypic variants.

HIV-1 can be found in multiple tissue compartments in the course of a human infection, which in some cases leads to the establishment of isolated, or compartmentalized, viral populations (311). We were therefore interested in investigating whether or not variants were compartmentalized in different tissue compartments in the mouse. Mouse 6 in particular, which harbored an X4 virus population, provided the opportunity to examine the tissue distribution of variants with distinct co-receptor phenotypes. Viral *env* genes (V1-V5) from this mouse were successfully amplified and sequenced from DNA extracted from spleen (SP), bone marrow (BM), and mesenteric lymphoid tissue (MLN) using the same limiting dilution technique employed for plasma RNA. Attempts to amplify viral DNA from the thymus were unsuccessful. Phylogenetic analysis of sequences recovered from these three

tissues together with sequences from peripheral blood plasma revealed the distinct clustering of X4 viruses within the tree, which was suggestive of clonal outgrowth of the X4 variant (Figure 7). In addition, X4-like variants comprised 95% of variants identified in the MLN, indicating compartmentalization of this phenotype in this tissue ($p<0.0001$). Phenotypic testing of a sample of variants with X4-like V3 sequences from the MLN confirmed their X4 phenotype (data not shown). Variants recovered from the spleen were phylogenetically intermingled with those from the peripheral blood and exhibited the same distribution. With these limited data we cannot determine if X4 compartmentalization in the MLN is due to stochastic seeding of or initial evolution in this tissue site, or if X4 viruses have a selective advantage in the MLN in this model. However, these data do demonstrate the potential for sub-populations of virus to disseminate, evolve and replicate independently in different tissues.

Genetic compartmentalization between the MLN and PB was assessed in mice 7, 8 and 64. Viral DNA was not successfully amplified from other mice or other tissues. In mice 7 and 8, sequences were well equilibrated between the PB plasma RNA and MLN tissue DNA. In mouse 64, a single synonymous mutation was enriched in the MLN ($P=0.0001$ Fisher's exact test), providing a second example of compartmentalization, although the overall genetic divergence between the two compartments was small (data not shown) and likely not based on phenotypic differences, at least within the Env protein.

3.5 DISCUSSION

Current models being used to study various aspects of HIV-1 infection include the genetically immunodeficient Rag2$^{-/-}\gamma_C^{-/-}$ mouse reconstituted with a human immune system by transplantation of human hematopoietic stem cells (DKO-hu-HSC mouse) (3, 7, 11, 94, 323). However, a detailed analysis of viral diversification and evolution in long-term infections has not been carried out in this system. In this study we examined the viral populations of DKO-hu-HSC mice with sustained infection for up to 44 weeks. We found that HIV-1 diversifies at nearly the same rate observed in human infections. We observed evolution of CXCR4 co-receptor use, a characteristic of many natural chronic infections. In addition we detected evolution towards increased sensitivity to a conformation-dependent V3 neutralizing antibody, increased CD4 binding affinity and a general loss of N-linked glycosylation sites.

Acute HIV-1 infection in humans is marked by high levels of viral replication. Within several weeks after infection, the CTL response appears and leads to suppression of peak viremia (22, 234). Following this initial immune response, variants emerge that have escaped CTL detection, marking the beginning of continuing evolution of HIV-1 in response to this selective pressure (22, 234). Between 4 and 5 weeks post infection (typically), HIV-1-specific antibodies appear (seroconversion), with some of the antibodies directed against the Env protein that can potentially select for neutralization escape variants (80, 87, 284). Selection of immune escape variants results in increasing viral diversity, which begins after seroconversion and continues into the chronic stage of infection, although the tempo of immune escape is highly variable and depends on the strength of the immune

response and the extent of immune dysregulation (87). Thus, the increasing variability in the *env* gene observed in human infection after seroconversion has a large component that is attributable to escape from immune pressure. In contrast, the DKO-hu-HSC model appears to lack a robust adaptive immune response to HIV-1 (3, 7, 94, 323). However, we observed similar rates of divergence and degrees of diversity in comparing viral populations from infected human subjects and DKO-hu-HSC mice. One interpretation is that the rates of divergence in DKO-hu-HSC mouse and human infections, while similar, are driven by different selective pressures acting on the population. For example, the virus is evolving either in response to constant immune pressure or as a result of selection for more efficient Env function in the absence of immune selection, as has been observed in cell culture (118, 143, 188, 192, 235), or perhaps also in the late stage of infection associated with immunodeficiency. The emergence of the same amino acid substitutions in multiple mice, particularly those that were linked to a phenotype such as enhanced CD4 binding or loss of glycosylation sites, was interpreted as evidence of positive selection. Analysis of selection based on the relative rates of synonymous (dS) and non-synonymous (dN) mutations across the V1-C5 region revealed no consistent pattern. However, this type of analysis is compromised when too few synonymous or non-synonymous mutations have accumulated to lend enough power to the analysis or if only a few sites are under strong positive or negative selection. For this model and over this period of time, the per-codon dN/dS rate ratio could not be reliably determined because of a lack of mutations at synonymous sites.

Some of the patterns of mutations were also similar to those observed in humans, with most substitutions concentrated in the variable loops, and detection of G-to-A hypermutations. However, evolution in this model is distinguished from natural infection by the quality of some mutations that grew out in the population. We observed that a number of Env variants isolated from several mice exhibited increased sensitivity to V3-specific antibodies such as 447-52D, which has been shown to be dependent on Env conformation and generally inactive against primary isolates, presumably as a result of occlusion of the V3 epitope in the wild-type, non-receptor-bound conformation of Env (13, 143). Specifically, we observed two mutations in V2 that were selected in most mice and resulted in amino acid substitutions I165R and D167N. We found that all of the viruses tested that evolved neutralization sensitivity to 447-52D had one of these two substitutions and that either of these alone, when reintroduced into the parental virus, HIV-1_{JRCSF}, rendered this virus more sensitive to neutralization. Variants with increased anti-V3 antibody sensitivity also exhibited increased resistance to competitive inhibition by the anti-CD4 antibody Leu3a. This was interpreted as increased CD4 binding efficiency.

Both 165R and 167N substitutions are represented at approximate frequencies of 3% and 12%, respectively, in the HIV Sequence Database (Los Alamos National Laboratories HIV Sequence database), whereas the most common amino acids at these positions, I165 and D167, are both found at frequencies of about 67%. These sites therefore exhibit some variability in human infections, and substitutions at these sites, along with other mutations that affect Env conformation,

may be markers of a loss of robust humoral immune pressure in late stage disease, although a direct link has yet to be made in natural infections. These substitutions have, however, been identified in several studies of virus passaged in cell culture (188, 235, 270, 312). While all of these studies find one or both of these substitutions to be linked to increased CD4 binding affinity (or sensitivity to CD4 mimics), the effects that these substitutions have on sensitivity to V3 antibodies in particular vary with the genetic background and the presence of different co-evolving substitutions. In our study, I165R/K and D167N appear to be mutually exclusive, and their appearing together, or in combination with other substitutions, may alter their neutralization phenotype. It is likely that these substitutions, along with others observed in viruses that have been passaged in cell culture systems, represent evolution toward heightened Env function through increased CD4 binding affinity or evolution toward CD4 independence, in the absence of neutralizing antibodies, as has been postulated previously (143, 192, 235). Further studies are required to ascertain whether or not these types of mutations are selected in people during profound immunosuppression and if they are linked to other phenotypes, such as CXCR4 tropism, that appear in late stage disease.

We also observed an overall loss of specific PNLG sites in multiple mice. Mutations that resulted in the loss of PNLG sites included sites that have been demonstrated to be conserved or selected in a long term infection in a Simian/Human Immunodeficiency Virus model (N339 and N386) (17). Other PNLG sites that were lost have been identified as central in a network of coevolving PNLG sites (N411) (231). The loss of the N386 site, which was observed at a high

frequency in three mice, has been implicated in enhancing HIV-1 replication in macrophage, which express low levels of CD4 and likely require changes in Env that increase CD4 affinity in order to be infected efficiently (74). Thus, the observed losses of N-linked glycosylation sites in mice, as with the changes affecting neutralization to V3 antibodies, also might represent selection for changes in Env that increase infectivity in the absence of neutralizing antibodies.

Another feature of natural HIV-1 infection is the emergence, usually late in chronic infection, of variants that use CXCR4 as a co-receptor. This occurs in about 50% of individuals infected with subtype B HIV-1 (49, 144). While this phenotypic switch in the population often coincides with a rapid drop in $CD4^+$ T cell count and disease progression (49), the selective pressures driving this switch are not clear. A stochastic model where the appearance of X4 variants is limited by the chance occurrence of the right combination of mutations does not explain their emergence in humans where the host likely has also to be immunodeficient (103, 114, 144). In one infected DKO-hu-HSC mouse we detected variants that could use CXCR4 as their co-receptor in addition to CCR5. These variants had distinct V3 sequences that were indicative of CXCR4 usage, and which were detected at weeks 43 and 44, but not at week 40. Coincidentally, 3 days prior to the detection of X4 variants, Ontak treatment (see Methods) was administered, which resulted in Treg depletion and increased T cell activation. Ontak treatment may therefore have played a role in creating an environment that potentiated X4 virus emergence in the periphery. However, it is also likely that the X4 variant preexisted in the MLN, the tissue in which it was found to be compartmentalized one week later. Only one of three mice

treated with Ontak developed detectible X4 virus, and no other biological characteristic of virus examined in this study could be attributed to an Ontak treatment effect. Early steps in the evolution of CXCR4 tropism may require the same conformational changes that render the virus sensitive to specific antibodies (28). A small effective population size in these mice, compared to humans, could also partly explain the emergence and outgrowth of X4 variants as following a stochastic process (26, 250). Nonetheless, this animal model provides the opportunity to explore further the link between X4 emergence and other Env phenotypes that evolve in the absence of a robust immune response.

Examination of the tissue distribution of variants in the mouse in which the X4 virus emerged showed that 95% of variants in the MLN were X4 compared to 15% in the peripheral blood and 22% in the spleen. While it is possible that apparent compartmentalization of X4 variants in the MLN was a result of chance seeding, there may also be a selective advantage for X4 viruses in this compartment. Previous studies have identified the thymus as a likely environment for X4 virus selection due to the high levels of CXCR4 expressed on resident T cells (257). In contrast, the MLN in wild type mice is responsible for linking both inductive and effector sites of the gut-associated lymphoid tissue (GALT), such as Peyer's Patches and the lamina propria and mucosal epithelium. As such, MLNs normally harbor a large population of activated T cells, predominantly with a memory phenotype, expressing high levels of CCR5. It is the large number of activated CD4+ CCR5+ T cells found in the GALT that are thought to support establishment and high levels of replication of the CCR5-tropic viruses responsible for initial infection. Indeed, this

tissue is decimated during peak viremia in the acute stage of infection (98, 163). Thus it is unclear how CXCR4-tropic viruses would have an advantage in this environment under normal conditions. However, the MNL in this model, populated by human T cells, may represent a different environment than that seen in normal humans or wild-type mice. The GALT has been shown to be underdeveloped in this model (116) indicating that the MLN may not be populated by the same CD4+ T cell subsets present in this tissue in a normal individual. Further exploration is required to assess more fully the cellular subsets populating this and other compartments in this model and the effect they have on the selection of viruses with different phenotypes.

3.6 ACKNOWLEDGMENTS

We thank the Los Alamos National Laboratories HIV Database group for helpful discussion and for the development of a vast array of user-friendly on-line tools for genetic analysis. We also thank Rachel Lovingood and Tom Denny of the CHAVI for the Western blot analysis of the mouse samples. This work was supported by NIH grant R37-AI44667 to RS and R01-AI077454 to LS. WLI was supported in part by NIH Training Grant T32-AI07419. This work was also supported by the UNC Center For AIDS Research (NIH award P30-AI50410) and the Lineberger Comprehensive Cancer Center (NIH award P30-CA16086).

Table 3.1: Immune reconstitution and CD4+ T cell depletion

Mouse	HSC Donor[a]	PB %hCD45+[b]	CD4/CD8 pre-infection[c]	CD4/CD8 at termination[d]
5	A	9.3	14.69	6.833
6	A	15.1	6.67	0.579
7	A	7.9	4.18	0.317
8	A	15.9	10.91	0.006
64	B	23.7	1.35	0.039
67	B	9.8	1.51	0.263

[a]Mice were reconstituted with one of two CD34+ HSC donors, A or B.
[b]Percentage of cells expressing human CD45 in the peripheral blood determined at 11.5 weeks after hCD34+ transplantation.
[c]The harmonic mean ratio of CD4+ to CD8+ T cells in the peripheral blood of 2 samplings prior to infection.
[d]Ratio of CD4+ to CD8+ T cells in the peripheral blood at termination: 44 weeks for mice 5-8 and 22 weeks for mice 64 and 67.

Table 3.2: Resistance to anti-CD4 antibody inhibition

	IC50	
Clone[a]	Leu3a (95% CI) (ng/ml)[b]	447-52D (ug/ml)[c]
6_38	40.9 (34.7 - 48.2)	<0.1
6_39	43.2 (39.3 - 47.6)	<0.1
JRCSF I165K	35.3 (31.0 - 40.2)	0.2
JRCSF D167N	33.0 (29.4 - 37.1)	1.4
7_16	23.2 (19.3 - 27.7)	>10
7_25	23.0 (19.6 - 27.1)	>10
JRCSF	23.5 (19.8 - 28.0)	>10

[a]First position in clone name indicates mouse number or parental clone for mutants.
[b]IC50 values were obtained from a sigmoidal dose-response curve fitted to 8-10 concentration data points (3 replicates per data point) ranging from 2 to 10^{-4} ug/ml.
[c]IC50 values were obtained from a linear curve fitted to 3 concentration data points at 10, 1 and 0.1 ug/ml as presented in Figure 5.

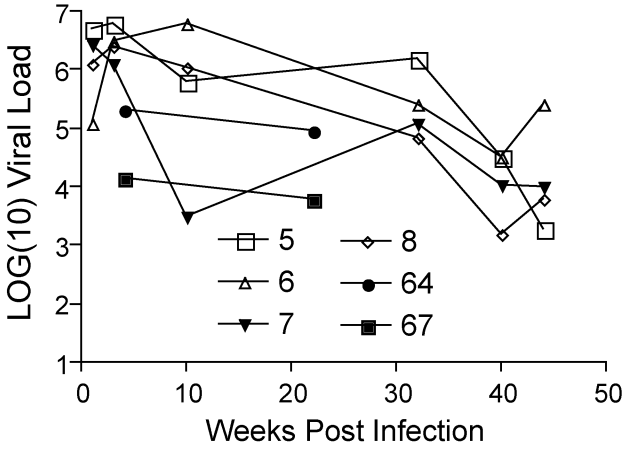

Figure 3.1. Plasma viral load over 44 weeks of infection for mice 5-8. The DKO-hu-HSC mice were infected intravenously with HIV-1_{JRCSF}. HIV-1 viremia in plasma samples (copies/ml) from all infected DKO-hu-HSC mice were measured at 3, 10, 22, 40, and 44 weeks post infection for mice 5-8 and 4 and 22 weeks post infection for mice 64 and 67.

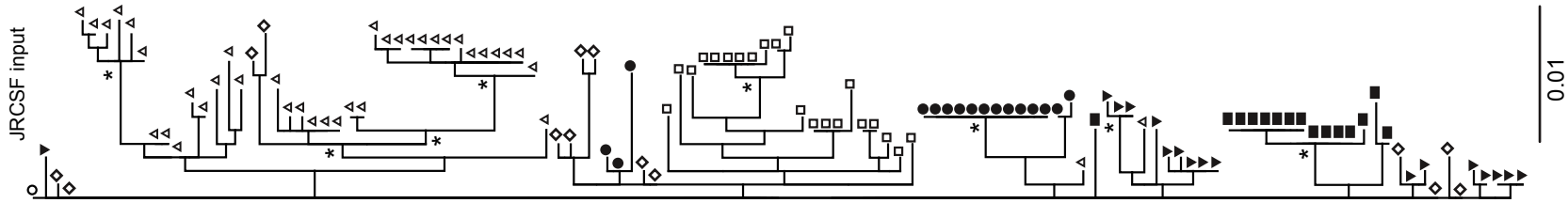

Figure 3.2. Phylogeny of HIV-1 sequences from all mice. Maximum likelihood tree of V1-C5 sequences from the peripheral blood (PB) at week 44 for mice 5-8 and week 22 for mice 64 and 67. Symbols at branch tips indicate mouse number. Open square: mouse 5; open triangle: mouse 6; closed triangle: mouse 7; diamond: mouse 8; closed circle: mouse 64; closed square: mouse 67. The open circle at the top of the tree indicates the JRCSF input sequence. Asterisks indicate bootstrap values >70%. Scale bar indicates substitutions per site.

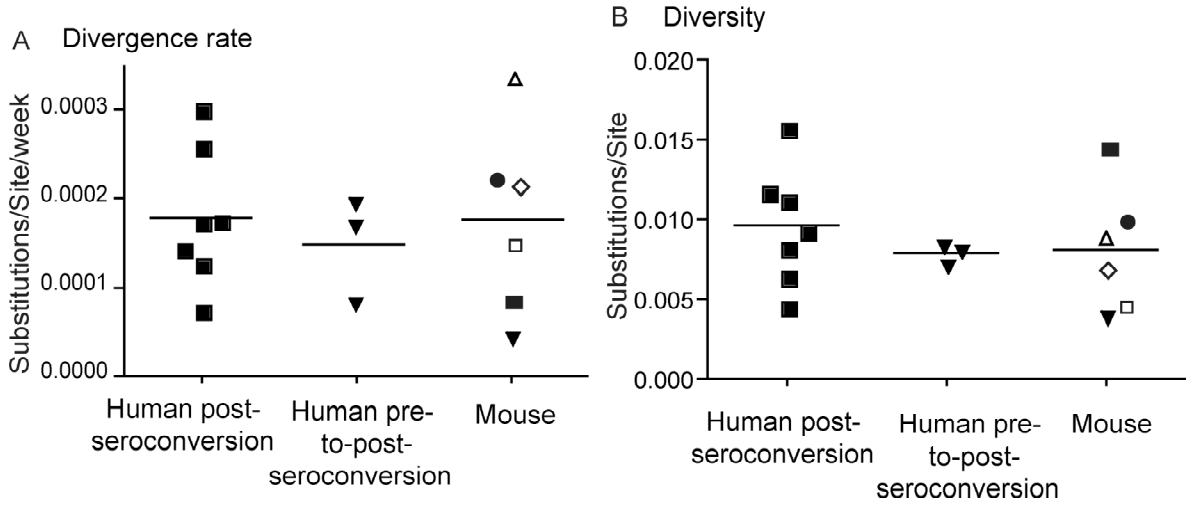

Figure 3.3. Comparison of divergence rate and diversity in mouse and humans. Distance measurements were based on branch lengths of maximum likelihood trees. Symbols in the Mouse group in A and B indicate the mouse number, as in figure 2. Open square: mouse 5; open triangle: mouse 6; closed triangle: mouse 7; diamond: mouse 8; closed circle: mouse 64; closed square: mouse 67. A) Divergence rates in mice and in human cohorts initially sampled post-seroconversion ("Human post-seroconversion" in A and B) (Shankarappa *et al.* 1999) and pre-seroconversion ("Human pre-to-post seroconversion" in A and B) (Salazar Gonzales *et al.* 2009) was measured for the C2-V5 region of *env*. For the post-seroconversion dataset, mean distance, based on branch lengths of a maximum likelihood tree, was measured from the consensus at a time point 3-5 months post-seroconversion for variants sampled at time points 9-24 months later. Sequences sampled at the first time point were relatively homogeneous but for 2 subjects which were likely infected with 2 variants and which were removed from the analysis. For the pre-to-post-seroconversion dataset, mean distance was measured from the consensus at time points estimated to be 20-24 days post infection, 9-16 days prior to seroconversion, for variants sampled 3-19 months later. Mean distance was divided by the time between sampling time-points to obtain rates of divergence. In mice, mean distance was measured from HIV-1_{JRCSF} for variants sampled at the last time point, either 22 or 44 weeks post infection. B) Population diversity is represented as the mean pairwise distances within populations at or extrapolated to 44 weeks post infection, for mouse and pre-to-post-seroconversion human samples, or post-seroconversion for the post-seroconversion human samples. A Student's *t*-Test was used to determine P-values for differences between distributions. P-values for all comparisons were >0.2.

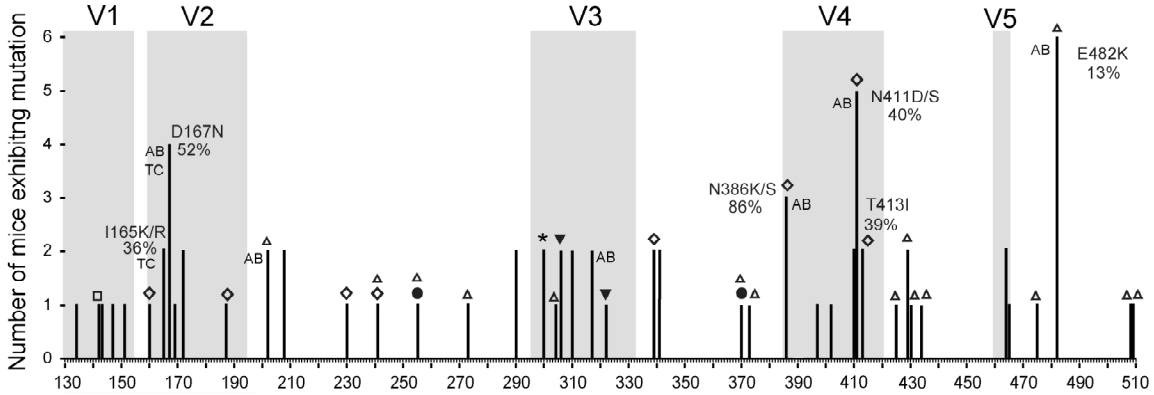

Figure 3.4. Positions and classifications of amino acid substitutions in the V1-C5 region of Env. Amino acid numbering on the abscissa corresponds to the HXB2 reference sequence. Bars on the graph indicate positions of substitutions and the frequency with which substitutions were identified in a mouse population at 44 weeks post-infection. Variable loops are shaded in grey. Substitution types are indicated by symbols. Square: addition of a PNLG site; diamond: loss of PNLG site; open triangle: >95% sequence conservation in subtype B; closed circle: component of the CD4 binding domain; asterisk: reversion to subtype B consensus; closed triangle: linked to co-receptor tropism. Substitutions at positions 165 and 167 that affected Env conformation and substitutions identified in 3 or more mice are indicated along with their mean percent abundance in the population. Substitutions identified in both donor sets are indicated by “AB” (see Table 1). “TC” indicates substitutions associated with tissue culture adaptation in other studies. Assessment of >95% sequence conservation was based on a random sampling of 300 sequences (one per patient) from the Los Alamos HIV Sequence Database. Sequencing of 30 SGA amplicons from the inoculum revealed 4 single point mutations among 3 amplicons. One of these mutations, at codon 151, was observed later in infection in mouse 67.

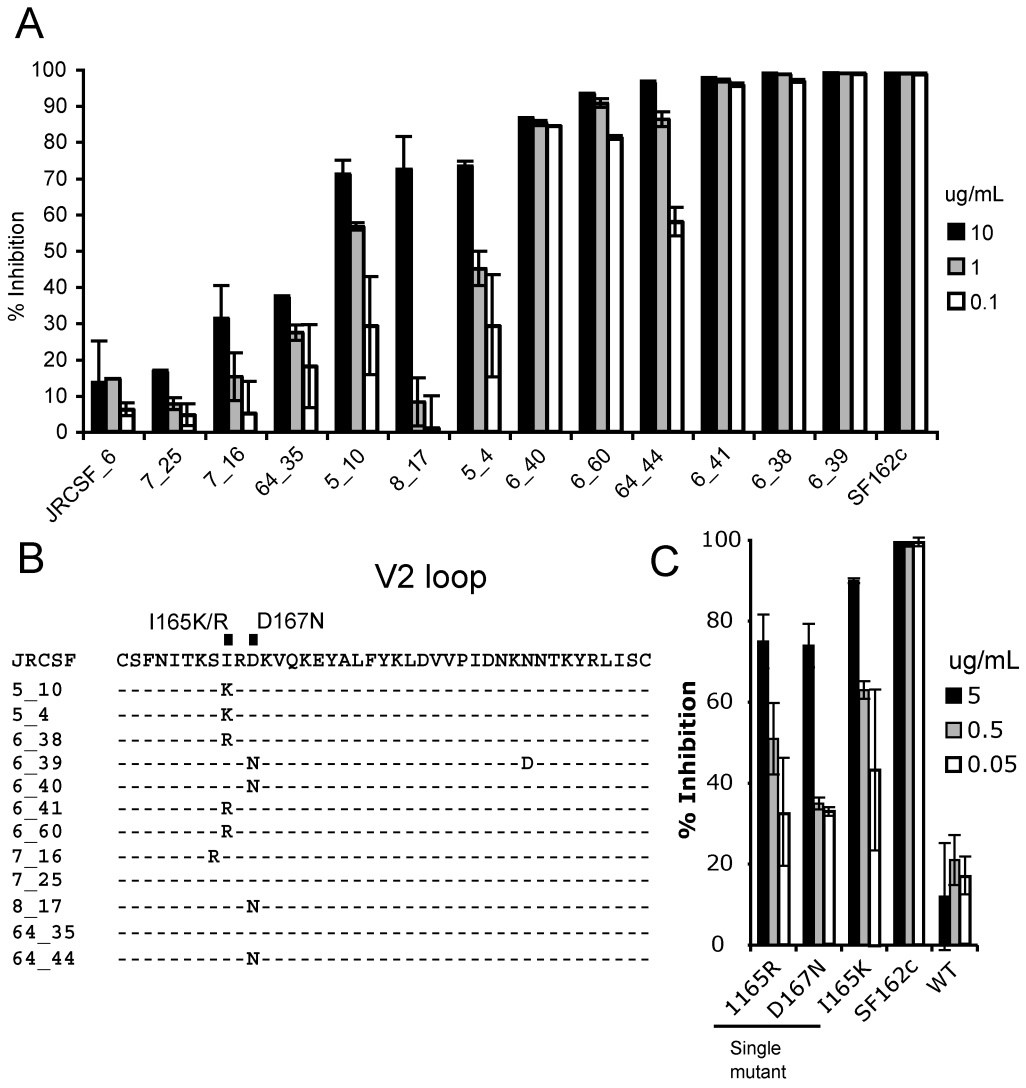

Figure 3.5. Neutralization sensitivities to 447-52D of selected envelope clones and mutants. A) Clone names identify the mouse followed by the clone number (e.g. 5_10). Percent inhibition is indicated for 447-52D antibody concentrations from 10-0.1 ug/ml. Error bars represent the range of 2 replicates. SF162c: a neutralization sensitive chimeric *env* in which the V3 region of HIV-1_{SF162} was replaced with the V3 loop from HIV-1_{JRFL} (Patel 2008). B) Alignment of the V2 loop of clones tested for neutralization sensitivity to 447-52D. Positions 165 and 167 are indicated. C) Neutralization sensitivity of HIV-1_{JRCSF} with substitutions I165R, D167N or I165K alone.

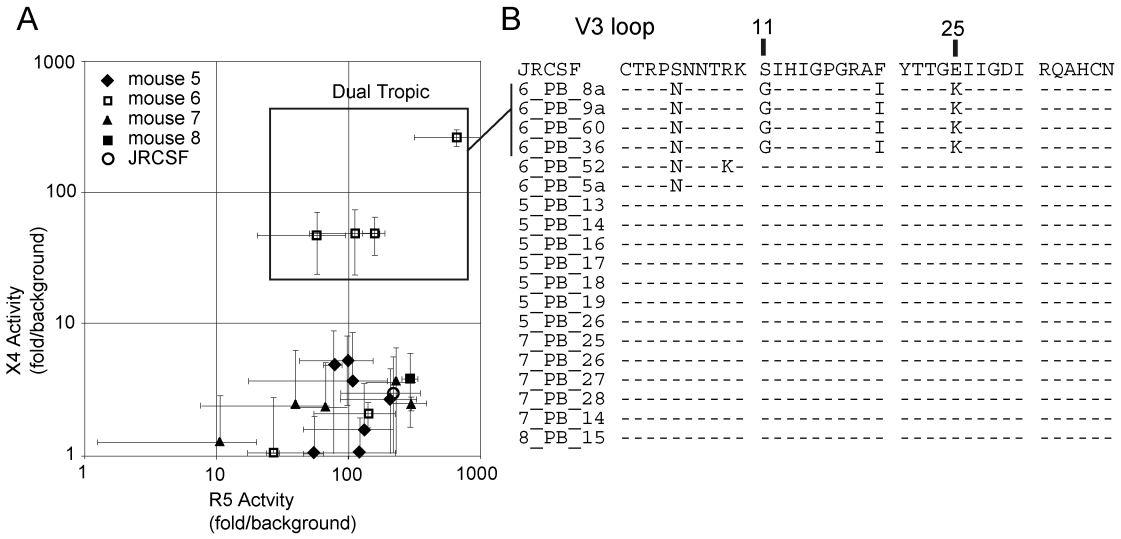

Figure 3.6. Phenotypic analysis of coreceptor tropism. A) Relative CXCR4 and CCR5 activity of *env* clones from 4 mice at week 44 post-infection in a pseudotype entry assay using U87.CD4 cells expressing either CXCR4 or CCR5. *env* clones exhibiting X4 usage are boxed and labeled “dual tropic”. Error bars represent the standard deviation of 3 replicates. These data are representative of multiple tropism assays. B) Alignment of the V3 loops of *env* clones tested in 6A. Clone names indicate mouse, tissue origin (peripheral blood - PB) and clone number. Env proteins exhibiting X4 tropism, boxed in 6A and indicated as “dual tropic”, are indicated in the alignment as those with changes in their V3 loops at positions 11 and 25 associated with the ability to use CXCR4. These variants were identified only in mouse 6 and comprised 15% of the population.

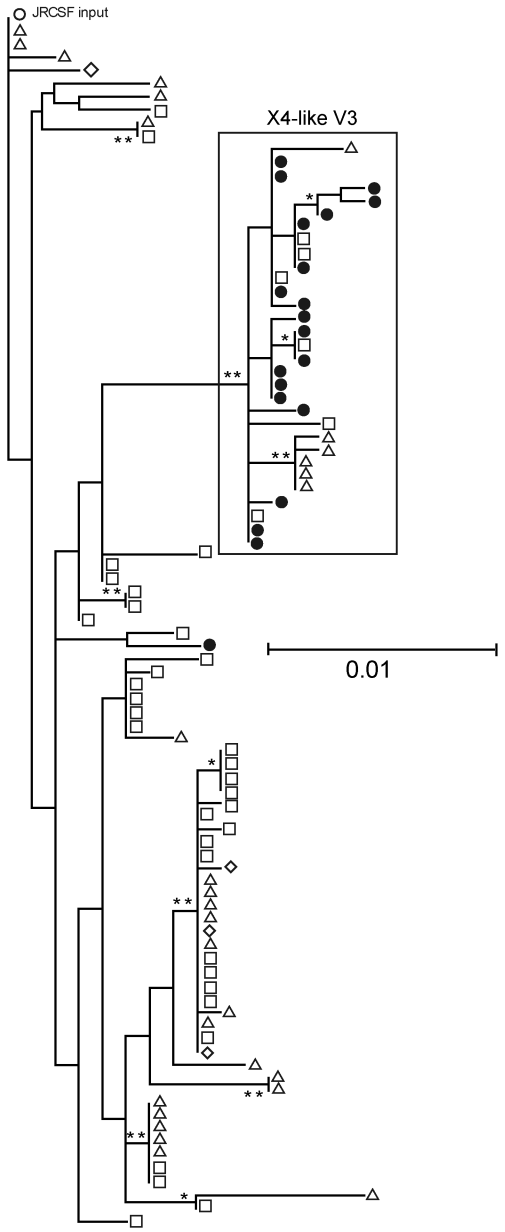

Figure 3.7. Maximum likelihood phylogeny of *env* variants (V1-C5) recovered from different tissue compartments in mouse 6. Bootstrap values >80% and >50% are indicated by double and single asterisks at nodes, respectively. Sequences were derived from viral DNA except in the case of sequences from the peripheral blood, which were from plasma viral RNA. The tissue of origin of sequences is indicated by symbols. Triangle: spleen; diamond: bone marrow; square: peripheral blood; closed circle: mesenteric lymph node. An open circle indicates the JRCSF input sequence. The boxed cluster indicates X4-like V3 sequences, which contain substitutions at positions 11 and 25 in addition to others and cluster together. A subset of these sequences was phenotypically tested to confirm tropism. Of the variants in the MLN, 95% contained an X4-like V3 sequence, indicating compartmentalization of this phenotype in this tissue in mouse 6 ($p<0.0001$).

Chapter 4

Forces Shaping Evolution In Late Stage Disease Contribute To The Evolution Of CXCR4 Tropism And May Contribute To Macrophage Tropism

The following individuals contributed to experiments presented in Chapter 4:

Kathryn Arrildt assisted with the generation of Env mutants and Sarah Joseph assisted with the entry assays using Affinofile cells.

4.1 ABSTRACT

I previously found that the Env protein of the CCR5- tropic HIV-1 isolate JRCSF evolved a more open conformation and increased CD4 binding affinity in a humanized mouse model of HIV-1 infection that lacked a strong HIV-1 antibody response. Within the context of this CCR5-tropic “background” phenotype, variants emerged that could efficiently use CXCR4 as their coreceptor. In this study, I further characterized the background R5 phenotype with regard to Env conformation, the ability to infect cells expressing low levels of CD4 and CCR5, mimicking macrophage, and infectivity using only CXCR4. I found that the background R5 phenotype included the ability to use low levels of CD4 and low level, but measurable, infectivity using CXCR4, compared to the parental virus JRCSF. I found that the major contributors to this phenotype were substitutions in the V2 loop that were linked to conformational changes, and I identified a similar pattern of substitutions in viruses from humans who were immunosuppressed and at risk of having CXCR4-tropic variants. These data are consistent with the hypothesis that specific conformational changes that are controlled by the conserved regions of the V2 loop and are constrained by adaptation to the humoral immune response, increase CD4 binding and promiscuous co-receptor usage and precede evolution of CXCR4 variants in the absence of strong humoral immune selective pressures.

4.2 INTRODUCTION

Defining the changes in the selective pressures that shape the evolution of HIV-1 envelope glycoprotein phenotypes during late stage disease is critical to understanding the environmental constraints placed on Env structures and functions that may affect viral pathogenesis and escape from pharmacological interventions directed at Env. Viral Env mediates entry into the host cell by sequential binding of the primary receptor CD4 and a coreceptor, either of two 7-transmembrane chemokine receptors, CCR5 or CXCR4. CXCR4-tropic (X4) viruses are rarely transmitted and HIV-1 infection is usually established by variants that require CCR5 as their coreceptor (R5 virus), a phenotype that typically dominates early infection (134). In about one-half of individuals infected with HIV-1 subtype B, a declining CD4+ T cell count marking late stage disease coincides with the emergence of viral variants that can efficiently use CXCR4 as a co-receptor (15, 48, 49, 244, 282). The primary genetic determinant of CXCR4 tropism is the composition of the relatively conserved (compared to the other variable loops) ~35 amino acid variable loop 3 (V3), a structural component of the coreceptor binding site in the gp120 subunit of Env, which determines co-receptor specificity through specific interactions with the extracellular loops of either CXCR4 or CCR5 (39, 50, 129). The reasons for the emergence of this new Env phenotype, and its link to disease progression, are not well understood.

As discussed in Chapter 2, X4 variants emerge as a clonal outgrowth of the preexisting R5 viral population and while these viruses are typically dual-tropic in tissue culture assays, they may be dependant on CXCR4 *in vivo* (318).

X4 variants also often continue to co-exist with R5 variants in the peripheral blood and show some degree of genetic mixing with R5 variants. X4 variants are not highly compartmentalized in separate anatomical or cellular niches, and it is not clear that X4 variants necessarily replace the existing R5 population. This apparent overlap in the X4 and R5 populations could indicate that strong niche selection itself is not required for X4 maintenance, even if it is in emergence.

While the selective pressures that drive (or select against) CXCR4 tropism are not clear, several hypotheses have been proposed. Changes in the relative numbers of target cells expressing CCR5 and CXCR4 may select for CXCR4 tropism in late stage disease as a result of CCR5+ CXCR4+ memory T-cell depletion over the course of infection leaving a larger proportion of CCR5- CXCR4+ naïve T cells which are vulnerable only to CXCR4 tropic virus (241). However, memory T cells express both CCR5 and CXCR4 and CXCR4+ CCR5- naïve T cells are abundant in healthy individuals. Importantly, in resistance selection experiments using viral inhibitors directed at CCR5 that block Env interactions with this coreceptor, inhibition more often selects for variants that can use inhibitor-bound CCR5 rather than for coreceptor switching (236, 286). *In vivo*, CCR5 inhibitors select pre-existing, but previously undetected minor X4 variants rather than *de novo* X4 variants, and once CCR5 inhibition is removed, R5 viruses regain dominance (reviewed in Kuritzkes 2009 (155)). As few as 2 mutations, are sufficient to confer X4 tropism (see below), a genetic barrier that is likely lower than resistance to many other inhibitors, if not CCR5 inhibitors themselves, indicating that CXCR4 variants are strongly selected against in

earlier stages of disease. This observation is consistent with the hypothesis that CXCR4-tropic variants evolve, perhaps to exploit CXCR4 on both memory and naïve T cells, only when released from immune selection constraints that exist in immunocompetent individuals.

X4 variants may be more susceptible to immune surveillance. It has been observed that X4 viruses are preferentially suppressed by a CTL response when Rhesus macaques are co-infected with X4 and R5 variants (103). It has also been found that emergent X4 variants in late stage human infection are more sensitive to neutralization by antibody specificities that suggest structural changes that expose otherwise cryptic epitopes, such as the CD4 binding site and the V3 loop (29, 114, 169). In Chapter 3, I found that in the environment of the humanized mouse, which did not exhibit a strong humoral response to HIV-1, the CCR5-tropic JRCSF isolate evolved to become highly sensitive to V3-specific antibody neutralization and exhibited increased CD4 binding affinity and that within this phenotypic background, X4 variants emerged. In the following study, I provide some additional evidence to support the hypothesis that structural changes that are required to evolve CXCR4 tropism render the virus more sensitive to immune selection. These structural changes allow increased CD4 binding and exposure of the V3 loop, which allow more promiscuous co-receptor usage and eventual evolution, based on V3 specificity, of efficient CXCR4 usage. Below, I further define the structural and phenotypic changes that occur on the path towards CXCR4 tropism in a virus that evolved in the absence of strong humoral immune pressure in the humanized mouse (mouse-adapted) and

attempt to link these genetic changes to changes observed in HIV-1 sequences from immunosuppressed humans.

4.3 MATERIALS AND METHODS

4.3.1 Cloning and mutagenesis of *env* genes.

As described in Chapter 3, *env* clone expression vectors were generated from selected SGA amplicons amplified from plasma viral RNA of mouse-adapted HIV-1 using the pcDNA3.1 Directional TOPO Expression kit (Invitrogen, Carlsbad, CA). Mutations in the wild-type JRCSF *env* were introduced by way of PCR re-synthesis of the JRCSF *env* expression vector using primers containing the desired base change (294).

4.3.2 Pseudovirus entry assays.

Generation of pseudotyped virus and pseudovirus phenotyping assays were carried out as described in Chapter 3. 293T cells were co-transfected with *env* expression vectors and the pNL4-3.Luc.R-E- luciferase reporter vector (109) (obtained from ARRRP) using the Fugene transfection reagent (Roche, Mannheim, Germany) according to the manufacturer's protocol to generate pseudovirus. Cells were washed with phosphate buffered saline 8-12 hours after transfection in order to reduce transfection complex carry-over and background luciferase expression in target cells, which was monitored with an *env*-negative control. Virus supernatant was collected 48 hours after transfection.

Co-receptor phenotype was determined based on detection of luciferase activity in U87.CD4+ cells expressing either CCR5 or CXCR4 (14) (obtained from ARRRP) using the Luciferase Assay System kit (Promega, Madison, WI). Pseudovirus was incubated with U87.CD4.CXCR4/CCR5 cells for 36-48 hours prior to lysis of cells and measurement of luciferase activity. Co-receptor-

dependent viral entry was confirmed using inhibitory concentrations of AMD3100 (112) (CXCR4 inhibitor) or TAK-779 (6) (CCR5 inhibitor) (both obtained from ARRRP).

Sensitivity to neutralization by the antibody b12 (32) (obtained from ARRRP), 4E10 (278) (obtained from ARRRP), 2G12 (27) (obtained from ARRRP) and the anti-V3 antibodies 447-52D (46) (obtained from ARRRP) and 19b (264) and 2.1E (gifts from Dr. James E. Robinson) was assessed on U87.CD4.CCR5 and TZM-BL cells (obtained from ARRRP), which are permissive to X4 and R5 viruses and contain an integrated, Tat-responsive luciferase cassette (65, 226). Sensitivity to the anti-CD4 antibody Leu3a (CD4 Pure) (BD Biosciences, San Jose, CA) was assessed on U87.CD4.CCR5 cells.

The ability of pseudovirus to infect cells expressing low levels of CD4 and CCR5 was assessed on Affinofile cells, transgenic 293T cells which express CD4 and CCR5 from independent inducible promoters (132). Cells were maintained in Dulbecco's Modified Eagle Medium containing 10% dialyzed Fetal Bovine Serum (2-14kD dialyzed; Atlanta Biologics) and 50 ug/ml blastocidin (D10F/B). Cells were seeded in poly-L-lysine-treated 96 well plates with 2.5×10^5 cells/well. Twenty-four hours after seeding, CD4 and CCR5 expression was differentially induced with the addition of tetracycline and ponasterone A, respectively. CD4 expression was induced at 6 levels (0-0.1 ug/ml tetracycline) and CCR5 at 4 levels (0-0.93 uM/ml ponasterone A) for a total of 24 induction levels. Eighteen hours later, the induction medium was removed and cells were spinoculated with pseudovirus or prepared for flow cytometry to measure induced CD4 and CCR5

densities. Cells were prepared for flow cytometry by staining at room temperature for 30 minutes with either phycoerythin (PE)-conjugated anti-human CD4 antibody (clone Q4120, BD Biosciences) or PE-conjugated mouse anti-human CCR5 antibody (clone 2D7, BD Biosciences). Cells were then fixed with 4% paraformaldehyde, washed and analyzed. CD4 and CCR5 levels were quantified using QuantiBRITE beads as a standard (BD Biosciences).

Analysis of neutralization activity in sera from HIV-1 infected subjects was assessed as follows. Sera or plasma was obtained from subjects from the cohorts described above. Neutralization assays were performed as previously described (189). An *env*-negative HIV-1 drug-resistant backbone (pNLCH-luciferase *env*$^-$ clone 1617 + K103N) was pseudotyped with wild type JRCSF or the antibody-sensitive mouse-adapted JRCSF 6-39 Env clone. Neutralization titers of sera were determined on TZM-BL cells in triplicate and the average relative infectivity determined.

4.3.3 Analysis of HIV-1 sequences from human subjects.

A total of 534 sequences were obtained by single genome amplification of viral RNA from the plasma of 33 subjects with CD4+ T cell counts ranging from 0 to 823 cells/ul. Sequences from eighteen chronically infected subjects with CD4+ T cell counts ranging from 241 to 823 cell/ul were from CHAVI-001 described previously (134). Sequences from 15 subjects with low CD4+ T cell counts, ranging from 0 to 233 cells/ul, were amplified from excess tissue obtained from the baseline blood draw of subjects participating in the virology sub-study of a ritonavir efficacy trial described previously (35) or from baseline blood draws of

subjects entering ACTG 359 described elsewhere (100). Potential N-linked glycosylation sites (PNGL) were predicted using N-Glycosite which infers a PNLG site in NXT/S motifs where X≠P (325) and was accessed through the Los Alamos National Laboratories HIV-1 Database website (http://www.hiv.lanl.gov/content/sequence/GLYCOSITE/glycosite.html).

4.3.4 Signature amino acid sequence analysis.

All sequences from 33 subjects were aligned in MAFFT (133) with manual editing of the alignment. One sequence per patient was sampled 5 times without replacement. Aligned sequences were then separated into high and low CD4+ T cell count groups. The amino acid frequency and statistical significance of frequency associations at each position for each sample set was determined using VESPA (147) accessed through the Los Alamos National Laboratories HIV-1 Database website http://www.hiv.lanl.gov/content/sequence/VESPA/vespa.html. The purpose of this analysis was to screen for positions that might be relevant to either the high or low CD4 environments; however, too few subjects' virus populations have been acquired thus far to power this analysis properly. The Bonferroni-corrected α of 0.00006 for differences at a given position was not met at any position in any of the five sequence sampling sets, although some positions did approach significance in >3 of 5 sequence samplings. Those observations are discussed in the results.

4.4 RESULTS

4.4.1 Previous observations

In Chapter 3, when variants from mouse 6 were screened for their sensitivity to antibodies directed at a conserved epitope in V3, I found that all clones tested, including those with an X4 phenotype, were >1000 fold more sensitive than the JRCSF parental virus to V3 antibodies (Figure 3.5 and Table 4.1), indicating the presence of a major structural change that had exposed the V3 loop in these variants. This was in contrast to the phenotypes of most primary isolates which are typically resistant to V3 antibodies (13), presumably due to structural masking of the V3 epitope, which is only exposed upon CD4 binding to allow interaction with the extracellular loops of the co-receptor. I found that either of two mutually exclusive amino acid substitutions in V2, I165R or D167N, was responsible for a large component of this phenotype (Figure 3.5, Table 4.1). I also showed that these V3 antibody-neutralization phenotypes correlated with increased resistance to an anti-CD4 antibody indicating increased CD4 binding affinity (Table 3.1 and Table 4.1). A subset of these Env variants in mouse 6 acquired the ability to efficiently use CXCR4, a specificity that was predominantly conferred by changes in the V3 loop. The specific changes distinguishing the X4 variant from the parental virus JRCSF were S5N, S11G, F20I and E25K (V3 numbering) (Figure 3.6), although the minimum combination of substitutions needed was not assessed. All but S5N were unique to X4 variants. In the present study, I followed up these observations with additional analyses of selected mouse-adapted clones and mutants (Table 4.1). I further defined the V3

mutations that are required for the X4 phenotype. I assessed sensitivities of these Envs to other monoclonal antibodies in order to further define the structural changes in these Envs. I then linked these structural changes to the ability to use low levels of CD4, and I mapped the phenotypic progression of CXCR4 usage in relation to the other phenotypes observed for these clones and mutants.

4.4.2 Mutations in V3 that confer strong X4 tropism

I determined the effect that different combinations of the V3 mutations identified in the X4 virus from mouse 6 had on entry of Env-pseudotyped virus in cells expressing CD4 and either CXCR4 (U87.CD4.CXCR4) or CCR5 (U87.CD4.CCR5) (Figure 4.1). S5N represents a reversion to the subtype B consensus and was present in over 90% of the variants sampled from mouse 6, which included the majority of variants that did not exhibit any other V3 substitution. S5N alone showed a modest but significant increase in the ability to infect CXCR4-expressing cells (CXCR4 infectivity), over 10-fold that of JRCSF. I also found that while the basic residue at position 25 is often the strongest predictor of an X4 virus in other studies (117, 129), CXCR4 infectivity was increased less than 2-fold that of JRCSF, although the overall infectivity of virus prepared with this Env mutant was greatly decreased. Addition of the S11G substitution to the E25K substitution conferred a significant increase in CXCR4 infectivity. Addition of the F20I to S11G and E25K increased CXCR4 infectivity further. When S11G was removed from the full set of mutations, leaving only S5N, F20I, and E25K, both absolute CXCR4 infectivity, and CXCR4 infectivity relative to CCR5 infectivity was maintained indicating that either F20I or S5N

plays a critical role in X4 tropism in this Env background. Interestingly, all V3 mutants, except for E25K alone, appeared to have minimal deficiencies in the ability to use CCR5 in these cells, although all 4 mutations together, S5N, S11G, F20I and E25K, conferred the highest level of both CXCR4 and CCR5 infectivity, but CXCR4 infectivity was relatively greater than CCR5 infectivity. Importantly, virus pseudotyped with X4 Env clones 6-45 and 6-60, isolated from the mouse 6 virus population exhibited nearly a 10-fold increase in CXCR4 infectivity relative to their CCR5 infectivity, whereas virus with changes only in V3 exhibited less CXCR4 infectivity as a proportion of CCR5 infectivity, indicating that in addition to mutations in V3, other mutations in these Env clones contribute to a stronger X4 phenotype.

4.4.3 Effect of mutations in gp120 on Env structure and antibody neutralization sensitivity.

In order to further characterize this structural change in gp120 indicated by increased sensitivity to V3 antibodies, I assessed the sensitivity of the selected mouse-adapted *env* clones and mutants listed in Table 4.1 to other antibodies to determine if sensitivity to V3 antibodies represented a global increase in neutralization sensitivity unrelated to specific structural changes. I found that the patterns of sensitivity to the broadly neutralizing antibody 4E10, which targets an epitope at the membrane proximal region of gp41, was uniform across clones, and sensitivity to 2G12, which targets specific glycans on gp120 correlated with the absence of specific glycan epitopes (in Env 6-39), but not with V3 antibody neutralization, indicating that antibody inhibition was a result of specific structural

changes in gp120 and not a general effect of reduced Env expression or virion loading, or another mechanisms unrelated to specific structural changes (Table 4.1).

In order to further define this structural rearrangement, I tested these *env* clones for their sensitivity to b12, an antibody directed at a conformational epitope overlapping the CD4 binding site. b12 is unique in its ability to access the conserved epitopes in the CD4 binding site that are otherwise obscured due to occlusion or conformational flexibility (327). b12 possesses an elongated CDR H3 loop that may be able to penetrate into the CD4 binding pocket to access and make more contacts with conserved residues (327). CD4 binding, on the other hand, requires increased avidity to counteract a relatively weak initial interaction between CD4 and the CD4 binding loop in gp120(327). While most primary isolates are sensitive to b12 to begin with, increased sensitivity to b12 has been shown to correlate with soluble CD4 sensitivity and increased CD4 binding affinity (72) and likely indicates a conformational change in the CD4 binding site, perhaps locking gp120 into a more CD4-accessible, and therefore more b12-sensitive form. Indeed, the mouse-adapted Envs 6-39 and 6-38, which were highly V3 antibody-sensitive and showed increased CD4 binding, were also increased in their sensitivity to b12. However, neither the I165R nor the D167N mutants displayed a measurable increase in b12 sensitivity (Table 4.1).

Another mutation, a loss of a glycosylation site at position 386 near the CD4 binding site, was also observed in nearly all mouse-adapted Envs from mouse 6, except those with X4 V3 genotypes, and this loss has been shown to

increase CD4 binding as well as b12 sensitivity (74). While I did not observe an increase in V3 antibody sensitivity or CD4 binding of the N386K mutant in JRCSF, I measured a small increase in b12 sensitivity, less than that measured for the highly V3 antibody-sensitive clones 6-38 and 6-39, indicating that this mutation acts specifically in the b12 interaction and that its effect on CD4 binding is at most subtle (Table 4.1). Furthermore, unlike the V2 mutations, it is absent in the background of *env* sequences with X4 V3s, indicating that it is not directly involved in the evolution of co-receptor tropism. The common feature that is found in both R5 and X4 mouse-adapted virus is the presence of mutations that both expose V3 and impact the structure of the CD4 binding site.

4.4.4 Env structural changes that expose V3 increase viral entry on cells when CD4 is limiting.

Increased CD4 binding is typically associated with macrophage tropism as it allows virus to utilize the low levels of CD4 and CCR5 expressed on macrophage. I was therefore interested in determining if this was a characteristic of the structurally evolved mouse-adapted X4 or R5 Envs and single V2 mutants that exhibited V3 antibody sensitivity and/or increased CD4 binding.

In order to assess the ability of *env* clones to mediate entry at limiting levels of CD4 and CCR5, viral infectivity was measured on 293T cells expressing different levels of CD4 and CCR5 (Affinofile cells) (132) for JRCSF wt, JRCSF with the I165R V2 mutation, mouse-adapted R5 clone 6-39, and mouse-adapted X4 clone 6-60 (Figure 4.2). Viral infectivity increased with both CD4 and CCR5

levels but was significantly more dependent on CD4 than CCR5 for all viruses tested (Figure 4.2 A-C).

Comparison of infectivity at low CD4 and low CCR5 levels, as a percentage of infectivity on cells expressing the maximum level of CD4, demonstrated a significant increase in entry of variants containing the V2 mutations affecting V3 exposure. The single substitution I165R, which is a phenocopy and mutually exclusive of D167N, alone conferred increased entry on low CD4/low CCR5 cells compared to JRCSF. Mouse-adapted clone 6-39 differs from JRCSF between V1 and C5 by 10 amino acid substitutions, including one substitution in V3, S5N, and the D167N substitution in V2, and showed a increase in relative infectivity on low CD4/CCR5 cells similar to that observed for the I165R single mutant. This was in spite of the observation that 6-39 Env showed greater CD4 binding affinity and sensitivity to V3 antibodies than the I165R mutant (Table 4.1). Mouse-adapted clone 6-60, which encodes an X4 Env, showed a significantly greater relative infectivity on CD4/CCR5 low cells compared to all other clones. The cells used in this assay express endogenous CXCR4, which may account for the increased infectivity of the 6-60 X4 clone, although, at low CD4, increasing CCR5 did not appear to increase infectivity appreciably for any Env. 6-60 differs from JRCSF by 7 substitutions in the V1-C5 region, including the 4 mutations in V3 (S5N, S11G, F20I, E25K) and the D167N substitution in V2. 6-60 differs from 6-39 by 7 substitutions, 6 that are absent in 6-60 and 1 that is present in 6-60, but absent in 6-39 (T202R).

The 6-39(R5) and 6-60(X4) Envs have 3 substitutions in common: I165R/D167N, S5N (V3), and the loss of an N-linked glycosylation site at position 411, at the base the V4 loop. As discussed in Chapter 3, the I165R/K/D167N mutation set was tightly linked to the loss of a glycosylation site at position 411, which was absent in virtually all clones that contained either I165R or D167N. Introduction of this mutation in combination with 165R had no effect on relative infectivity in low CD4/CCR5 cells (data not shown), as might be expected based on the similar infectivity of the single I165R mutant and 6-39, which contains both mutations; the significance of the loss of the glycan at position 411 requires further investigation.

In summary, the single substitution at position 165 was able to increase relative infectivity at low CD4 levels compared to JRCSF. The additional mutations in 6-39, which contributed to increased CD4 binding affinity, as measured by Leu3a resistance, and b12 sensitivity, did not increase infectivity at low CD4 and CCR5 concentrations compared to the I165R mutant alone, highlighting the importance of I165R, and by extension D167N, in conferring this specific phenotype.

4.4.5 Effect on relative CXCR4 usage of mutations external to V3.

I have shown thus far that the mutations that accumulate in mouse-adapted Env clones, increased sensitivity to V3 (19b, 447-52D, 2.1E) and CD4 binding site (b12) antibodies, increased CD4 binding and, separately, increased the ability to use low levels of CD4 and CCR5. Sensitivity to V3 antibodies in particular, which was the most common feature of mouse-adapted Envs (Chapter

3), indicates a more open conformation of Env that increases V3 exposure and plays a role in enhancing entry into cells expressing low levels of CD4 and CCR5.

I hypothesized that these features of Env, which evolved prior to the emergence of X4 tropism conferred by changes in V3, represent prerequisite or intermediate features of X4 tropism. If so, they might confer some level of X4 tropism, as has been observed in primary isolates that lack strong V3-driven X4 tropism but show low-level infectivity on cells expressing only CD4 and CXCR4 (CXCR4 infectivity), compared to their infectivity on cells expressing only CD4 and CCR5 (CCR5 infectivity) (84, 121). I therefore determined infectivity of Env mutants and mouse-adapted clones on U87.CD4.CXCR4 cells and compared this to infectivity on U87.CD4.CCR5 cells.

Relative CXCR4 and CCR5 infectivities are shown in Figure 4.3 for Env clones exhibiting a range of V3 antibody sensitivities and CD4 affinities. Mutant (I165R or D167N) and mouse-adapted Env clones with R5-like V3 loops, 6-38 and 6-39, showed significant and progressive increases in CXCR4 infectivity, relative to CCR5 infectivity, that correlated with sensitivity to V3 antibody and CD4 binding. Envs 6-38 and 6-39, which showed increased CXCR4 infectivity compared to the single mutants I165R and D167N, also contained the S5N mutation in V3, which was shown to confer low level X4 tropism alone (Figure 4.1). Clones with X4-like V3 loops (6-60 and NL4-3, a prototypical X4 virus) (V3 geno. In Figure 4.3) exhibited at least ten-fold greater CXCR4 infectivity than clones with R5-like V3 loops. Env clones with R5-like V3 loops that displayed the

highest activity on U87.CD4.CXCR4 cells (6-38 and 6-39) exhibited greater resistance to AMD3100, a small molecule antagonist of CXCR4, compared to variants with X4-like V3 loops (Figure 4.3c).

The curve of increasing X4 activity appeared to have multiple phases (Figure 4.3b). The single mutations I165R and D167N increased CXCR4 infectivity by nearly ten-fold compared to JRCSF, but without an increase in CCR5 infectivity. Mouse-adapted clones 6-38 and 6-39, which showed higher sensitivity to V3 antibodies and increased CD4 binding compared to the single mutants I165R and D167N, exhibited equal increases in both CXCR4 and CCR5 infectivity, perhaps illustrating an overall increase in infectivity regardless of co-receptor use. The presence of an X4-like V3 in 6-60 was associated with a ten-fold increase in CXCR4 infectivity over the R5 clones 6-39 and 6-39, but also a decrease in the ability to use CCR5 by nearly the same magnitude. Thus in these data, it appears that variants with R5-like V3 loops but with more open conformations and increased V3 exposure, acquire the ability to infect, at a low level, cells bearing only CXCR4 and CD4 (I165R and D167N). Increasing CD4 binding affinity may enhance this effect (6-38 and 6-39) by compensating further for the weak interaction with CXCR4, which creates an evolutionary path for further changes in V3 to enhance interaction with CXCR4; the acquisition of these V3 changes likely diminishes the ability of V3 to interact with CCR5. This pathway may only be initiated by the absence of an antibody response, perhaps specifically a loss of antibodies targeted to V3 that would otherwise select for a closed Env conformation.

4.4.6 Sequence analysis of gp120 from HIV-1-infected subjects with high and low CD4+ T cell counts.

The phenotypes that I observed in this study likely depended on the absence of humoral immune pressure, based on previous studies also linking these phenotypes, as well as some of these specific mutations, to passage in tissue culture and therefore in the absence of immune selective pressures (discussed in Chapter 3). I therefore wanted to know if any of the mutational patterns identified in mouse-adapted isolates were present in HIV-1 populations from human subjects with low CD4+ T cell counts, compared to populations from subjects with relatively high CD4+ T cell counts, with the assumption that immune selective pressures would be weaker when CD4+ T cell counts are low. A total of 33 subjects with a range of CD4+ T cell counts were divided into low and high CD4+ T cell count groups (low CD4 and high CD4, respectively). For the 15 subjects in the high CD4 group, CD4+ T cell counts (cells/ul) ranged from 241 to 823, with a median of 382. For the 18 subjects in the low CD4 group, counts ranged between 0 and 233, with a median of 93. For each subject, between 7 and 27 viral genomes encompassing V2-V4 were amplified using SGA (as described in chapter 2). X4 variants were inferred (by PSSM) to be present in 15 of the 18 subjects with low CD4+ T cell counts and in 1 of the 15 subjects with high CD4+ T cell counts; these variants represented less than 50% of the population in most cases. Analyses were carried out to determine if there were any positions at which amino acid substitutions were disproportionately represented in the low versus the high CD4 groups. The average number of

glycosylation sites, sequence length, and V2 charge were also compared between low and high CD4 groups.

Analysis of the differences in amino acid substitutions in HIV-1 populations between groups was carried out by sampling one sequence per patient multiple times without replacement. While this analysis was not powered to detect differences on a sequence-wide basis, several positions approached significance. Only one position in V3, 319 (V3 position 22) with a T to an A substitution, approached significant enrichment in the low CD4 group. Also approaching significance were differences at positions 164 (N in high CD4, S in low CD4) and 169 (I in high CD4, M in low CD4), near the structurally important positions 165 and 167 in V2. Several other positions were identified in the C2, V4 and C5 regions, although none that was also identified in mouse-adapted clones. Determining the significance of these mutations requires further sequence analysis in a larger dataset in addition to functional analysis.

No significant difference in the average number of glycosylation sites was detected between high and low CD4 groups, although there was a trend toward a lower number of glycosylation sites in the low CD4 group (Figure 4a), which was consistent with the loss of glycosylation sites observed in the mouse-adapted virus populations. Sequence length (Figure 4.4b), which would be a consequence of length variability in the variable loops, was also not significantly different, but again showed a trend toward shorter sequence length in the low CD4 group, which was perhaps linked to the number of glycosylation sites as

glycosylation sites are often added and subtracted through insertion and deletion in the variable loops.

I detected two distinct substitutions (I165R/K and D167N) in the V2 region in mouse-adapted JRCSF that conferred the same structural change in Env indicating that while V2 may be important in Env conformational changes and phenotypes, multiple pathways exist to achieve the same result, analogous to V3 and co-receptor tropism. This may confound an attempt to identify specific sites that are responsible for a specific phenotype. I therefore probed for differences in amino acid composition in V2 by comparing differences in charge. I determined the average charge within a subject of HIV-1 amino acid sequences for a region encompassing positions 158-198 (HXB2 numbering), which includes both the non-length-variable N-terminal region along with the length-variable region of V2. Figure 4.4c illustrates the distribution of average V2 charges for each subject in the high and low CD4+ T cell count groups. I found that V2 sequences from low CD4+ T cell count subjects exhibited a significant increase in charge, which is consistent with the types of mutations identified in V2 sequences of mouse-adapted clones (I- to R/K or D to N), which also increase overall V2 charge in JRCSF. Increased V2 charge was linked to X4 phenotypes in some but not all sequences in subjects with X4 virus (data not shown).

4.4.7 Determining the prevalence of V3 antibody activity in sera from low and high CD4+ T cell count subjects

I have identified a pathway to CXCR4 tropism in mouse-adapted variants that may depend on reduced humoral immune pressure in late stage disease.

Given that I had Envs that exhibited exquisite neutralization sensitivity to V3 antibodies, and increased sensitivity to the CD4bs antibody b12, but not antibodies targeting other epitopes, as with Env 6-39 compared to the parental JRCSF (Table 4.1), I wanted to know if I could use these Envs to screen plasma samples for the presence of V3 antibody and b12-like neutralization activity. In a preliminary analysis of plasma from 8 subjects, 6 with low CD4+ T cell counts and 2 with high CD4+ T cell counts, I found that 3 of 6 low CD4+ T cell count sera, and 1 of 2 high CD4+ T cell count sera exhibited little to no neutralization activity against either a sensitive or resistant Env, while the other sera exhibited neutralization activity comparable to a V3 monoclonal antibody against the sensitive clone only (Figure 4.5). These Envs represent useful tools to further investigate larger sample sets for a link between the absence of specific neutralizing antibody activity and contemporaneous HIV-1 Env phenotypes in human subjects.

4.5 DISCUSSION

In Chapter 3, I identified Env variants of the CCR5-tropic JRCSF isolate that had evolved CXCR4 tropism in a humanized mouse model of HIV-1 infection. These X4 variants emerged in a “background” Env phenotype characterized by increased sensitivity to V3-directed antibodies and increased CD4 affinity, consistent with the lack of a strong humoral immune response in these mice and the evolution of a more open conformation of Env that exposed V3 (188, 192, 235). I hypothesized that the more open Env conformation that conferred the background phenotype was a prerequisite for the acquisition of CXCR4 tropism. Further analysis in Chapter 4 of both the background and X4 phenotypes revealed that conformational changes that increased V3 exposure and CD4 binding affinity could allow low-level utilization of CXCR4 by Envs that had yet to acquire tropism-defining V3 substitutions associated with efficient CXCR4 use. I also found a correlation between increased positive charge in the V2 region that controls V3 exposure, and low CD4+ T cell counts and the presence of X4 virus in humans.

In Chapter 3, I established that the V3 loop of the X4 variants was sufficient to confer X4 tropism in the mouse-adapted JRCSF. In this chapter, I further defined the impact on CXCR4 tropism of specific combinations of the 4 substitutions in V3 associated with the tropism switch. Co-receptor tropism can be predicted based on the composition of the V3 loop. In particular, basic amino acid substitutions at positions 11 and/or 25, or an overall increase in positive charge, is indicative of CXCR4 tropism (117, 129, 184). The single substitution of

E25K, the only one of the 4 substitutions in X4 V3s that increased positive charge, only appeared to diminish viral infectivity of the pseudotyped virus (Figure 4.1). However, addition of the S11G substitution significantly increased infectivity and measurable X4 tropism, although further work needs to be done to confirm the effect of E25K alone. Positions 11 and 25 lie on opposite sides of the V3 stem, with the charge-changing E25K substitution located near the V3 tip. The increased positive charge of V3, and in particular at position 25 in V3, is thought to determine specificity for CXCR4 by facilitating interaction with the anionic surface of the extracellular loop 2 (ECL-2) of CXCR4 (23, 39, 306). The X4-associated change F20I in V3 tip maintains a hydrophobic residue at that position, which is thought to be important for ECL-2 interactions (50) and also gp120/gp41 interactions in the un-liganded structure (317). Although this substitution appeared to have a positive effect on both CCR4 and CXCR4 infectivity when added to the S11G and E25K substitutions, the functional significance of this conservative change remains unclear and requires further investigation. While S11G and E25K are sufficient to confer high-level CXCR4 infectivity, the additional substitutions F20I and S5N enhance overall infectivity and in particular CXCR4 infectivity (Figure 4.1). The fitness advantage conferred by this particular combination of four substitutions is consistent with our not finding in the peripheral blood any other V3 variants with an X4 phenotype in our analysis (Chapter 3). If I were able to examine the mesenteric lymph node, the likely site of origin of these variants in the mouse, I may have identified the immediate predecessor to the X4 phenotypes that emerged.

The base of V3 is also thought to play a role in co-receptor engagement (50). The S5N substitution in the base of V3, unlike the substitutions at positions 11, 20 and 25, was not unique to X4 variants and was found throughout the virus population in mouse 6 (the mouse in which X4 variants emerged) at 92% frequency. It was identified at a low frequency in only one other mouse, in which X4 variants were not detected. This substitution represents a reversion to the subtype B consensus. The S5N substitution is the first of a conserved triplet of asparagines, and is in close proximity and just outside the binding pocket for one of the sulfonated tyrosines in the N-terminus of the CCR5. Structural evidence using a Y-sulfonated N-terminal peptide and antibody mimic indicates that the latter 2 asparagines in this triplet directly interact with the C-terminal sulfonated tyrosine, and while a dramatic acidic substitution at V3 position 5 had little effect on binding of gp120 with these reagents (119), the consequences of a serine at this position and it's implication for coreceptor switching are unknown. Interestingly, this substitution appeared to have a positive impact on relative X4 activity in combination with F20I and E25K, similar to S11G, and also exhibited modest X4 activity alone, strongly suggesting it does play a role, although further work is required to ascertain its impact on co-receptor switching.

The background phenotype in which X4 variants emerged exhibited profound sensitivity to antibodies directed at V3 and showed increased CD4 binding conferred by structural rearrangements that resulted in a more open conformation of Env (Table 4.1). b12 sensitivity is linked to increased CD4 binding affinity and macrophage tropism (72). I also found increased b12

sensitivity in Envs that were highly sensitive to V3 antibodies along with having increased CD4 binding affinity, further linking these structural changes with phenotypes found in human infections, and in virus that may have escaped antibody selective pressures by invading the CNS (72-74, 283).

Mutations in the non-length-variable N-terminal side of the V2 loop that increased the overall positive charge of the loop (I165R/K or D167N) were responsible for a major structural rearrangement that leads to increased V3 exposure, indicated by increased V3 antibody sensitivity. The V2 region of Env has been shown in other studies to play a pivotal role in the conformational masking of conserved epitopes targeted by neutralizing antibody responses and those directed at V3 in particular (44, 225, 270, 315). It has been demonstrated in multiple settings that removal of antibody selective pressures results in the selection of mutations in V2 that result in a more open, neutralization sensitive Env conformation that has enhanced CD4 and co-receptor engagement through exposure of these binding sites (9, 83, 127, 164, 188, 235, 315). The recently-identified gp120 trimer-specific, potent, broadly neutralizing antibody PG9 (and the somatic variant PG16) recognizes an epitope involving the conserved V1/V2 base and conserved regions of the V2 and V3 loops, or at least is dramatically affected by changes in these regions. PG9 also exhibits increased affinity to trimers with an E168K substitution, perhaps a result of a conformational change (299). This provides additional evidence that basic substitutions at specific sites in V2 can increase neutralization sensitivity to antibodies with specificities for this region and V3. Substitutions in the V1/V2 region have also been shown to play a

compensatory role by increasing infectivity in viruses that acquire V3 mutations on the pathway to CXCR4 tropism that confer a loss of infectivity (199, 215). The question of whether or not this involves increased dependence on the N-terminus of the co-receptor requires further investigation. The changes I identified in V2, while not conferring a detectible increase in CD4 binding affinity in a competitive inhibition assay with an anti-CD4 antibody (Table 4.1), were sufficient to increase relative infectivity when CD4 was limiting, analogous to a pathway that may confer some level of macrophage tropism. Thus the same conformational change in gp120 may have three related effects: first, changes may allow more efficient CD4 binding for more rapid growth in T cells (presumably the source of the selection); second, more efficient CD4 binding may also allow entry into cells with fewer CD4 molecules; and third, the altered conformation may allow increased interaction with CXCR4, which may also depend on increased CD4 binding affinity. Because the initial gp120:CD4 interaction is weak and likely requires the binding of multiple CD4 molecules in order to increase avidity for most primary isolates, conformational changes that allow increased CD4 affinity can compensate for the reduced avidity when CD4 molecules are scarce, such as on macrophages (327). An alternative hypothesis is that changes in V2 which increase positive charge may enhance interactions, in a less specific manner, with negatively charged cell membrane-associated molecules, such as heparan sulfate proteoglycans, thereby increasing avidity when CD4 is low, although the data are conflicting on the positive effect of heparan sulfate in HIV-1 binding to target cells (194, 216, 296, 297).

When I compared V2 sequences from subjects with low CD4+ T cell counts, and therefore with a high risk of having X4 virus, to those with high CD4+ T cell counts, I found an increase in overall V2 charge in the low CD4+ T cell count subjects. Because more than one mutation in the mouse-adapted virus, in an isogenic viral background, was sufficient to confer the same phenotype, it is likely that a basic or positive charge at any of multiple sites in V2 can confer this phenotype. This is consistent with a lack of detection of a signal at a single position in V2 that distinguishes these high and low CD4 environments. Whether or not variants with increased V2 charge show the same phenotypes, either increased V3 antibody neutralization or increased infectivity when CD4 is limiting, is an important question.

Increased CD4 binding affinity and sensitivity to neutralization by soluble CD4 and antibodies, phenotypes also associated with macrophage-tropism, have been linked to co-receptor switching in simian/human immunodeficiency virus (SHIV) Rhesus macaque models (114). In addition, X4 variants have been shown to be more neutralization sensitive compared to R5 variants in human infections (29, 169). Emergence of X4 SHIV variants in the Rhesus macaque was shown to follow, rather than precede, the development of an immunosuppressed environment and coincided with an increase in a macrophage-tropic phenotype (114, 115). Thus, the same environmental change, immunosuppression, may link macrophage tropism, as defined by increased CD4 binding affinity and the ability to use low levels of CD4, and X4 emergence if both

of these phenotypes depend on the same conformational changes which are selected against by humoral immune pressure.

Evolution of X4 tropism may depend on the same functional changes that confer macrophage tropism. This is demonstrated in Figure 4.3a and b, which show that increasing V3 antibody sensitivity and CD4 binding affinity correlate with increased infectivity on cells expressing only CD4 and CXCR4. This pathway suggests a mechanism of X4 evolution whereby substitutions, such as those at positions 165 or 167, that result in conformational unmasking of receptor and co-receptor binding sites, and which may increase CD4 binding affinity and infectivity, compensate for weak or non-specific interactions with the alternative co-receptor CXCR4. A reduced dependance on the specific interactions between V3 and coreceptor is indicated by increased relative resistance to the CXCR4 inhibitor AMD3100, of the Envs with R5 V3s that exhibit some infectivity using CXCR4, compared to bona fide X4 viruses (Figure 4.3c). AMD3100 specifically inhibits the interactions between V3 and the extracellular loop, but not necessarily interactions with the N-terminus of the co-receptor, which may be how these R5 viruses are interacting with CXCR4 (69). As CD4 binding and V3 exposure become more pronounced, the ability to utilize CXCR4 is increased. The pathway of X4 and macrophage tropism bifurcates when V3 mutations accumulate to a degree that CXCR4 engagement is enhanced at the expense of CCR5 engagement. Thus the early stages of X4 evolution may be shared with those of macrophage tropism evolution. This is consistent with some evidence linking the emergence of macrophage-tropic virus in tissue other than the brain

with late stage disease (97, 114, 124), although further investigation is required to link the emergence macrophage tropism to immunosuppression.

Why do X4 variants emerge? The early stages of X4 evolution allowing low-level utilization of CXCR4 may allow expansion of host cell range to cells that only express CXCR4 and not CCR5, such as naïve T cells. While the initial viruses infecting these cells may exhibit reduced replication capacity, at first, in these cell types, un-rivaled competition for this cellular pool may allow a less fit viral population time to evolve V3 changes that increase replication capacity in this cell type and fitness relative to R5 variants. This model is consistent with the observation made in Chapter 2 that X4 variants in the population represent a clonal expansion. This is presumably because of the jump in viral fitness when variants acquire the correct combination of V3 mutations, an event that needs to occur only once. However, the evolution of this initially poorly fit virus in naïve T cells likely requires an immunodeficient host that is either incapable of neutralizing the newly-evolved, neutralization-sensitive and promiscuous virus or incapable of monitoring infection of this new target cell population.

Linking genetic pathways of these phenotypes to the environmental change of reduced antibody pressure will require parallel tracking of the host antibody response and the genetic and phenotypic changes in the viral population. Alternatively, a cross-sectional approach with a large enough dataset could also lend further evidence to this connection. The exquisitely V3-antibody-sensitive Envs identified in this study, along with the parental JRCSF Env, can be used to probe for specific antibody neutralization activity in patient sera. The

neutralization profile of the sera can then be correlated to the genetic and phenotypic features of the contemporaneous virus. Ultimately, however, proof of this link will require evolutionary modeling in the appropriate system where specific immune pressures can be carefully controlled.

It is also possible that while this hypothesis for the evolutionary path of CXCR4 tropism might be validated for Envs evolving in the absence of a specific humoral response, different selective pressures and a different evolutionary pathway may be operating in humans. It is also possible that the correlates identified in the perpheral blood, such as a lack of a specific antibody neutralization activity may not be relevant. Instead, what may be more relevant is the local environment, either in a specific tissue or cellular compartment, which may select for or potentiate X4 evolution. Further work is needed to understand the local environmental factors at play that select for phenotypic variants in the compartment where they originate, which is still unknown for X4 variants.

Table 4.1: Neutralization phenotypes of selected mouse-adated and mutant Env

Env clone	V3 antibody sensitivity[b]	CD4 binding affinity (mAb Leu3a resistance)[c]	mAb b12 sensitivity	mAb 4E10 sensitvity	mAb 2G12 senstivity
JRCSF wt	-	-	-	+	+
6-39 (R5)[a]	+++	+	++	+	-
6-38 (R5)[a]	+++	+	++	ND	ND
6-60 (X4)[a]	+++	ND	ND	ND	ND
JRCSF I165R	+	+/-	-	+	+
JRCSF D167N	+	+/-	-	+	+
JRCSF N386K	-	-	+	+	+

[a] Data from Chapter 3. For mouse adapted clones 6-39, 6-38 and 6-60, the co-receptor phenotype predicted by the V3 sequence is indicated in parenthesis
[b]Data from Chapter 3. Sensitvity was tested using 1 or more of 3 antibodies directed at overlapping epitopes at the tip of V3 (447-52D, 19b, 2.1E) all results were concordant
[c]Leu3a competatively inhibits Env binding

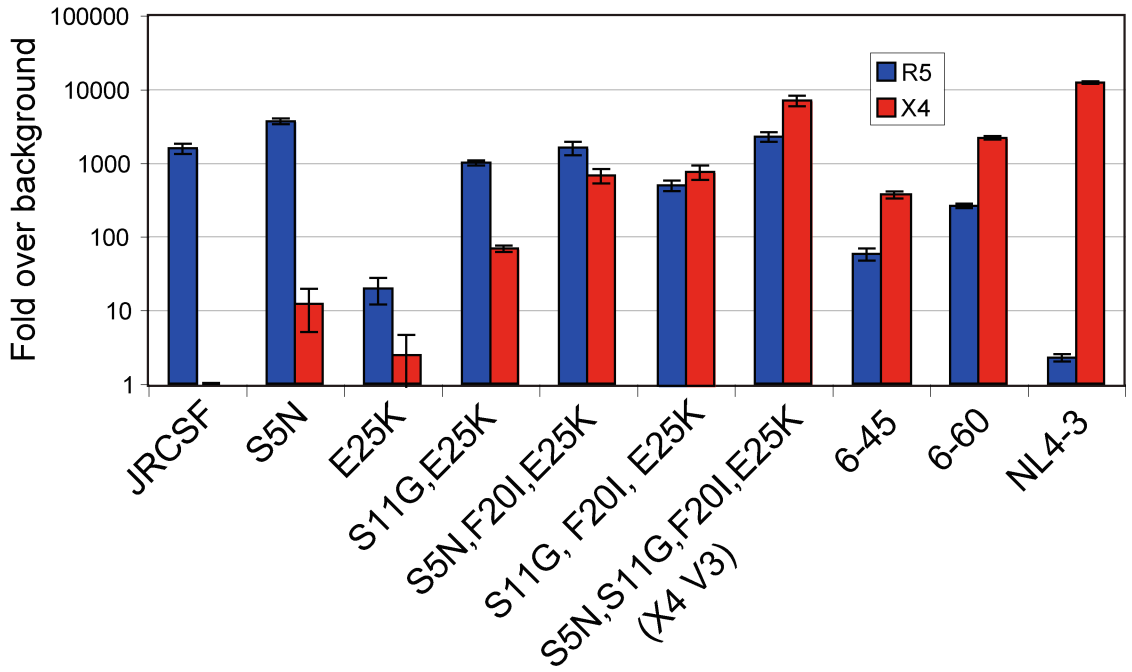

Figure 4.1. X4 and R5 activity JRCSF V3 mutants. Entry activity of virus pseudotyped with various Env mutants on U87.CD4.CCR5 and U87.CD4.CXCR4 was quantitated by luciferase expression. Background was set to un-infected cells. *x*-Axis labels indicate the Env clone or V3 amino acid substitution and position (1-35) and in JRCSF Env. JRCSF is the wild type R5 Env, 6-45 and 6-60 are JRCSF-derived, mouse-adapted X4 viruses. NL4-3 is a prototypical X4 virus.

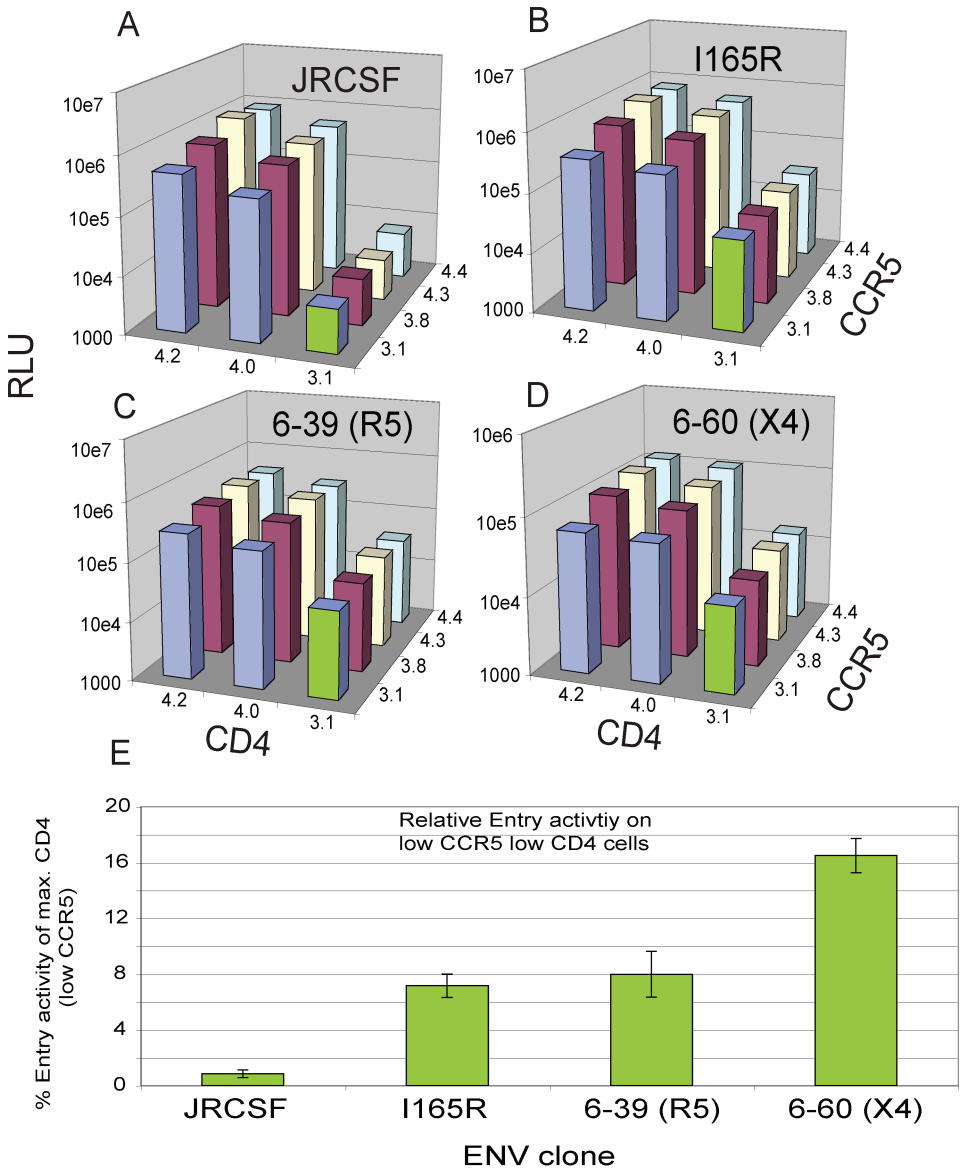

Figure 4.2. Entry activity of pseudotyped virus on cells expressing different levels of CD4 and CCR5. Affinofile cells, 293T cells with differentially inducible CD4 and CCR5 expression, were infected with pseudovirus containing a luciferase expression cassette. Viral entry activity was quantitated by luciferase expression (relative light units (RLU)). A-D. Entry activity at different CD4 (*x*-axis) and CCR5 (*y*-axis) expression levels, indicated as the log(10) antibody binding sites/cell. E. Entry activity of pseudovirus at the lowest CD4 and CCR5 expression levels relative to entry at the low CCR5 and the highest CD4 expression level ($10^{4.7}$ ABS/cell and not presented in A-D).

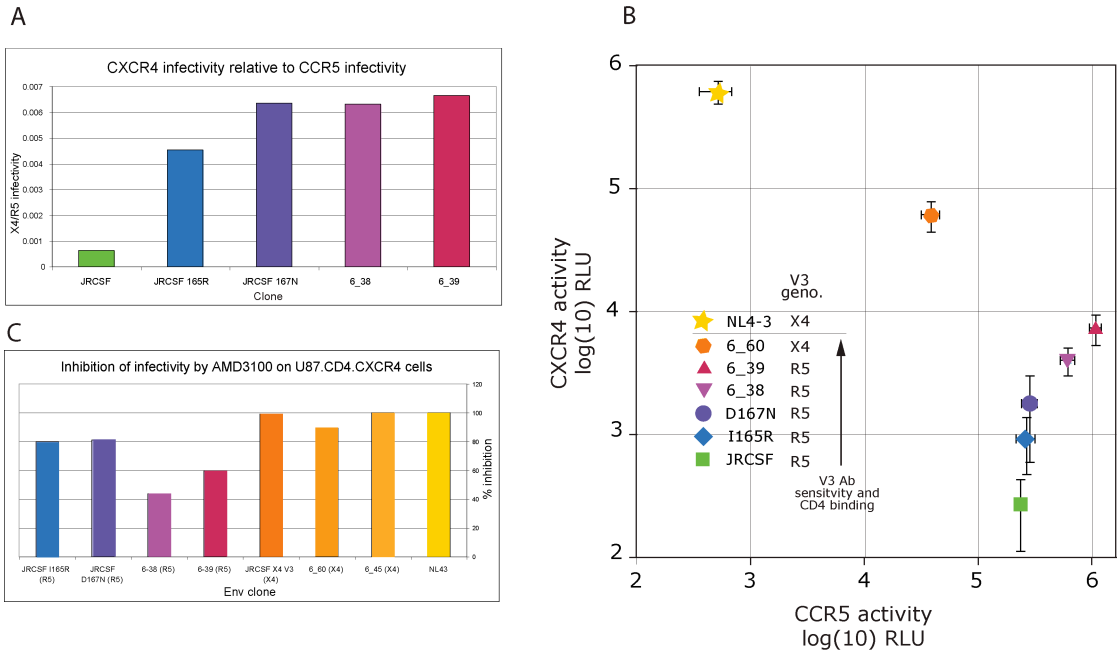

Figure 4.3. Relative X4 and R5 activity and AMD3100 resistance of JRCSF-derived mouse-adapted and mutant Envs. Luciferase activity was assessed for pseudovirus infecting either U87.CD4.CCR5 (*x*-axis) and U87.CD4.CXCR4 (*y*-axis) cells and plotted as the log(10) RLU. A) Infectivty using CD4 and CXCR4 relative to infectivity usingCD4 and CCR5 using data plotted in (B). B) Infectivity on using CD4 and CXCR4 or CCR5. V3 antibody sensitivity and CD4 binding affinity are as indicated in Table 1. V3 genotype (V3 geno.) was determined using X4R5 PSSM (Jensen). C) % inhibiton by a 2.5uM dose of AMD3100.

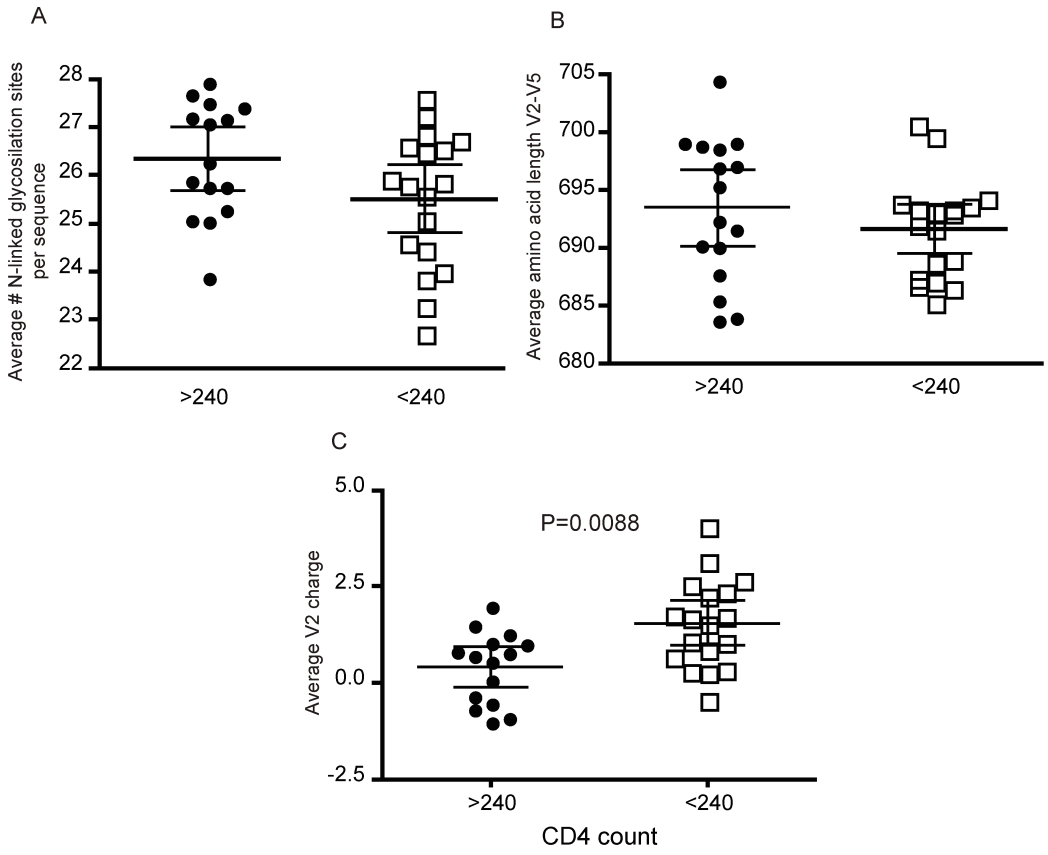

Figure 4.4. Sequence characteristics of V2-V5 region of Env from HIV-1 infected subjects with high and low CD4+ T cell counts. Subjects were divided in to two groups based on CD4+ T cell count (*x*-axis). High: >240; low: <240. A. Average number of N-linked glycosylation sites in the V2-V5 region. Potential N-linked glycosylation sites (PNGL) were predicted using N-Glycosite accessed through the Los Alamos National Laboratories HIV-1 Database website which infers a PNLGS in NXT/S motifs where X≠ P. B. Average amino acid length for the V2-V5 region. C. Average charge of the V2 loop (HXB2 positions 158-198). V2 charge was significantly different between the sequences obtained from subjects with high and low CD4+ T cell counts.

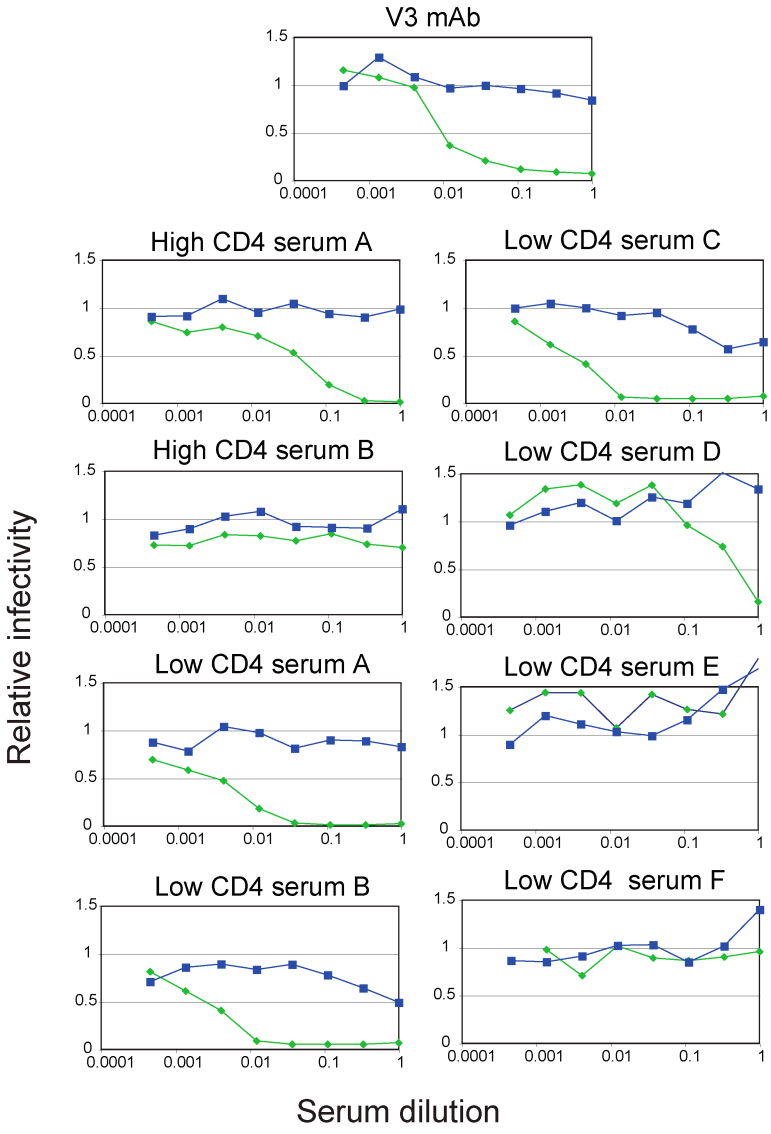

Figure 4.5. Neutralization activity in HIV-1-infected patient sera. Neutralization curves for sera against mouse-derived clone 6-39 (green line), which is highly sensitive to V3 antibodies, and JRCSF (blue line) pseudotyped virus. The viral backbone used contains antiviral resistance mutations. Entry was measured as luciferase activity in TZM-BL cells which contain a viral Tat-responsive luciferase expression cassette. Infectivity was measure relative to entry activity in the absence of serum.

Chapter 5

Conclusions and Future Directions

In this work, I have attempted to shed more light on how HIV-1 Env evolution is shaped by its interaction with a dynamic host environment, particularly the evolving immune response, which is itself shaped by pathogenic effects of the virus. In Chapter 2, I showed that the diverse population of Env variants that develops in the peripheral blood over the course of chronic infection does not represent compartmentalized populations, based on the observation that individual variants decayed at the same rate upon initiation of therapy. I also showed how the gain-of-function phenotype of CXCR4 tropism, which is correlated with immunosuppression, affects the viral population. I found that X4 variants emerge from a single founder and that these variants can co-exist with R5 variants in the host yet replicate in an overlapping cellular compartment. These results indicated that diverse Env phenotypes were not driving compartmentalization in different cell types, as might be expected if CXCR4 and CCR5 are differentially expressed on different susceptible cellular subsets. In Chapter 3, I characterized the evolution of Env in a humanized mouse model, which may be representative of late stage immunosuppression in humans. There

was no detectible HIV-1-specific antibody response in these animals, and it is possible that this is similar to the environment encountered by HIV-1 in humans when CD4+ T helper cell counts are very low and when B cell function has been shown to be impaired. In this environment in the mouse, Env evolved in a manner indicative of a reduced or absent humoral immune response. These changes included a widely observed opening up of Env conformation and a switch in co-receptor tropism in one population. Given these observations, in Chapter 4 I began to explore the factors responsible for the emergence of virus with CXCR4 tropism by dissecting the relationship between different Env phenotypes associated with immunosuppression and CXCR4 tropism. I found that an open Env conformation and increased CD4 binding potentiated entry using CXCR4 and may be a prerequisite phenotype for evolution of CXCR4 tropism in general. I also compared some features of virus adapted to the immunodeficient environment in the mouse to HIV-1 from immunosuppressed individuals, a high percentage of whom had CXCR4-tropic virus, and found that basic changes (that increase charge) in V2 are common among Env variants evolving in immunosuppressed environments in both humans and the humanized mouse.

While the hypothesis that a the loss of a specific antibody response is required for, or at least potentiates, CXCR4-tropism evolution remains viable, additional evidence is required to prove the causative link between the loss of specific antibody pressures and the structural and phenotypic changes that allow HIV-1 to expand its host cell range and ultimately optimize its CXCR4 tropism.

The environmental pressures that select for CXCR4 tropism remain unknown, and are not directly addressed by this hypothesis. It may be determined that evolution of CXCR4 tropism is independent of antibody selective pressures and only dependent on target cell availability or other selective forces. Also, the relationship between CXCR4 emergence and disease progression remain unclear and could provide clues to the selection of CXCR4-tropism emergence.

5.1 Origin of V3 antibodies.

The more open Env conformation that evolves in the absence of antibody selective pressure is thought to resemble more closely the CD4-bound state of gp120 that is primed to bind the coreceptor. One consequence of a more open Env conformation, along with enhanced CD4 binding, sensitivity to soluble CD4, and exposure of other CD4 binding-induced epitopes, is the exposure of V3 and increased V3 antibody sensitivity (9, 77, 192, 235, 270, 313). V3 has also been found to be a potent antigen as evidenced by the abundance of V3 antibodies in patient sera (51, 261, 293). The relative insensitivity of primary isolates to anti-V3 antibodies (13, 192, 293) indicates that the antigen responsible for eliciting this antibody may not be in the neutralization-resistant virion-associated trimer, but rather may be gp120 monomers shed from the cell or particle. V3 antibodies in particular show greatly increased binding to monomers compared to membrane-associated trimers (82). Furthermore, antibody titers generated from monomer-based vaccines show poor neutralization activity. Thus it is likely that the presence of V3 antibody, perhaps by accident of gp120 shedding, keeps Env from evolving a more open conformation.

I should note here that these findings point toward a mechanism of epitope masking that involves inter-molecular interactions between members of the trimer. Whether or not this is the case may be addressed by assessing the phenotypes of heterotrimers assembled with different Env mutants (259). Do Envs that exhibit the loss of conformational masking due to different mechanisms complement each other in a trimer?

5.2 Characterizing the humoral immune response in late stage infection.

The humoral immune response is impaired in HIV-1 infection, particularly in late stage disease (56, 57, 153, 246, 281). However, the extent to which the ability to produce specific antibodies (such as those directed at V3) is lost when the CD4+ T cell count is very low remains unclear. As discussed in Chapter 4, I have generated reagents that may be used to probe for the neutralization activity of specific antibodies in patient sera. Screening with a highly V3 antibody-sensitive Env clone can be used to identify the loss of this activity. This assay can be refined by further confirming the breadth of sensitivity of this Env, perhaps by depletion of V3-specific antibodies from sera. We can then ask the question of whether or not V3 antibody-deficient sera correlate with the presence of specific Env phenotypes, such as the loss of sensitivity to specific antibodies and other phenotypes that are on the path to CXCR4 tropism, as described in Chapter 4. This type of experimental approach can also be used in the case where longitudinal samples are available that span the time when an X4 virus emerges. Are specific antibodies lost prior to CXCR4 emergence? Do V2 mutations that open Env conformation precede and show linkage to the emergent CXCR4 *env*

variant? Finally, a comprehensive assessment of the differences in neutralization sensitivities of HIV-1 populations in which CXCR4 variants have emerged, compared to populations that do not harbor CXCR4 variants, should be carried out, as the current data on this issue are incomplete and conflicting (29, 31, 38, 114, 158, 169, 190).

5.3 Modeling of coreceptor switching.

The role that background phenotypes play in the evolution of CXCR4 tropism can be modeled directly in vitro. Do either of the V2 mutations identified in the humanized mouse (described in Chapter 3), or any V2 mutations identified in human infections with low CD4+ T cell counts (described in Chapter 4), lead to more rapid evolution of CXCR4 tropism in vitro when this phenotype is selected for? The role that particular antibody specificities play in inhibiting Env phenotypic evolution that leads to CXCR4 tropism can also be addressed more directly by modeling evolution in vitro using different monoclonal antibodies as selective agents (8, 173, 270). These types of experiments can be extended to in vivo models, using passive immunization in models that lack a natural antibody response, and depletion of specific B cells or antibodies in models that do.

The interactions between the co-receptor and Envs with background or intermediate CXCR4 tropism phenotypes requires further investigation. It is still unclear how CXCR4 mediates fusion of a virus with a CCR5-tropic V3 loop. One hypothesis is that Interactions with the new coreceptor are mediated predominantly by the N-terminus of the coreceptor. This is suggested by the observation that the CXCR4-binding inhibitor AMD3100 only partially impairs the

low level CXCR4-mediated infectivity of Envs with R5 V3 sequences. This can be tested directly using a peptide that mimics the sulfonated N-terminus of the coreceptor, binds to gp120, and inhibits its interactions with this portion of the coreceptor.

5.4 Compartmentalization and the tissue of origin.

A major factor that likely plays a role in CXCR4 tropism emergence, and also in pathogenesis, is compartmentalization. Where in the body is CXCR4 tropism first selected and in what cell types? Other than a few studies examining autopsy tissue, and only one study that adequately addresses compartmentalization of X4 virus in different cell type (15, 257), there is very little evidence in people that points to the compartment where X4 viruses first emerge. Understanding this aspect of evolution will not only shed light on the selective pressures driving X4 emergence, but also on the pathogenic role of X4 virus. In Chapter 2, I observed that X4 and R5 virus populations were not highly compartmentalized in cross-sectional analysis, making clear that pinpointing the source will be challenging. While studies in SHIV models in which a tropism switch has occurred have provided the opportunity to explore this question (237), it has not been rigorously explored in this setting. Only one study that I am aware of has adequately addressed the question of the tissue compartment origin of CXCR4 tropism in humans (257). In Salemi, *at al*, longitudinal analysis of sequences from the peripheral blood was coupled with sequences obtained from *post mortem* tissue from therapy naïve children that had died of AIDS. Using phylogenetic reconstruction, they found that the X4 variants first emerged in the thymus. This

is not surprising given that this organ harbors highly HIV-susceptible CXCR4-expressing thymocytes and a very limited number of CCR5-expressing cells (25, 138, 321). They also found X4 evolution to be a sequential process, with mutations in the V1/V2 and C2 regions appearing first, similar to my findings in the humanized mouse model. The findings in this study are consistent with the hypothesis that X4 variants take hold in the CXCR4+ CCR5- population of CD4+ T cells, a cell type that is abundant in the thymus, an organ in which active viral replication has observed pathogenic consequences. Whether or not the observation of a thymic origin of X4 virus extends to adults, in whom the cellular population of this organ is altered, remains unclear. While X4 variants may be highly pathogenic in the thymus, this does not necessarily indicate it is the tissue of origin in immunosuppressed adults. Identifying the environmental factors, both systemic and in the tissue and cellular compartments, that select for the changes in the Env phenotypes that coincide with disease progression will aid not only in our understanding HIV-1 pathogenesis but also in our understanding of the fundamental features of enveloped virus evolution.

5.5 Exceptions that prove the rule.

The environmental and Env-intrinsic constraints on Env evolution can also be better understood by examining the factors that limit the emergence of specific phenotypes, such as CXCR4 tropism. For example, the frequent emergence of CXCR4-tropic virus in late stage disease is a typical feature of subtypes B and D, but not subtype C HIV-1 (121, 224). This may be due to intrinsic structural constraints of subtype C (217). Further exploration of the

differences in the structural constraints between subtypes B, C and D may provide clues to the genetic barriers to X4 emergence in these different subtypes. Differences in the environments experienced by different subtypes may also be a factor in determining the different frequencies of Env phenotypes. What is the impact of the fact that the population supporting subtype B infections is relatively homogeneous compared to that supporting subtype C infections?

Finally, what factors limit the transmission of specific phenotypic variants, such as CXCR4- and macrophage-tropic viruses? Understanding the environmental factors that select for the highly CD4-dependent R5 virus that is typically responsible for establishing infection will not only inform the development of transmission prevention strategies, but will also tell us something about the environmental requirements of the phenotypic variants that are not typically transmitted. Conversely, exceptions often prove the rule. CXCR4-tropic variants are transmitted in a limited number of cases and often lead to rapid disease progression. What are the characteristics of the recipients of the phenotypic variants that might lend clues to the selective pressures driving its emergence?

A significant amount of data has been collected in an attempt to answer many of the questions posed above, although a definitive answer to why HIV-1 Env evolves on its relatively predictable path remains elusive. One task that remains is a more thorough re-examination of the assumptions, especially those that have become dogma, some of which are based on weak or possibly misinterpreted data. Testing the hypotheses that I have presented and that flow

from my results will go a long way toward a deeper understanding of Env protein evolution during late-stage HIV-1 infection.

References

1. **Abrahams, M. R., J. A. Anderson, E. E. Giorgi, C. Seoighe, K. Mlisana, L. H. Ping, G. S. Athreya, F. K. Treurnicht, B. F. Keele, N. Wood, J. F. Salazar-Gonzalez, T. Bhattacharya, H. Chu, I. Hoffman, S. Galvin, C. Mapanje, P. Kazembe, R. Thebus, S. Fiscus, W. Hide, M. S. Cohen, S. A. Karim, B. F. Haynes, G. M. Shaw, B. H. Hahn, B. T. Korber, R. Swanstrom, and C. Williamson.** 2009. Quantitating the multiplicity of infection with human immunodeficiency virus type 1 subtype C reveals a non-poisson distribution of transmitted variants. J Virol **83:**3556-67.

2. **Allan, J. S., J. E. Coligan, F. Barin, M. F. McLane, J. G. Sodroski, C. A. Rosen, W. A. Haseltine, T. H. Lee, and M. Essex.** 1985. Major glycoprotein antigens that induce antibodies in AIDS patients are encoded by HTLV-III. Science **228:**1091-4.

3. **An, D. S., B. Poon, R. Ho Tsong Fang, K. Weijer, B. Blom, H. Spits, I. S. Chen, and C. H. Uittenbogaart.** 2007. Use of a novel chimeric mouse model with a functionally active human immune system to study human immunodeficiency virus type 1 infection. Clin Vaccine Immunol **14:**391-6.

4. **An, W., and A. Telesnitsky.** 2002. HIV-1 genetic recombination: experimental approaches and observations. AIDS Rev **4:**195-212.

5. **Arthos, J., C. Cicala, E. Martinelli, K. Macleod, D. Van Ryk, D. Wei, Z. Xiao, T. D. Veenstra, T. P. Conrad, R. A. Lempicki, S. McLaughlin, M. Pascuccio, R. Gopaul, J. McNally, C. C. Cruz, N. Censoplano, E. Chung, K. N. Reitano, S. Kottilil, D. J. Goode, and A. S. Fauci.** 2008. HIV-1 envelope protein binds to and signals through integrin alpha4beta7, the gut mucosal homing receptor for peripheral T cells. Nat Immunol **9:**301-9.

6. **Baba, M., O. Nishimura, N. Kanzaki, M. Okamoto, H. Sawada, Y. Iizawa, M. Shiraishi, Y. Aramaki, K. Okonogi, Y. Ogawa, K. Meguro, and M. Fujino.** 1999. A small-molecule, nonpeptide CCR5 antagonist with highly potent and selective anti-HIV-1 activity. Proc Natl Acad Sci U S A **96:**5698-703.

7. **Baenziger, S., R. Tussiwand, E. Schlaepfer, L. Mazzucchelli, M. Heikenwalder, M. O. Kurrer, S. Behnke, J. Frey, A. Oxenius, H. Joller, A. Aguzzi, M. G. Manz, and R. F. Speck.** 2006. Disseminated and sustained HIV infection in CD34+ cord blood cell-transplanted Rag2-/-gamma c-/- mice. Proc Natl Acad Sci U S A **103:**15951-6.

8. **Beaumont, T., S. Broersen, A. van Nuenen, H. G. Huisman, A. M. de Roda Husman, J. L. Heeney, and H. Schuitemaker.** 2000. Increased neutralization sensitivity and reduced replicative capacity of human

immunodeficiency virus type 1 after short-term in vivo or in vitro passage through chimpanzees. J Virol **74:**7699-707.

9. **Beaumont, T., E. Quakkelaar, A. van Nuenen, R. Pantophlet, and H. Schuitemaker.** 2004. Increased sensitivity to CD4 binding site-directed neutralization following in vitro propagation on primary lymphocytes of a neutralization-resistant human immunodeficiency virus IIIB strain isolated from an accidentally infected laboratory worker. Journal of Virology **78:**5651-5657.

10. **Berges, B. K., S. R. Akkina, J. M. Folkvord, E. Connick, and R. Akkina.** 2008. Mucosal transmission of R5 and X4 tropic HIV-1 via vaginal and rectal routes in humanized Rag2-/- gammac -/- (RAG-hu) mice. Virology **373:**342-51.

11. **Berges, B. K., W. H. Wheat, B. E. Palmer, E. Connick, and R. Akkina.** 2006. HIV-1 infection and CD4 T cell depletion in the humanized Rag2-/- gamma c-/- (RAG-hu) mouse model. Retrovirology **3:**76.

12. **Binley, J. M., E. A. Lybarger, E. T. Crooks, M. S. Seaman, E. Gray, K. L. Davis, J. M. Decker, D. Wycuff, L. Harris, N. Hawkins, B. Wood, C. Nathe, D. Richman, G. D. Tomaras, F. Bibollet-Ruche, J. E. Robinson, L. Morris, G. M. Shaw, D. C. Montefiori, and J. R. Mascola.** 2008. Profiling the specificity of neutralizing antibodies in a large panel of plasmas from patients chronically infected with human immunodeficiency virus type 1 subtypes B and C. J Virol **82:**11651-68.

13. **Binley, J. M., T. Wrin, B. Korber, M. B. Zwick, M. Wang, C. Chappey, G. Stiegler, R. Kunert, S. Zolla-Pazner, H. Katinger, C. J. Petropoulos, and D. R. Burton.** 2004. Comprehensive cross-clade neutralization analysis of a panel of anti-human immunodeficiency virus type 1 monoclonal antibodies. J Virol **78:**13232-52.

14. **Bjorndal, A., H. Deng, M. Jansson, J. R. Fiore, C. Colognesi, A. Karlsson, J. Albert, G. Scarlatti, D. R. Littman, and E. M. Fenyo.** 1997. Coreceptor usage of primary human immunodeficiency virus type 1 isolates varies according to biological phenotype. J Virol **71:**7478-87.

15. **Blaak, H., A. B. van't Wout, M. Brouwer, B. Hooibrink, E. Hovenkamp, and H. Schuitemaker.** 2000. In vivo HIV-1 infection of CD45RA(+)CD4(+) T cells is established primarily by syncytium-inducing variants and correlates with the rate of CD4(+) T cell decline. Proc Natl Acad Sci U S A **97:**1269-74.

16. **Blankson, J. N., D. Finzi, T. C. Pierson, B. P. Sabundayo, K. Chadwick, J. B. Margolick, T. C. Quinn, and R. F. Siliciano.** 2000. Biphasic decay of

latently infected CD4+ T cells in acute human immunodeficiency virus type 1 infection. J Infect Dis **182:**1636-42.

17. **Blay, W. M., S. Gnanakaran, B. Foley, N. A. Doria-Rose, B. T. Korber, and N. L. Haigwood.** 2006. Consistent patterns of change during the divergence of human immunodeficiency virus type 1 envelope from that of the inoculated virus in simian/human immunodeficiency virus-infected macaques. J Virol **80:**999-1014.

18. **Bleul, C. C., M. Farzan, H. Choe, C. Parolin, I. Clark-Lewis, J. Sodroski, and T. A. Springer.** 1996. The lymphocyte chemoattractant SDF-1 is a ligand for LESTR/fusin and blocks HIV-1 entry. Nature **382:**829-33.

19. **Bleul, C. C., L. Wu, J. A. Hoxie, T. A. Springer, and C. R. Mackay.** 1997. The HIV coreceptors CXCR4 and CCR5 are differentially expressed and regulated on human T lymphocytes. Proc Natl Acad Sci U S A **94:**1925-30.

20. **Boots, L. J., P. M. McKenna, B. A. Arnold, P. M. Keller, M. K. Gorny, S. Zolla-Pazner, J. E. Robinson, and A. J. Conley.** 1997. Anti-human immunodeficiency virus type 1 human monoclonal antibodies that bind discontinuous epitopes in the viral glycoproteins can identify mimotopes from recombinant phage peptide display libraries. AIDS Res Hum Retroviruses **13:**1549-59.

21. **Borrow, P., H. Lewicki, B. H. Hahn, G. M. Shaw, and M. B. Oldstone.** 1994. Virus-specific CD8+ cytotoxic T-lymphocyte activity associated with control of viremia in primary human immunodeficiency virus type 1 infection. J Virol **68:**6103-10.

22. **Borrow, P., H. Lewicki, X. Wei, M. S. Horwitz, N. Peffer, H. Meyers, J. A. Nelson, J. E. Gairin, B. H. Hahn, M. B. Oldstone, and G. M. Shaw.** 1997. Antiviral pressure exerted by HIV-1-specific cytotoxic T lymphocytes (CTLs) during primary infection demonstrated by rapid selection of CTL escape virus. Nat Med **3:**205-11.

23. **Brelot, A., N. Heveker, K. Adema, M. J. Hosie, B. Willett, and M. Alizon.** 1999. Effect of mutations in the second extracellular loop of CXCR4 on its utilization by human and feline immunodeficiency viruses. J Virol **73:**2576-86.

24. **Brenchley, J. M., B. J. Hill, D. R. Ambrozak, D. A. Price, F. J. Guenaga, J. P. Casazza, J. Kuruppu, J. Yazdani, S. A. Migueles, M. Connors, M. Roederer, D. C. Douek, and R. A. Koup.** 2004. T-cell subsets that harbor human immunodeficiency virus (HIV) in vivo: implications for HIV pathogenesis. J Virol **78:**1160-8.

25. **Brooks, D. G., S. G. Kitchen, C. M. Kitchen, D. D. Scripture-Adams, and J. A. Zack.** 2001. Generation of HIV latency during thymopoiesis. Nat Med **7:**459-64.

26. **Brown, A. J.** 1997. Analysis of HIV-1 env gene sequences reveals evidence for a low effective number in the viral population. Proc Natl Acad Sci U S A **94:**1862-5.

27. **Buchacher, A., R. Predl, K. Strutzenberger, W. Steinfellner, A. Trkola, M. Purtscher, G. Gruber, C. Tauer, F. Steindl, A. Jungbauer, and et al.** 1994. Generation of human monoclonal antibodies against HIV-1 proteins; electrofusion and Epstein-Barr virus transformation for peripheral blood lymphocyte immortalization. AIDS Res Hum Retroviruses **10:**359-69.

28. **Bunnik, E. M., E. D. Quakkelaar, A. C. van Nuenen, B. Boeser-Nummink, and H. Schuitemaker.** 2007. Increased neutralization sensitivity of recently emerged CXCR4-using human immunodeficiency virus type 1 strains compared to coexisting CCR5-using variants from the same patient. Journal of Virology **81:**525-531.

29. **Bunnik, E. M., E. D. Quakkelaar, A. C. van Nuenen, B. Boeser-Nunnink, and H. Schuitemaker.** 2007. Increased neutralization sensitivity of recently emerged CXCR4-using human immunodeficiency virus type 1 strains compared to coexisting CCR5-using variants from the same patient. J Virol **81:**525-31.

30. **Burkala, E. J., J. He, J. T. West, C. Wood, and C. K. Petito.** 2005. Compartmentalization of HIV-1 in the central nervous system: role of the choroid plexus. Aids **19:**675-84.

31. **Burke, B., N. R. Derby, Z. Kraft, C. J. Saunders, C. Dai, N. Llewellyn, I. Zharkikh, L. Vojtech, T. Zhu, I. K. Srivastava, S. W. Barnett, and L. Stamatatos.** 2006. Viral evolution in macaques coinfected with CCR5- and CXCR4-tropic SHIVs in the presence or absence of vaccine-elicited anti-CCR5 SHIV neutralizing antibodies. Virology **355:**138-51.

32. **Burton, D. R., C. F. Barbas, 3rd, M. A. Persson, S. Koenig, R. M. Chanock, and R. A. Lerner.** 1991. A large array of human monoclonal antibodies to type 1 human immunodeficiency virus from combinatorial libraries of asymptomatic seropositive individuals. Proc Natl Acad Sci U S A **88:**10134-7.

33. **Burton, D. R., J. Pyati, R. Koduri, S. J. Sharp, G. B. Thornton, P. W. Parren, L. S. Sawyer, R. M. Hendry, N. Dunlop, P. L. Nara, and et al.** 1994. Efficient neutralization of primary isolates of HIV-1 by a recombinant human monoclonal antibody. Science **266:**1024-7.

34. **Calarese, D. A., H. K. Lee, C. Y. Huang, M. D. Best, R. D. Astronomo, R. L. Stanfield, H. Katinger, D. R. Burton, C. H. Wong, and I. A. Wilson.** 2005. Dissection of the carbohydrate specificity of the broadly neutralizing anti-HIV-1 antibody 2G12. Proc Natl Acad Sci U S A **102:**13372-7.

35. **Cameron, D. W., M. Heath-Chiozzi, S. Danner, C. Cohen, S. Kravcik, C. Maurath, E. Sun, D. Henry, R. Rode, A. Potthoff, and J. Leonard.** 1998. Randomised placebo-controlled trial of ritonavir in advanced HIV-1 disease. The Advanced HIV Disease Ritonavir Study Group. Lancet **351:**543-9.

36. **Cao, Y. Z., D. Dieterich, P. A. Thomas, Y. X. Huang, M. Mirabile, and D. D. Ho.** 1992. Identification and quantitation of HIV-1 in the liver of patients with AIDS. Aids **6:**65-70.

37. **Casper, C., M. Mild, M. Jansson, A. Karlsson, V. Holmberg, G. Bratt, H. Van Paaschen, P. Biberfeld, A. Bjorndal, J. Albert, M. Popovic, and E. M. Fenyo.** 2005. Coreceptor usage of primary HIV type 1 isolates obtained from different lymph node subsets. AIDS Res Hum Retroviruses **21:**1003-10.

38. **Cecilia, D., V. N. KewalRamani, J. O'Leary, B. Volsky, P. Nyambi, S. Burda, S. Xu, D. R. Littman, and S. Zolla-Pazner.** 1998. Neutralization profiles of primary human immunodeficiency virus type 1 isolates in the context of coreceptor usage. J Virol **72:**6988-96.

39. **Chabot, D. J., and C. C. Broder.** 2000. Substitutions in a homologous region of extracellular loop 2 of CXCR4 and CCR5 alter coreceptor activities for HIV-1 membrane fusion and virus entry. J Biol Chem **275:**23774-82.

40. **Chackerian, B., L. M. Rudensey, and J. Overbaugh.** 1997. Specific N-linked and O-linked glycosylation modifications in the envelope V1 domain of simian immunodeficiency virus variants that evolve in the host alter recognition by neutralizing antibodies. J Virol **71:**7719-27.

41. **Chen, J., D. Powell, and W. S. Hu.** 2006. High frequency of genetic recombination is a common feature of primate lentivirus replication. J Virol **80:**9651-8.

42. **Cheynier, R., S. Henrichwark, F. Hadida, E. Pelletier, E. Oksenhendler, B. Autran, and S. Wain-Hobson.** 1995. Clonal expansion of T cells and HIV genotypes in microdissected splenic white pulps indicates viral replication in situ and infiltration of HIV-specific cytotoxic T lymphocytes. Adv Exp Med Biol **374:**173-82.

43. **Choudhary, S. K., N. L. Rezk, W. L. Ince, M. Cheema, L. Zhang, L. Su, R. Swanstrom, A. D. Kashuba, and D. M. Margolis.** 2009. Suppression of HIV-

1 viremia with reverse transcriptase and integrase inhibitors, CD4+ T cell recovery, and viral rebound upon therapy interruption in a new model for HIV treatment in the humanized Rag2-/- {gamma}c-/- mice. J Virol.

44. **Cole, K. S., J. D. Steckbeck, J. L. Rowles, R. C. Desrosiers, and R. C. Montelaro.** 2004. Removal of N-linked glycosylation sites in the V1 region of simian immunodeficiency virus gp120 results in redirection of B-cell responses to V3. J Virol **78:**1525-39.

45. **Collins, K. L., B. K. Chen, S. A. Kalams, B. D. Walker, and D. Baltimore.** 1998. HIV-1 Nef protein protects infected primary cells against killing by cytotoxic T lymphocytes. Nature **391:**397-401.

46. **Conley, A. J., M. K. Gorny, J. A. Kessler, 2nd, L. J. Boots, M. Ossorio-Castro, S. Koenig, D. W. Lineberger, E. A. Emini, C. Williams, and S. Zolla-Pazner.** 1994. Neutralization of primary human immunodeficiency virus type 1 isolates by the broadly reactive anti-V3 monoclonal antibody, 447-52D. J Virol **68:**6994-7000.

47. **Connor, R. I., B. K. Chen, S. Choe, and N. R. Landau.** 1995. Vpr is required for efficient replication of human immunodeficiency virus type-1 in mononuclear phagocytes. Virology **206:**935-44.

48. **Connor, R. I., H. Mohri, Y. Cao, and D. D. Ho.** 1993. Increased viral burden and cytopathicity correlate temporally with CD4+ T-lymphocyte decline and clinical progression in human immunodeficiency virus type 1-infected individuals. J Virol **67:**1772-7.

49. **Connor, R. I., K. E. Sheridan, D. Ceradini, S. Choe, and N. R. Landau.** 1997. Change in coreceptor use coreceptor use correlates with disease progression in HIV-1--infected individuals. J Exp Med **185:**621-8.

50. **Cormier, E. G., and T. Dragic.** 2002. The crown and stem of the V3 loop play distinct roles in human immunodeficiency virus type 1 envelope glycoprotein interactions with the CCR5 coreceptor. J Virol **76:**8953-7.

51. **Corti, D., J. P. Langedijk, A. Hinz, M. S. Seaman, F. Vanzetta, B. M. Fernandez-Rodriguez, C. Silacci, D. Pinna, D. Jarrossay, S. Balla-Jhagjhoorsingh, B. Willems, M. J. Zekveld, H. Dreja, E. O'Sullivan, C. Pade, C. Orkin, S. A. Jeffs, D. C. Montefiori, D. Davis, W. Weissenhorn, A. McKnight, J. L. Heeney, F. Sallusto, Q. J. Sattentau, R. A. Weiss, and A. Lanzavecchia.** 2010. Analysis of memory B cell responses and isolation of novel monoclonal antibodies with neutralizing breadth from HIV-1-infected individuals. PLoS One **5:**e8805.

52. **Crowe, S., T. Zhu, and W. A. Muller.** 2003. The contribution of monocyte infection and trafficking to viral persistence, and maintenance of the viral reservoir in HIV infection. J Leukoc Biol **74:**635-41.

53. **Cummings, C. J., and H. Y. Zoghbi.** 2000. Trinucleotide repeats: mechanisms and pathophysiology. Annu Rev Genomics Hum Genet **1:**281-328.

54. **Dalgleish, A. G., P. C. Beverley, P. R. Clapham, D. H. Crawford, M. F. Greaves, and R. A. Weiss.** 1984. The CD4 (T4) antigen is an essential component of the receptor for the AIDS retrovirus. Nature **312:**763-7.

55. **De Cock, K. M., M. G. Fowler, E. Mercier, I. de Vincenzi, J. Saba, E. Hoff, D. J. Alnwick, M. Rogers, and N. Shaffer.** 2000. Prevention of mother-to-child HIV transmission in resource-poor countries: translating research into policy and practice. Jama **283:**1175-82.

56. **De Milito, A.** 2004. B lymphocyte dysfunctions in HIV infection. Curr HIV Res **2:**11-21.

57. **De Milito, A., C. Morch, A. Sonnerborg, and F. Chiodi.** 2001. Loss of memory (CD27) B lymphocytes in HIV-1 infection. Aids **15:**957-64.

58. **Delwart, E., M. Magierowska, M. Royz, B. Foley, L. Peddada, R. Smith, C. Heldebrant, A. Conrad, and M. Busch.** 2002. Homogeneous quasispecies in 16 out of 17 individuals during very early HIV-1 primary infection. Aids **16:**189-95.

59. **Delwart, E. L., J. I. Mullins, P. Gupta, G. H. Learn, Jr., M. Holodniy, D. Katzenstein, B. D. Walker, and M. K. Singh.** 1998. Human immunodeficiency virus type 1 populations in blood and semen. J Virol **72:**617-23.

60. **Delwart, E. L., H. W. Sheppard, B. D. Walker, J. Goudsmit, and J. I. Mullins.** 1994. Human immunodeficiency virus type 1 evolution in vivo tracked by DNA heteroduplex mobility assays. J Virol **68:**6672-83.

61. **Deng, H., R. Liu, W. Ellmeier, S. Choe, D. Unutmaz, M. Burkhart, P. Di Marzio, S. Marmon, R. E. Sutton, C. M. Hill, C. B. Davis, S. C. Peiper, T. J. Schall, D. R. Littman, and N. R. Landau.** 1996. Identification of a major co-receptor for primary isolates of HIV-1. Nature **381:**661-6.

62. **Denton, P. W., J. D. Estes, Z. Sun, F. A. Othieno, B. L. Wei, A. K. Wege, D. A. Powell, D. Payne, A. T. Haase, and J. V. Garcia.** 2008. Antiretroviral pre-exposure prophylaxis prevents vaginal transmission of HIV-1 in humanized BLT mice. PLoS Med **5:**e16.

63. **Denton, P. W., and J. V. Garcia.** 2009. Novel humanized murine models for HIV research. Curr HIV/AIDS Rep **6:**13-9.

64. **Derdeyn, C. A., J. M. Decker, F. Bibollet-Ruche, J. L. Mokili, M. Muldoon, S. A. Denham, M. L. Heil, F. Kasolo, R. Musonda, B. H. Hahn, G. M. Shaw, B. T. Korber, S. Allen, and E. Hunter.** 2004. Envelope-constrained neutralization-sensitive HIV-1 after heterosexual transmission. Science **303:**2019-22.

65. **Derdeyn, C. A., J. M. Decker, J. N. Sfakianos, X. Wu, W. A. O'Brien, L. Ratner, J. C. Kappes, G. M. Shaw, and E. Hunter.** 2000. Sensitivity of human immunodeficiency virus type 1 to the fusion inhibitor T-20 is modulated by coreceptor specificity defined by the V3 loop of gp120. J Virol **74:**8358-67.

66. **Des Jarlais, D. C., K. Arasteh, S. Semaan, and E. Wood.** 2009. HIV among injecting drug users: current epidemiology, biologic markers, respondent-driven sampling, and supervised-injection facilities. Curr Opin HIV AIDS **4:**308-13.

67. **Dey, B., M. Pancera, K. Svehla, Y. Shu, S. H. Xiang, J. Vainshtein, Y. Li, J. Sodroski, P. D. Kwong, J. R. Mascola, and R. Wyatt.** 2007. Characterization of human immunodeficiency virus type 1 monomeric and trimeric gp120 glycoproteins stabilized in the CD4-bound state: antigenicity, biophysics, and immunogenicity. J Virol **81:**5579-93.

68. **Diem, K., D. C. Nickle, A. Motoshige, A. Fox, S. Ross, J. I. Mullins, L. Corey, R. W. Coombs, and J. N. Krieger.** 2008. Male genital tract compartmentalization of human immunodeficiency virus type 1 (HIV). AIDS Res Hum Retroviruses **24:**561-71.

69. **Donzella, G. A., D. Schols, S. W. Lin, J. A. Este, K. A. Nagashima, P. J. Maddon, G. P. Allaway, T. P. Sakmar, G. Henson, E. De Clercq, and J. P. Moore.** 1998. AMD3100, a small molecule inhibitor of HIV-1 entry via the CXCR4 co-receptor. Nat Med **4:**72-7.

70. **Doranz, B. J., M. J. Orsini, J. D. Turner, T. L. Hoffman, J. F. Berson, J. A. Hoxie, S. C. Peiper, L. F. Brass, and R. W. Doms.** 1999. Identification of CXCR4 domains that support coreceptor and chemokine receptor functions. J Virol **73:**2752-61.

71. **Doranz, B. J., J. Rucker, Y. Yi, R. J. Smyth, M. Samson, S. C. Peiper, M. Parmentier, R. G. Collman, and R. W. Doms.** 1996. A dual-tropic primary HIV-1 isolate that uses fusin and the beta-chemokine receptors CKR-5, CKR-3, and CKR-2b as fusion cofactors. Cell **85:**1149-58.

72. **Dunfee, R. L., E. R. Thomas, and D. Gabuzda.** 2009. Enhanced macrophage tropism of HIV in brain and lymphoid tissues is associated with sensitivity to the broadly neutralizing CD4 binding site antibody b12. Retrovirology **6:**69.

73. **Dunfee, R. L., E. R. Thomas, P. R. Gorry, J. Wang, J. Taylor, K. Kunstman, S. M. Wolinsky, and D. Gabuzda.** 2006. The HIV Env variant N283 enhances macrophage tropism and is associated with brain infection and dementia. Proc Natl Acad Sci U S A **103:**15160-5.

74. **Dunfee, R. L., E. R. Thomas, J. Wang, K. Kunstman, S. M. Wolinsky, and D. Gabuzda.** 2007. Loss of the N-linked glycosylation site at position 386 in the HIV envelope V4 region enhances macrophage tropism and is associated with dementia. Virology **367:**222-34.

75. **Edinger, A. L., J. L. Mankowski, B. J. Doranz, B. J. Margulies, B. Lee, J. Rucker, M. Sharron, T. L. Hoffman, J. F. Berson, M. C. Zink, V. M. Hirsch, J. E. Clements, and R. W. Doms.** 1997. CD4-independent, CCR5-dependent infection of brain capillary endothelial cells by a neurovirulent simian immunodeficiency virus strain. Proc Natl Acad Sci U S A **94:**14742-7.

76. **Edmonson, P. F., and J. I. Mullins.** 1992. Efficient amplification of HIV half-genomes from tissue DNA. Nucleic Acids Res **20:**4933.

77. **Edwards, T. G., T. L. Hoffman, F. Baribaud, S. Wyss, C. C. LaBranche, J. Romano, J. Adkinson, M. Sharron, J. A. Hoxie, and R. W. Doms.** 2001. Relationships between CD4 independence, neutralization sensitivity, and exposure of a CD4-induced epitope in a human immunodeficiency virus type 1 envelope protein. J Virol **75:**5230-9.

78. **Endres, M. J., P. R. Clapham, M. Marsh, M. Ahuja, J. D. Turner, A. McKnight, J. F. Thomas, B. Stoebenau-Haggarty, S. Choe, P. J. Vance, T. N. Wells, C. A. Power, S. S. Sutterwala, R. W. Doms, N. R. Landau, and J. A. Hoxie.** 1996. CD4-independent infection by HIV-2 is mediated by fusin/CXCR4. Cell **87:**745-56.

79. **Feng, Y., C. C. Broder, P. E. Kennedy, and E. A. Berger.** 1996. HIV-1 entry cofactor: functional cDNA cloning of a seven-transmembrane, G protein-coupled receptor. Science **272:**872-7.

80. **Fiebig, E. W., D. J. Wright, B. D. Rawal, P. E. Garrett, R. T. Schumacher, L. Peddada, C. Heldebrant, R. Smith, A. Conrad, S. H. Kleinman, and M. P. Busch.** 2003. Dynamics of HIV viremia and antibody seroconversion in plasma donors: implications for diagnosis and staging of primary HIV infection. Aids **17:**1871-9.

81. **Fouchier, R. A., M. Groenink, N. A. Kootstra, M. Tersmette, H. G. Huisman, F. Miedema, and H. Schuitemaker.** 1992. Phenotype-associated sequence variation in the third variable domain of the human immunodeficiency virus type 1 gp120 molecule. J Virol **66:**3183-7.

82. **Fouts, T. R., J. M. Binley, A. Trkola, J. E. Robinson, and J. P. Moore.** 1997. Neutralization of the human immunodeficiency virus type 1 primary isolate JR-FL by human monoclonal antibodies correlates with antibody binding to the oligomeric form of the envelope glycoprotein complex. J Virol **71:**2779-85.

83. **Fox, D. G., P. Balfe, C. P. Palmer, J. C. May, C. Arnold, and J. A. McKeating.** 1997. Length polymorphism within the second variable region of the human immunodeficiency virus type 1 envelope glycoprotein affects accessibility of the receptor binding site. J Virol **71:**759-65.

84. **Fransen, S., G. Bridger, J. M. Whitcomb, J. Toma, E. Stawiski, N. Parkin, C. J. Petropoulos, and W. Huang.** 2008. Suppression of dualtropic human immunodeficiency virus type 1 by the CXCR4 antagonist AMD3100 is associated with efficiency of CXCR4 use and baseline virus composition. Antimicrob Agents Chemother **52:**2608-15.

85. **Frost, S. D., M. J. Dumaurier, S. Wain-Hobson, and A. J. Brown.** 2001. Genetic drift and within-host metapopulation dynamics of HIV-1 infection. Proc Natl Acad Sci U S A **98:**6975-80.

86. **Frost, S. D., Y. Liu, S. L. Pond, C. Chappey, T. Wrin, C. J. Petropoulos, S. J. Little, and D. D. Richman.** 2005. Characterization of human immunodeficiency virus type 1 (HIV-1) envelope variation and neutralizing antibody responses during transmission of HIV-1 subtype B. J Virol **79:**6523-7.

87. **Frost, S. D., T. Wrin, D. M. Smith, S. L. Kosakovsky Pond, Y. Liu, E. Paxinos, C. Chappey, J. Galovich, J. Beauchaine, C. J. Petropoulos, S. J. Little, and D. D. Richman.** 2005. Neutralizing antibody responses drive the evolution of human immunodeficiency virus type 1 envelope during recent HIV infection. Proc Natl Acad Sci U S A **102:**18514-9.

88. **Fulcher, J. A., Y. Hwangbo, R. Zioni, D. Nickle, X. Lin, L. Heath, J. I. Mullins, L. Corey, and T. Zhu.** 2004. Compartmentalization of human immunodeficiency virus type 1 between blood monocytes and CD4+ T cells during infection. J Virol **78:**7883-93.

89. **Gao, F., E. Bailes, D. L. Robertson, Y. Chen, C. M. Rodenburg, S. F. Michael, L. B. Cummins, L. O. Arthur, M. Peeters, G. M. Shaw, P. M. Sharp, and B. H. Hahn.** 1999. Origin of HIV-1 in the chimpanzee Pan troglodytes troglodytes. Nature **397:**436-41.

90. **Gartner, S., P. Markovits, D. M. Markovitz, M. H. Kaplan, R. C. Gallo, and M. Popovic.** 1986. The role of mononuclear phagocytes in HTLV-III/LAV infection. Science **233:**215-9.

91. **Gavel, Y., and G. von Heijne.** 1990. Sequence differences between glycosylated and non-glycosylated Asn-X-Thr/Ser acceptor sites: implications for protein engineering. Protein Eng **3:**433-42.

92. **Gondois-Rey, F., A. Biancotto, M. A. Fernandez, L. Bettendroffer, J. Blazkova, K. Trejbalova, M. Pion, and I. Hirsch.** 2006. R5 variants of human immunodeficiency virus type 1 preferentially infect CD62L- CD4+ T cells and are potentially resistant to nucleoside reverse transcriptase inhibitors. J Virol **80:**854-65.

93. **Goonetilleke, N., M. K. Liu, J. F. Salazar-Gonzalez, G. Ferrari, E. Giorgi, V. V. Ganusov, B. F. Keele, G. H. Learn, E. L. Turnbull, M. G. Salazar, K. J. Weinhold, S. Moore, N. Letvin, B. F. Haynes, M. S. Cohen, P. Hraber, T. Bhattacharya, P. Borrow, A. S. Perelson, B. H. Hahn, G. M. Shaw, B. T. Korber, and A. J. McMichael.** 2009. The first T cell response to transmitted/founder virus contributes to the control of acute viremia in HIV-1 infection. J Exp Med **206:**1253-72.

94. **Gorantla, S., H. Sneller, L. Walters, J. G. Sharp, S. J. Pirruccello, J. T. West, C. Wood, S. Dewhurst, H. E. Gendelman, and L. Poluektova.** 2007. Human immunodeficiency virus type 1 pathobiology studied in humanized BALB/c-Rag2-/-gammac-/- mice. J Virol **81:**2700-12.

95. **Gorry, P. R., J. Taylor, G. H. Holm, A. Mehle, T. Morgan, M. Cayabyab, M. Farzan, H. Wang, J. E. Bell, K. Kunstman, J. P. Moore, S. M. Wolinsky, and D. Gabuzda.** 2002. Increased CCR5 affinity and reduced CCR5/CD4 dependence of a neurovirulent primary human immunodeficiency virus type 1 isolate. J Virol **76:**6277-92.

96. **Gratton, S., R. Cheynier, M. J. Dumaurier, E. Oksenhendler, and S. Wain-Hobson.** 2000. Highly restricted spread of HIV-1 and multiply infected cells within splenic germinal centers. Proc Natl Acad Sci U S A **97:**14566-71.

97. **Gray, L., J. Sterjovski, M. Churchill, P. Ellery, N. Nasr, S. R. Lewin, S. M. Crowe, S. L. Wesselingh, A. L. Cunningham, and P. R. Gorry.** 2005. Uncoupling coreceptor usage of human immunodeficiency virus type 1 (HIV-1) from macrophage tropism reveals biological properties of CCR5-restricted

HIV-1 isolates from patients with acquired immunodeficiency syndrome. Virology **337:**384-98.

98. **Guadalupe, M., E. Reay, S. Sankaran, T. Prindiville, J. Flamm, A. McNeil, and S. Dandekar.** 2003. Severe CD4+ T-cell depletion in gut lymphoid tissue during primary human immunodeficiency virus type 1 infection and substantial delay in restoration following highly active antiretroviral therapy. J Virol **77:**11708-17.

99. **Guindon, S., and O. Gascuel.** 2003. A simple, fast, and accurate algorithm to estimate large phylogenies by maximum likelihood. Syst Biol **52:**696-704.

100. **Gulick, R. M., X. J. Hu, S. A. Fiscus, C. V. Fletcher, R. Haubrich, H. Cheng, E. Acosta, S. W. Lagakos, R. Swanstrom, W. Freimuth, S. Snyder, C. Mills, M. Fischl, C. Pettinelli, and D. Katzenstein.** 2000. Randomized study of saquinavir with ritonavir or nelfinavir together with delavirdine, adefovir, or both in human immunodeficiency virus-infected adults with virologic failure on indinavir: AIDS Clinical Trials Group Study 359. J Infect Dis **182:**1375-84.

101. **Haddad, D. N., C. Birch, T. Middleton, D. E. Dwyer, A. L. Cunningham, and N. K. Saksena.** 2000. Evidence for late stage compartmentalization of HIV-1 resistance mutations between lymph node and peripheral blood mononuclear cells. Aids **14:**2273-81.

102. **Hallenberger, S., V. Bosch, H. Angliker, E. Shaw, H. D. Klenk, and W. Garten.** 1992. Inhibition of furin-mediated cleavage activation of HIV-1 glycoprotein gp160. Nature **360:**358-61.

103. **Harouse, J. M., C. Buckner, A. Gettie, R. Fuller, R. Bohm, J. Blanchard, and C. Cheng-Mayer.** 2003. CD8+ T cell-mediated CXC chemokine receptor 4-simian/human immunodeficiency virus suppression in dually infected rhesus macaques. Proc Natl Acad Sci U S A **100:**10977-82.

104. **Harrington, P. R., M. J. Connell, R. B. Meeker, P. R. Johnson, and R. Swanstrom.** 2007. Dynamics of simian immunodeficiency virus populations in blood and cerebrospinal fluid over the full course of infection. J Infect Dis **196:**1058-67.

105. **Harrington, P. R., D. W. Haas, K. Ritola, and R. Swanstrom.** 2005. Compartmentalized human immunodeficiency virus type 1 present in cerebrospinal fluid is produced by short-lived cells. J Virol **79:**7959-66.

106. **Harrington, P. R., J. A. Nelson, K. M. Kitrinos, and R. Swanstrom.** 2007. Independent evolution of human immunodeficiency virus type 1 env V1/V2 and V4/V5 hypervariable regions during chronic infection. J Virol **81:**5413-7.

107. **Harris, R. S., K. N. Bishop, A. M. Sheehy, H. M. Craig, S. K. Petersen-Mahrt, I. N. Watt, M. S. Neuberger, and M. H. Malim.** 2003. DNA deamination mediates innate immunity to retroviral infection. Cell **113:**803-9.

108. **He, J., S. Choe, R. Walker, P. Di Marzio, D. O. Morgan, and N. R. Landau.** 1995. Human immunodeficiency virus type 1 viral protein R (Vpr) arrests cells in the G2 phase of the cell cycle by inhibiting p34cdc2 activity. J Virol **69:**6705-11.

109. **He, J., and N. R. Landau.** 1995. Use of a novel human immunodeficiency virus type 1 reporter virus expressing human placental alkaline phosphatase to detect an alternative viral receptor. J Virol **69:**4587-92.

110. **Heinzinger, N. K., M. I. Bukinsky, S. A. Haggerty, A. M. Ragland, V. Kewalramani, M. A. Lee, H. E. Gendelman, L. Ratner, M. Stevenson, and M. Emerman.** 1994. The Vpr protein of human immunodeficiency virus type 1 influences nuclear localization of viral nucleic acids in nondividing host cells. Proc Natl Acad Sci U S A **91:**7311-5.

111. **Henderson, G. J., N. G. Hoffman, L. H. Ping, S. A. Fiscus, I. F. Hoffman, K. M. Kitrinos, T. Banda, F. E. Martinson, P. N. Kazembe, D. A. Chilongozi, M. S. Cohen, and R. Swanstrom.** 2004. HIV-1 populations in blood and breast milk are similar. Virology **330:**295-303.

112. **Hendrix, C. W., C. Flexner, R. T. MacFarland, C. Giandomenico, E. J. Fuchs, E. Redpath, G. Bridger, and G. W. Henson.** 2000. Pharmacokinetics and safety of AMD-3100, a novel antagonist of the CXCR-4 chemokine receptor, in human volunteers. Antimicrob Agents Chemother **44:**1667-73.

113. **Ho, D. D., A. U. Neumann, A. S. Perelson, W. Chen, J. M. Leonard, and M. Markowitz.** 1995. Rapid turnover of plasma virions and CD4 lymphocytes in HIV-1 infection. Nature **373:**123-6.

114. **Ho, S. H., S. Tasca, L. Shek, A. Li, A. Gettie, J. Blanchard, D. Boden, and C. Cheng-Mayer.** 2007. Coreceptor switch in R5-tropic simian/human immunodeficiency virus-infected macaques. J Virol **81:**8621-33.

115. **Ho, S. H., N. Trunova, A. Gettie, J. Blanchard, and C. Cheng-Mayer.** 2008. Different mutational pathways to CXCR4 coreceptor switch of CCR5-using simian-human immunodeficiency virus. J Virol **82:**5653-6.

116. **Hofer, U., S. Baenziger, M. Heikenwalder, E. Schlaepfer, N. Gehre, S. Regenass, T. Brunner, and R. F. Speck.** 2008. RAG2-/- gamma(c)-/- mice transplanted with CD34+ cells from human cord blood show low levels of intestinal engraftment and are resistant to rectal transmission of human immunodeficiency virus. J Virol **82:**12145-53.

117. **Hoffman, N. G., F. Seillier-Moiseiwitsch, J. Ahn, J. M. Walker, and R. Swanstrom.** 2002. Variability in the human immunodeficiency virus type 1 gp120 Env protein linked to phenotype-associated changes in the V3 loop. J Virol **76:**3852-64.

118. **Hoffman, T. L., C. C. LaBranche, W. Zhang, G. Canziani, J. Robinson, I. Chaiken, J. A. Hoxie, and R. W. Doms.** 1999. Stable exposure of the coreceptor-binding site in a CD4-independent HIV-1 envelope protein. Proc Natl Acad Sci U S A **96:**6359-64.

119. **Huang, C. C., S. N. Lam, P. Acharya, M. Tang, S. H. Xiang, S. S. Hussan, R. L. Stanfield, J. Robinson, J. Sodroski, I. A. Wilson, R. Wyatt, C. A. Bewley, and P. D. Kwong.** 2007. Structures of the CCR5 N terminus and of a tyrosine-sulfated antibody with HIV-1 gp120 and CD4. Science **317:**1930-4.

120. **Huang, C. C., M. Tang, M. Y. Zhang, S. Majeed, E. Montabana, R. L. Stanfield, D. S. Dimitrov, B. Korber, J. Sodroski, I. A. Wilson, R. Wyatt, and P. D. Kwong.** 2005. Structure of a V3-containing HIV-1 gp120 core. Science **310:**1025-8.

121. **Huang, W., S. H. Eshleman, J. Toma, S. Fransen, E. Stawiski, E. E. Paxinos, J. M. Whitcomb, A. M. Young, D. Donnell, F. Mmiro, P. Musoke, L. A. Guay, J. B. Jackson, N. T. Parkin, and C. J. Petropoulos.** 2007. Coreceptor tropism in human immunodeficiency virus type 1 subtype D: high prevalence of CXCR4 tropism and heterogeneous composition of viral populations. J Virol **81:**7885-93.

122. **Hudson, R. R., D. D. Boos, and N. L. Kaplan.** 1992. A statistical test for detecting geographic subdivision. Mol Biol Evol **9:**138-51.

123. **Igarashi, T., O. K. Donau, H. Imamichi, Y. Nishimura, T. S. Theodore, R. Iyengar, C. Erb, A. Buckler-White, C. E. Buckler, and M. A. Martin.** 2007. Although macrophage-tropic simian/human immunodeficiency viruses can exhibit a range of pathogenic phenotypes, a majority of isolates induce no clinical disease in immunocompetent macaques. J Virol **81:**10669-79.

124. **Igarashi, T., H. Imamichi, C. R. Brown, V. M. Hirsch, and M. A. Martin.** 2003. The emergence and characterization of macrophage-tropic SIV/HIV chimeric viruses (SHIVs) present in CD4+ T cell-depleted rhesus monkeys. J Leukoc Biol **74:**772-80.

125. **Imamichi, H., T. Igarashi, T. Imamichi, O. K. Donau, Y. Endo, Y. Nishimura, R. L. Willey, A. F. Suffredini, H. C. Lane, and M. A. Martin.** 2002. Amino acid deletions are introduced into the V2 region of gp120 during independent pathogenic simian immunodeficiency virus/HIV chimeric virus

(SHIV) infections of rhesus monkeys generating variants that are macrophage tropic. Proc Natl Acad Sci U S A **99:**13813-8.

126. **Ince, W. L., P. R. Harrington, G. L. Schnell, M. Patel-Chhabra, C. L. Burch, P. Menezes, R. W. Price, J. J. Eron, Jr., and R. I. Swanstrom.** 2009. Major coexisting human immunodeficiency virus type 1 env gene subpopulations in the peripheral blood are produced by cells with similar turnover rates and show little evidence of genetic compartmentalization. J Virol **83:**4068-80.

127. **Ince, W. L., L. Zhang, Q. Jiang, K. Arrildt, L. Su, and R. Swanstrom.** 2010. Evolution of the HIV-1 env gene in the Rag2-/- gammaC-/- humanized mouse model. J Virol **84:**2740-52.

128. **Ishikawa, F., M. Yasukawa, B. Lyons, S. Yoshida, T. Miyamoto, G. Yoshimoto, T. Watanabe, K. Akashi, L. D. Shultz, and M. Harada.** 2005. Development of functional human blood and immune systems in NOD/SCID/IL2 receptor {gamma} chain(null) mice. Blood **106:**1565-73.

129. **Jensen, M. A., F. S. Li, A. B. van 't Wout, D. C. Nickle, D. Shriner, H. X. He, S. McLaughlin, R. Shankarappa, J. B. Margolick, and J. I. Mullins.** 2003. Improved coreceptor usage prediction and genotypic monitoring of R5-to-X4 transition by motif analysis of human immunodeficiency virus type 1 env V3 loop sequences. J Virol **77:**13376-88.

130. **Jern, P., R. A. Russell, V. K. Pathak, and J. M. Coffin.** 2009. Likely role of APOBEC3G-mediated G-to-A mutations in HIV-1 evolution and drug resistance. PLoS Pathog **5:**e1000367.

131. **Jiang, Q., L. Zhang, R. Wang, J. Jeffrey, M. L. Washburn, D. Brouwer, S. Barbour, G. I. Kovalev, D. Unutmaz, and L. Su.** 2008. FoxP3+CD4+ regulatory T cells play an important role in acute HIV-1 infection in humanized Rag2-/-gammaC-/- mice in vivo. Blood **112:**2858-68.

132. **Johnston, S. H., M. A. Lobritz, S. Nguyen, K. Lassen, S. Delair, F. Posta, Y. J. Bryson, E. J. Arts, T. Chou, and B. Lee.** 2009. A quantitative affinity-profiling system that reveals distinct CD4/CCR5 usage patterns among human immunodeficiency virus type 1 and simian immunodeficiency virus strains. J Virol **83:**11016-26.

133. **Katoh, K., and H. Toh.** 2008. Recent developments in the MAFFT multiple sequence alignment program. Brief Bioinform **9:**286-98.

134. **Keele, B. F., E. E. Giorgi, J. F. Salazar-Gonzalez, J. M. Decker, K. T. Pham, M. G. Salazar, C. Sun, T. Grayson, S. Wang, H. Li, X. Wei, C. Jiang, J. L. Kirchherr, F. Gao, J. A. Anderson, L. H. Ping, R. Swanstrom, G. D. Tomaras, W. A. Blattner, P. A. Goepfert, J. M. Kilby, M. S. Saag, E.**

L. Delwart, M. P. Busch, M. S. Cohen, D. C. Montefiori, B. F. Haynes, B. Gaschen, G. S. Athreya, H. Y. Lee, N. Wood, C. Seoighe, A. S. Perelson, T. Bhattacharya, B. T. Korber, B. H. Hahn, and G. M. Shaw. 2008. Identification and characterization of transmitted and early founder virus envelopes in primary HIV-1 infection. Proc Natl Acad Sci U S A **105:**7552-7.

135. **Keele, B. F., F. Van Heuverswyn, Y. Li, E. Bailes, J. Takehisa, M. L. Santiago, F. Bibollet-Ruche, Y. Chen, L. V. Wain, F. Liegeois, S. Loul, E. M. Ngole, Y. Bienvenue, E. Delaporte, J. F. Brookfield, P. M. Sharp, G. M. Shaw, M. Peeters, and B. H. Hahn.** 2006. Chimpanzee reservoirs of pandemic and nonpandemic HIV-1. Science **313:**523-6.

136. **Kemal, K. S., B. Foley, H. Burger, K. Anastos, H. Minkoff, C. Kitchen, S. M. Philpott, W. Gao, E. Robison, S. Holman, C. Dehner, S. Beck, W. A. Meyer, 3rd, A. Landay, A. Kovacs, J. Bremer, and B. Weiser.** 2003. HIV-1 in genital tract and plasma of women: compartmentalization of viral sequences, coreceptor usage, and glycosylation. Proc Natl Acad Sci U S A **100:**12972-7.

137. **Kirchherr, J. L., X. Lu, W. Kasongo, V. Chalwe, L. Mwananyanda, R. M. Musonda, S. M. Xia, R. M. Scearce, H. X. Liao, D. C. Montefiori, B. F. Haynes, and F. Gao.** 2007. High throughput functional analysis of HIV-1 env genes without cloning. J Virol Methods **143:**104-11.

138. **Kitchen, S. G., and J. A. Zack.** 1997. CXCR4 expression during lymphopoiesis: implications for human immunodeficiency virus type 1 infection of the thymus. J Virol **71:**6928-34.

139. **Kitrinos, K. M., N. G. Hoffman, J. A. Nelson, and R. Swanstrom.** 2003. Turnover of env variable region 1 and 2 genotypes in subjects with late-stage human immunodeficiency virus type 1 infection. J Virol **77:**6811-22.

140. **Klatzmann, D., E. Champagne, S. Chamaret, J. Gruest, D. Guetard, T. Hercend, J. C. Gluckman, and L. Montagnier.** 1984. T-lymphocyte T4 molecule behaves as the receptor for human retrovirus LAV. Nature **312:**767-8.

141. **Koch, M., M. Pancera, P. D. Kwong, P. Kolchinsky, C. Grundner, L. Wang, W. A. Hendrickson, J. Sodroski, and R. Wyatt.** 2003. Structure-based, targeted deglycosylation of HIV-1 gp120 and effects on neutralization sensitivity and antibody recognition. Virology **313:**387-400.

142. **Koito, A., G. Harrowe, J. A. Levy, and C. Cheng-Mayer.** 1994. Functional role of the V1/V2 region of human immunodeficiency virus type 1 envelope glycoprotein gp120 in infection of primary macrophages and soluble CD4 neutralization. J Virol **68:**2253-9.

143. **Kolchinsky, P., E. Kiprilov, and J. Sodroski.** 2001. Increased neutralization sensitivity of CD4-independent human immunodeficiency virus variants. Journal of Virology **75:**2041-2050.

144. **Koot, M., R. van Leeuwen, R. E. de Goede, I. P. Keet, S. Danner, J. K. Eeftinck Schattenkerk, P. Reiss, M. Tersmette, J. M. Lange, and H. Schuitemaker.** 1999. Conversion rate towards a syncytium-inducing (SI) phenotype during different stages of human immunodeficiency virus type 1 infection and prognostic value of SI phenotype for survival after AIDS diagnosis. J Infect Dis **179:**254-8.

145. **Korber, B.** 2000. HIV Signature and Sequence Variation Analysis, p. 55-72. *In* A. G. a. L. Rodrigo, G. H. (ed.), Computational Analysis of HIV Molecular Sequences. Kluwer Academic Publishers, Dordrecht, Netherlands.

146. **Korber, B., B. Gaschen, K. Yusim, R. Thakallapally, C. Kesmir, and V. Detours.** 2001. Evolutionary and immunological implications of contemporary HIV-1 variation. Br Med Bull **58:**19-42.

147. **Korber, B., and G. Myers.** 1992. Signature pattern analysis: a method for assessing viral sequence relatedness. AIDS Res Hum Retroviruses **8:**1549-60.

148. **Korber, B. T., K. J. Kunstman, B. K. Patterson, M. Furtado, M. M. McEvilly, R. Levy, and S. M. Wolinsky.** 1994. Genetic differences between blood- and brain-derived viral sequences from human immunodeficiency virus type 1-infected patients: evidence of conserved elements in the V3 region of the envelope protein of brain-derived sequences. J Virol **68:**7467-81.

149. **Koup, R. A., J. T. Safrit, Y. Cao, C. A. Andrews, G. McLeod, W. Borkowsky, C. Farthing, and D. D. Ho.** 1994. Temporal association of cellular immune responses with the initial control of viremia in primary human immunodeficiency virus type 1 syndrome. J Virol **68:**4650-5.

150. **Koyanagi, Y., S. Miles, R. T. Mitsuyasu, J. E. Merrill, H. V. Vinters, and I. S. Chen.** 1987. Dual infection of the central nervous system by AIDS viruses with distinct cellular tropisms. Science **236:**819-22.

151. **Kraase, M., R. Sloan, D. Klein, N. Logan, L. McMonagle, R. Biek, B. J. Willett, and M. J. Hosie.** 2010. Feline immunodeficiency virus env gene evolution in experimentally infected cats. Vet Immunol Immunopathol **134:**96-106.

152. **Krachmarov, C., A. Pinter, W. J. Honnen, M. K. Gorny, P. N. Nyambi, S. Zolla-Pazner, and S. C. Kayman.** 2005. Antibodies that are cross-reactive for human immunodeficiency virus type 1 clade a and clade B v3 domains are

common in patient sera from Cameroon, but their neutralization activity is usually restricted by epitope masking. J Virol **79:**780-90.

153. **Kroon, F. P., J. T. van Dissel, E. Ravensbergen, P. H. Nibbering, and R. van Furth.** 1999. Impaired antibody response after immunization of HIV-infected individuals with the polysaccharide vaccine against Salmonella typhi (Typhim-Vi). Vaccine **17:**2941-5.

154. **Kumar, P., H. S. Ban, S. S. Kim, H. Wu, T. Pearson, D. L. Greiner, A. Laouar, J. Yao, V. Haridas, K. Habiro, Y. G. Yang, J. H. Jeong, K. Y. Lee, Y. H. Kim, S. W. Kim, M. Peipp, G. H. Fey, N. Manjunath, L. D. Shultz, S. K. Lee, and P. Shankar.** 2008. T cell-specific siRNA delivery suppresses HIV-1 infection in humanized mice. Cell **134:**577-86.

155. **Kuritzkes, D. R.** 2009. HIV-1 entry inhibitors: an overview. Curr Opin HIV AIDS **4:**82-7.

156. **Kwong, P. D., M. L. Doyle, D. J. Casper, C. Cicala, S. A. Leavitt, S. Majeed, T. D. Steenbeke, M. Venturi, I. Chaiken, M. Fung, H. Katinger, P. W. Parren, J. Robinson, D. Van Ryk, L. Wang, D. R. Burton, E. Freire, R. Wyatt, J. Sodroski, W. A. Hendrickson, and J. Arthos.** 2002. HIV-1 evades antibody-mediated neutralization through conformational masking of receptor-binding sites. Nature **420:**678-82.

157. **Kwong, P. D., R. Wyatt, J. Robinson, R. W. Sweet, J. Sodroski, and W. A. Hendrickson.** 1998. Structure of an HIV gp120 envelope glycoprotein in complex with the CD4 receptor and a neutralizing human antibody. Nature **393:**648-59.

158. **LaCasse, R. A., K. E. Follis, T. Moudgil, M. Trahey, J. M. Binley, V. Planelles, S. Zolla-Pazner, and J. H. Nunberg.** 1998. Coreceptor utilization by human immunodeficiency virus type 1 is not a primary determinant of neutralization sensitivity. J Virol **72:**2491-5.

159. **Learn, G. H., D. Muthui, S. J. Brodie, T. Zhu, K. Diem, J. I. Mullins, and L. Corey.** 2002. Virus population homogenization following acute human immunodeficiency virus type 1 infection. J Virol **76:**11953-9.

160. **Lee, B., M. Sharron, L. J. Montaner, D. Weissman, and R. W. Doms.** 1999. Quantification of CD4, CCR5, and CXCR4 levels on lymphocyte subsets, dendritic cells, and differentially conditioned monocyte-derived macrophages. Proc Natl Acad Sci U S A **96:**5215-20.

161. **LeMaistre, C. F.** 2000. DAB(389)IL-2 (denileukin diftitox, ONTAK): other potential applications. Clin Lymphoma **1 Suppl 1:**S37-40.

162. **Leonard, C. K., M. W. Spellman, L. Riddle, R. J. Harris, J. N. Thomas, and T. J. Gregory.** 1990. Assignment of intrachain disulfide bonds and characterization of potential glycosylation sites of the type 1 recombinant human immunodeficiency virus envelope glycoprotein (gp120) expressed in Chinese hamster ovary cells. J Biol Chem **265:**10373-82.

163. **Li, Q., L. Duan, J. D. Estes, Z. M. Ma, T. Rourke, Y. Wang, C. Reilly, J. Carlis, C. J. Miller, and A. T. Haase.** 2005. Peak SIV replication in resting memory CD4+ T cells depletes gut lamina propria CD4+ T cells. Nature **434:**1148-52.

164. **Li, Y., B. Cleveland, I. Klots, B. Travis, B. A. Richardson, D. Anderson, D. Montefiori, P. Polacino, and S. L. Hu.** 2008. Removal of a single N-linked glycan in human immunodeficiency virus type 1 gp120 results in an enhanced ability to induce neutralizing antibody responses. J Virol **82:**638-51.

165. **Li, Y., L. Luo, N. Rasool, and C. Y. Kang.** 1993. Glycosylation is necessary for the correct folding of human immunodeficiency virus gp120 in CD4 binding. J Virol **67:**584-8.

166. **Librado, P., and J. Rozas.** 2009. DnaSP v5: a software for comprehensive analysis of DNA polymorphism data. Bioinformatics **25:**1451-2.

167. **Lichtenstein, D. L., C. J. Issel, and R. C. Montelaro.** 1996. Genomic quasispecies associated with the initiation of infection and disease in ponies experimentally infected with equine infectious anemia virus. J Virol **70:**3346-54.

168. **Llewellyn, N., R. Zioni, H. Zhu, T. Andrus, Y. Xu, L. Corey, and T. Zhu.** 2006. Continued evolution of HIV-1 circulating in blood monocytes with antiretroviral therapy: genetic analysis of HIV-1 in monocytes and CD4+ T cells of patients with discontinued therapy. J Leukoc Biol **80:**1118-26.

169. **Lusso, P., P. L. Earl, F. Sironi, F. Santoro, C. Ripamonti, G. Scarlatti, R. Longhi, E. A. Berger, and S. E. Burastero.** 2005. Cryptic nature of a conserved, CD4-inducible V3 loop neutralization epitope in the native envelope glycoprotein oligomer of CCR5-restricted, but not CXCR4-using, primary human immunodeficiency virus type 1 strains. J Virol **79:**6957-68.

170. **Malim, M. H., J. Hauber, S. Y. Le, J. V. Maizel, and B. R. Cullen.** 1989. The HIV-1 rev trans-activator acts through a structured target sequence to activate nuclear export of unspliced viral mRNA. Nature **338:**254-7.

171. **Malkevitch, N., D. H. McDermott, Y. Yi, J. C. Grivel, D. Schols, E. De Clercq, P. M. Murphy, S. Glushakova, R. G. Collman, and L. Margolis.** 2001. Coreceptor choice and T cell depletion by R5, X4, and R5X4 HIV-1

variants in CCR5-deficient (CCR5delta32) and normal human lymphoid tissue. Virology **281:**239-47.

172. **Mangeat, B., P. Turelli, G. Caron, M. Friedli, L. Perrin, and D. Trono.** 2003. Broad antiretroviral defence by human APOBEC3G through lethal editing of nascent reverse transcripts. Nature **424:**99-103.

173. **Manrique, A., P. Rusert, B. Joos, M. Fischer, H. Kuster, C. Leemann, B. Niederost, R. Weber, G. Stiegler, H. Katinger, H. F. Gunthard, and A. Trkola.** 2007. In vivo and in vitro escape from neutralizing antibodies 2G12, 2F5, and 4E10. J Virol **81:**8793-808.

174. **Mansky, L. M., and H. M. Temin.** 1995. Lower in vivo mutation rate of human immunodeficiency virus type 1 than that predicted from the fidelity of purified reverse transcriptase. J Virol **69:**5087-94.

175. **Marchlik, E., R. Kalman, and N. Rosenberg.** 2005. Decreased virus population diversity in p53-null mice infected with weakly oncogenic Abelson virus. J Virol **79:**11618-26.

176. **Markowitz, M., M. Louie, A. Hurley, E. Sun, M. Di Mascio, A. S. Perelson, and D. D. Ho.** 2003. A novel antiviral intervention results in more accurate assessment of human immunodeficiency virus type 1 replication dynamics and T-cell decay in vivo. J Virol **77:**5037-8.

177. **Martin, D. P., D. Posada, K. A. Crandall, and C. Williamson.** 2005. A modified bootscan algorithm for automated identification of recombinant sequences and recombination breakpoints. AIDS Res Hum Retroviruses **21:**98-102.

178. **Martin, J., C. C. LaBranche, and F. Gonzalez-Scarano.** 2001. Differential CD4/CCR5 utilization, gp120 conformation, and neutralization sensitivity between envelopes from a microglia-adapted human immunodeficiency virus type 1 and its parental isolate. J Virol **75:**3568-80.

179. **Martin-Garcia, J., W. Cao, A. Varela-Rohena, M. L. Plassmeyer, and F. Gonzalez-Scarano.** 2006. HIV-1 tropism for the central nervous system: Brain-derived envelope glycoproteins with lower CD4 dependence and reduced sensitivity to a fusion inhibitor. Virology **346:**169-79.

180. **Mbah, H. A., S. Burda, M. K. Gorny, C. Williams, K. Revesz, S. Zolla-Pazner, and P. N. Nyambi.** 2001. Effect of soluble CD4 on exposure of epitopes on primary, intact, native human immunodeficiency virus type 1 virions of different genetic clades. J Virol **75:**7785-8.

181. **Melkus, M. W., J. D. Estes, A. Padgett-Thomas, J. Gatlin, P. W. Denton, F. A. Othieno, A. K. Wege, A. T. Haase, and J. V. Garcia.** 2006. Humanized

mice mount specific adaptive and innate immune responses to EBV and TSST-1. Nat Med **12:**1316-22.

182. **Mellors, J. W., C. R. Rinaldo, Jr., P. Gupta, R. M. White, J. A. Todd, and L. A. Kingsley.** 1996. Prognosis in HIV-1 infection predicted by the quantity of virus in plasma. Science **272:**1167-70.

183. **Mild, M., J. Esbjornsson, E. M. Fenyo, and P. Medstrand.** 2007. Frequent intrapatient recombination between human immunodeficiency virus type 1 R5 and X4 envelopes: implications for coreceptor switch. J Virol **81:**3369-76.

184. **Milich, L., B. H. Margolin, and R. Swanstrom.** 1997. Patterns of amino acid variability in NSI-like and SI-like V3 sequences and a linked change in the CD4-binding domain of the HIV-1 Env protein. Virology **239:**108-18.

185. **Miller, C. J., Q. Li, K. Abel, E. Y. Kim, Z. M. Ma, S. Wietgrefe, L. La Franco-Scheuch, L. Compton, L. Duan, M. D. Shore, M. Zupancic, M. Busch, J. Carlis, S. Wolinsky, and A. T. Haase.** 2005. Propagation and dissemination of infection after vaginal transmission of simian immunodeficiency virus. J Virol **79:**9217-27.

186. **Mitsuya, Y., V. Varghese, C. Wang, T. F. Liu, S. P. Holmes, P. Jayakumar, B. Gharizadeh, M. Ronaghi, D. Klein, W. J. Fessel, and R. W. Shafer.** 2008. Minority human immunodeficiency virus type 1 variants in antiretroviral-naive persons with reverse transcriptase codon 215 revertant mutations. J Virol **82:**10747-55.

187. **Miyauchi, K., M. M. Kozlov, and G. B. Melikyan.** 2009. Early steps of HIV-1 fusion define the sensitivity to inhibitory peptides that block 6-helix bundle formation. PLoS Pathog **5:**e1000585.

188. **Mo, H. M., L. Stamatatos, J. E. Ip, C. F. Barbas, P. Parren, D. R. Burton, J. P. Moore, and D. D. Ho.** 1997. Human immunodeficiency virus type 1 mutants that escape neutralization by human monoclonal antibody IgG1b12. Journal of Virology **71:**6869-6874.

189. **Montefiori, D. C.** 2004. Evaluating neutralizing antibodies against HIV, SIV and SHIV in luciferase reporter gene assays, p. 12.11.1-12.11.15. *In* J. E. Coligan, A. M. Kruisbeek, D. H. Margulies, E. M. Shevach, W. Strober, and R. Coico (ed.), Current Protocols in Immunology. John Wiley & Sons, New York, NY.

190. **Montefiori, D. C., R. G. Collman, T. R. Fouts, J. Y. Zhou, M. Bilska, J. A. Hoxie, J. P. Moore, and D. P. Bolognesi.** 1998. Evidence that antibody-mediated neutralization of human immunodeficiency virus type 1 by sera from infected individuals is independent of coreceptor usage. J Virol **72:**1886-93.

191. **Moore, J. P., Y. Cao, D. D. Ho, and R. A. Koup.** 1994. Development of the anti-gp120 antibody response during seroconversion to human immunodeficiency virus type 1. J Virol **68:**5142-55.

192. **Moore, J. P., Y. Cao, L. Qing, Q. J. Sattentau, J. Pyati, R. Koduri, J. Robinson, C. F. Barbas, 3rd, D. R. Burton, and D. D. Ho.** 1995. Primary isolates of human immunodeficiency virus type 1 are relatively resistant to neutralization by monoclonal antibodies to gp120, and their neutralization is not predicted by studies with monomeric gp120. J Virol **69:**101-9.

193. **Moore, J. P., and D. D. Ho.** 1995. HIV-1 neutralization: the consequences of viral adaptation to growth on transformed T cells. Aids **9 Suppl A:**S117-36.

194. **Moulard, M., H. Lortat-Jacob, I. Mondor, G. Roca, R. Wyatt, J. Sodroski, L. Zhao, W. Olson, P. D. Kwong, and Q. J. Sattentau.** 2000. Selective interactions of polyanions with basic surfaces on human immunodeficiency virus type 1 gp120. J Virol **74:**1948-60.

195. **Moutouh, L., J. Corbeil, and D. D. Richman.** 1996. Recombination leads to the rapid emergence of HIV-1 dually resistant mutants under selective drug pressure. Proc Natl Acad Sci U S A **93:**6106-11.

196. **Murray, J. M., S. Emery, A. D. Kelleher, M. Law, J. Chen, D. J. Hazuda, B. Y. Nguyen, H. Teppler, and D. A. Cooper.** 2007. Antiretroviral therapy with the integrase inhibitor raltegravir alters decay kinetics of HIV, significantly reducing the second phase. Aids **21:**2315-21.

197. **Musey, L., J. Hughes, T. Schacker, T. Shea, L. Corey, and M. J. McElrath.** 1997. Cytotoxic-T-cell responses, viral load, and disease progression in early human immunodeficiency virus type 1 infection. N Engl J Med **337:**1267-74.

198. **Myers G, R. A., Berzofsky JA, Smith TF and Wong-Staal F (ed.).** 1990. Human Retroviruses and AIDS 1990: A Compilation and Analysis of Nucleic Acid and Amino Acid Sequences. Theoretical Biology and Biophysics Group, Los Alamos National Laboratory., Los Alamos, NM.

199. **Nabatov, A. A., G. Pollakis, T. Linnemann, A. Kliphius, M. I. Chalaby, and W. A. Paxton.** 2004. Intrapatient alterations in the human immunodeficiency virus type 1 gp120 V1V2 and V3 regions differentially modulate coreceptor usage, virus inhibition by CC/CXC chemokines, soluble CD4, and the b12 and 2G12 monoclonal antibodies. J Virol **78:**524-30.

200. **Nei, M., and T. Gojobori.** 1986. Simple methods for estimating the numbers of synonymous and nonsynonymous nucleotide substitutions. Mol Biol Evol **3:**418-26.

201. **Neil, S. J., T. Zang, and P. D. Bieniasz.** 2008. Tetherin inhibits retrovirus release and is antagonized by HIV-1 Vpu. Nature **451:**425-30.

202. **Nelson, J. A., F. Baribaud, T. Edwards, and R. Swanstrom.** 2000. Patterns of changes in human immunodeficiency virus type 1 V3 sequence populations late in infection. J Virol **74:**8494-501.

203. **Nelson, J. A., S. A. Fiscus, and R. Swanstrom.** 1997. Evolutionary variants of the human immunodeficiency virus type 1 V3 region characterized by using a heteroduplex tracking assay. J Virol **71:**8750-8.

204. **Nicholson, J. K., S. W. Browning, R. L. Hengel, E. Lew, L. E. Gallagher, D. Rimland, and J. S. McDougal.** 2001. CCR5 and CXCR4 expression on memory and naive T cells in HIV-1 infection and response to highly active antiretroviral therapy. J Acquir Immune Defic Syndr **27:**105-15.

205. **Niewiadomska, A. M., and X. F. Yu.** 2010. Host Restriction of HIV-1 by APOBEC3 and Viral Evasion Through Vif. Curr Top Microbiol Immunol **339:**1-25.

206. **Ohagen, A., A. Devitt, K. J. Kunstman, P. R. Gorry, P. P. Rose, B. Korber, J. Taylor, R. Levy, R. L. Murphy, S. M. Wolinsky, and D. Gabuzda.** 2003. Genetic and functional analysis of full-length human immunodeficiency virus type 1 env genes derived from brain and blood of patients with AIDS. J Virol **77:**12336-45.

207. **Ostrowski, M. A., T. W. Chun, S. J. Justement, I. Motola, M. A. Spinelli, J. Adelsberger, L. A. Ehler, S. B. Mizell, C. W. Hallahan, and A. S. Fauci.** 1999. Both memory and CD45RA+/CD62L+ naive CD4(+) T cells are infected in human immunodeficiency virus type 1-infected individuals. J Virol **73:**6430-5.

208. **Ostrowski, M. A., S. J. Justement, A. Catanzaro, C. A. Hallahan, L. A. Ehler, S. B. Mizell, P. N. Kumar, J. A. Mican, T. W. Chun, and A. S. Fauci.** 1998. Expression of chemokine receptors CXCR4 and CCR5 in HIV-1-infected and uninfected individuals. J Immunol **161:**3195-201.

209. **Ostrowski, M. A., D. C. Krakauer, Y. Li, S. J. Justement, G. Learn, L. A. Ehler, S. K. Stanley, M. Nowak, and A. S. Fauci.** 1998. Effect of immune activation on the dynamics of human immunodeficiency virus replication and on the distribution of viral quasispecies. J Virol **72:**7772-84.

210. **Ota, T., and M. Nei.** 1994. Variance and covariances of the numbers of synonymous and nonsynonymous substitutions per site. Mol Biol Evol **11:**613-9.

211. **Overbaugh, J., R. J. Anderson, J. O. Ndinya-Achola, and J. K. Kreiss.** 1996. Distinct but related human immunodeficiency virus type 1 variant populations in genital secretions and blood. AIDS Res Hum Retroviruses **12:**107-15.

212. **Palmer, S., M. Kearney, F. Maldarelli, E. K. Halvas, C. J. Bixby, H. Bazmi, D. Rock, J. Falloon, R. T. Davey, Jr., R. L. Dewar, J. A. Metcalf, S. Hammer, J. W. Mellors, and J. M. Coffin.** 2005. Multiple, linked human immunodeficiency virus type 1 drug resistance mutations in treatment-experienced patients are missed by standard genotype analysis. J Clin Microbiol **43:**406-13.

213. **Parker, C. E., L. J. Deterding, C. Hager-Braun, J. M. Binley, N. Schulke, H. Katinger, J. P. Moore, and K. B. Tomer.** 2001. Fine definition of the epitope on the gp41 glycoprotein of human immunodeficiency virus type 1 for the neutralizing monoclonal antibody 2F5. J Virol **75:**10906-11.

214. **Parren, P. W., J. P. Moore, D. R. Burton, and Q. J. Sattentau.** 1999. The neutralizing antibody response to HIV-1: viral evasion and escape from humoral immunity. Aids **13 Suppl A:**S137-62.

215. **Pastore, C., R. Nedellec, A. Ramos, S. Pontow, L. Ratner, and D. E. Mosier.** 2006. Human immunodeficiency virus type 1 coreceptor switching: V1/V2 gain-of-fitness mutations compensate for V3 loss-of-fitness mutations. J Virol **80:**750-8.

216. **Patel, M., M. Yanagishita, G. Roderiquez, D. C. Bou-Habib, T. Oravecz, V. C. Hascall, and M. A. Norcross.** 1993. Cell-surface heparan sulfate proteoglycan mediates HIV-1 infection of T-cell lines. AIDS Res Hum Retroviruses **9:**167-74.

217. **Patel, M. B., N. G. Hoffman, and R. Swanstrom.** 2007. Subtype-Specific Conformational Differences Within the V3 Region of Subtype B and Subtype C Human Immunodeficiency Virus Type 1 Env Protein. J Virol.

218. **Perelson, A. S., P. Essunger, Y. Cao, M. Vesanen, A. Hurley, K. Saksela, M. Markowitz, and D. D. Ho.** 1997. Decay characteristics of HIV-1-infected compartments during combination therapy. Nature **387:**188-91.

219. **Perelson, A. S., A. U. Neumann, M. Markowitz, J. M. Leonard, and D. D. Ho.** 1996. HIV-1 dynamics in vivo: virion clearance rate, infected cell life-span, and viral generation time. Science **271:**1582-6.

220. **Peters, P. J., J. Bhattacharya, S. Hibbitts, M. T. Dittmar, G. Simmons, J. Bell, P. Simmonds, and P. R. Clapham.** 2004. Biological analysis of human

immunodeficiency virus type 1 R5 envelopes amplified from brain and lymph node tissues of AIDS patients with neuropathology reveals two distinct tropism phenotypes and identifies envelopes in the brain that confer an enhanced tropism and fusigenicity for macrophages. J Virol **78:**6915-26.

221. **Peters, P. J., W. M. Sullivan, M. J. Duenas-Decamp, J. Bhattacharya, C. Ankghuambom, R. Brown, K. Luzuriaga, J. Bell, P. Simmonds, J. Ball, and P. R. Clapham.** 2006. Non-macrophage-tropic human immunodeficiency virus type 1 R5 envelopes predominate in blood, lymph nodes, and semen: implications for transmission and pathogenesis. J Virol **80:**6324-32.

222. **Philpott, S., H. Burger, C. Tsoukas, B. Foley, K. Anastos, C. Kitchen, and B. Weiser.** 2005. Human immunodeficiency virus type 1 genomic RNA sequences in the female genital tract and blood: compartmentalization and intrapatient recombination. J Virol **79:**353-63.

223. **Philpott, S., B. Weiser, K. Anastos, C. M. Kitchen, E. Robison, W. A. Meyer, 3rd, H. S. Sacks, U. Mathur-Wagh, C. Brunner, and H. Burger.** 2001. Preferential suppression of CXCR4-specific strains of HIV-1 by antiviral therapy. J Clin Invest **107:**431-8.

224. **Ping, L. H., J. A. Nelson, I. F. Hoffman, J. Schock, S. L. Lamers, M. Goodman, P. Vernazza, P. Kazembe, M. Maida, D. Zimba, M. M. Goodenow, J. J. Eron, Jr., S. A. Fiscus, M. S. Cohen, and R. Swanstrom.** 1999. Characterization of V3 sequence heterogeneity in subtype C human immunodeficiency virus type 1 isolates from Malawi: underrepresentation of X4 variants. J Virol **73:**6271-81.

225. **Pinter, A., W. J. Honnen, Y. X. He, M. K. Gorny, S. Zolla-Pazner, and S. C. Kayman.** 2004. The V1/V2 domain of gp120 is a global regulator of the sensitivity of primary human immunodeficiency virus type 1 isolates to neutralization by antibodies commonly induced upon infection. Journal of Virology **78:**5205-5215.

226. **Platt, E. J., K. Wehrly, S. E. Kuhmann, B. Chesebro, and D. Kabat.** 1998. Effects of CCR5 and CD4 cell surface concentrations on infections by macrophagetropic isolates of human immunodeficiency virus type 1. J Virol **72:**2855-64.

227. **Poignard, P., M. Moulard, E. Golez, V. Vivona, M. Franti, S. Venturini, M. Wang, P. Parren, and D. R. Burton.** 2003. Heterogeneity of envelope molecules expressed on primary human immunodeficiency virus type 1 particles as probed by the binding of neutralizing and nonneutralizing antibodies. Journal of Virology **77:**353-365.

228. **Poles, M. A., W. J. Boscardin, J. Elliott, P. Taing, M. M. Fuerst, I. McGowan, S. Brown, and P. A. Anton.** 2006. Lack of decay of HIV-1 in gut-associated lymphoid tissue reservoirs in maximally suppressed individuals. J Acquir Immune Defic Syndr **43:**65-8.

229. **Pollakis, G., S. Kang, A. Kliphuis, M. I. Chalaby, J. Goudsmit, and W. A. Paxton.** 2001. N-linked glycosylation of the HIV type-1 gp120 envelope glycoprotein as a major determinant of CCR5 and CXCR4 coreceptor utilization. J Biol Chem **276:**13433-41.

230. **Pond, S. L., S. D. Frost, and S. V. Muse.** 2005. HyPhy: hypothesis testing using phylogenies. Bioinformatics **21:**676-9.

231. **Poon, A. F., F. I. Lewis, S. L. Pond, and S. D. Frost.** 2007. Evolutionary interactions between N-linked glycosylation sites in the HIV-1 envelope. PLoS Comput Biol **3:**e11.

232. **Posada, D., and K. A. Crandall.** 1998. MODELTEST: testing the model of DNA substitution. Bioinformatics **14:**817-8.

233. **Poss, M., A. G. Rodrigo, J. J. Gosink, G. H. Learn, D. de Vange Panteleeff, H. L. Martin, Jr., J. Bwayo, J. K. Kreiss, and J. Overbaugh.** 1998. Evolution of envelope sequences from the genital tract and peripheral blood of women infected with clade A human immunodeficiency virus type 1. J Virol **72:**8240-51.

234. **Price, D. A., P. J. Goulder, P. Klenerman, A. K. Sewell, P. J. Easterbrook, M. Troop, C. R. Bangham, and R. E. Phillips.** 1997. Positive selection of HIV-1 cytotoxic T lymphocyte escape variants during primary infection. Proc Natl Acad Sci U S A **94:**1890-5.

235. **Pugach, P., S. E. Kuhmann, J. Taylor, A. J. Marozsan, A. Snyder, T. Ketas, S. M. Wolinsky, B. T. Korber, and J. P. Moore.** 2004. The prolonged culture of human immunodeficiency virus type 1 in primary lymphocytes increases its sensitivity to neutralization by soluble CD4. Virology **321:**8-22.

236. **Pugach, P., A. J. Marozsan, T. J. Ketas, E. L. Landes, J. P. Moore, and S. E. Kuhmann.** 2007. HIV-1 clones resistant to a small molecule CCR5 inhibitor use the inhibitor-bound form of CCR5 for entry. Virology **361:**212-28.

237. **Ren, W., S. Tasca, K. Zhuang, A. Gettie, J. Blanchard, and C. Cheng-Mayer.** 2010. Different tempo and anatomic location of dual-tropic and X4 virus emergence in a model of R5 simian-human immunodeficiency virus infection. J Virol **84:**340-51.

238. **Rencher, S. D., and J. L. Hurwitz.** 1997. Effect of natural HIV-1 envelope V1-V2 sequence diversity on the binding of V3-specific and non-V3-specific antibodies. J Acquir Immune Defic Syndr Hum Retrovirol **16:**69-73.

239. **Resch, W., N. Parkin, E. L. Stuelke, T. Watkins, and R. Swanstrom.** 2001. A multiple-site-specific heteroduplex tracking assay as a tool for the study of viral population dynamics. Proc Natl Acad Sci U S A **98:**176-81.

240. **Rhodes, T., H. Wargo, and W. S. Hu.** 2003. High rates of human immunodeficiency virus type 1 recombination: near-random segregation of markers one kilobase apart in one round of viral replication. J Virol **77:**11193-200.

241. **Ribeiro, R. M., M. D. Hazenberg, A. S. Perelson, and M. P. Davenport.** 2006. Naive and memory cell turnover as drivers of CCR5-to-CXCR4 tropism switch in human immunodeficiency virus type 1: implications for therapy. J Virol **80:**802-9.

242. **Rice, A. P., and M. B. Mathews.** 1988. Transcriptional but not translational regulation of HIV-1 by the tat gene product. Nature **332:**551-3.

243. **Rich, E. A., I. S. Chen, J. A. Zack, M. L. Leonard, and W. A. O'Brien.** 1992. Increased susceptibility of differentiated mononuclear phagocytes to productive infection with human immunodeficiency virus-1 (HIV-1). J Clin Invest **89:**176-83.

244. **Richman, D. D., and S. A. Bozzette.** 1994. The impact of the syncytium-inducing phenotype of human immunodeficiency virus on disease progression. J Infect Dis **169:**968-74.

245. **Richman, D. D., T. Wrin, S. J. Little, and C. J. Petropoulos.** 2003. Rapid evolution of the neutralizing antibody response to HIV type 1 infection. Proc Natl Acad Sci U S A **100:**4144-9.

246. **Rigaud, M., W. Borkowsky, P. Muresan, A. Weinberg, P. Larussa, T. Fenton, J. S. Read, P. Jean-Philippe, E. Fergusson, B. Zimmer, D. Smith, and J. Kraimer.** 2008. Impaired immunity to recall antigens and neoantigens in severely immunocompromised children and adolescents during the first year of effective highly active antiretroviral therapy. J Infect Dis **198:**1123-30.

247. **Ritola, K., K. Robertson, S. A. Fiscus, C. Hall, and R. Swanstrom.** 2005. Increased human immunodeficiency virus type 1 (HIV-1) env compartmentalization in the presence of HIV-1-associated dementia. J Virol **79:**10830-4.

248. **Rose, P. P., and B. T. Korber.** 2000. Detecting hypermutations in viral sequences with an emphasis on G --> A hypermutation. Bioinformatics **16:**400-1.

249. **Ross, H. A., and A. G. Rodrigo.** 2002. Immune-mediated positive selection drives human immunodeficiency virus type 1 molecular variation and predicts disease duration. J Virol **76:**11715-20.

250. **Rouzine, I. M., and J. M. Coffin.** 1999. Linkage disequilibrium test implies a large effective population number for HIV in vivo. Proc Natl Acad Sci U S A **96:**10758-63.

251. **Royce, R. A., A. Sena, W. Cates, Jr., and M. S. Cohen.** 1997. Sexual transmission of HIV. N Engl J Med **336:**1072-8.

252. **Rozas, J., and R. Rozas.** 1999. DnaSP version 3: an integrated program for molecular population genetics and molecular evolution analysis. Bioinformatics **15:**174-5.

253. **Rybarczyk, B. J., D. Montefiori, P. R. Johnson, A. West, R. E. Johnston, and R. Swanstrom.** 2004. Correlation between env V1/V2 region diversification and neutralizing antibodies during primary infection by simian immunodeficiency virus sm in rhesus macaques. J Virol **78:**3561-71.

254. **Sagar, M., X. Wu, S. Lee, and J. Overbaugh.** 2006. Human immunodeficiency virus type 1 V1-V2 envelope loop sequences expand and add glycosylation sites over the course of infection, and these modifications affect antibody neutralization sensitivity. J Virol **80:**9586-98.

255. **Salazar-Gonzalez, J. F., E. Bailes, K. T. Pham, M. G. Salazar, M. B. Guffey, B. F. Keele, C. A. Derdeyn, P. Farmer, E. Hunter, S. Allen, O. Manigart, J. Mulenga, J. A. Anderson, R. Swanstrom, B. F. Haynes, G. S. Athreya, B. T. Korber, P. M. Sharp, G. M. Shaw, and B. H. Hahn.** 2008. Deciphering human immunodeficiency virus type 1 transmission and early envelope diversification by single-genome amplification and sequencing. J Virol **82:**3952-70.

256. **Salazar-Gonzalez, J. F., M. G. Salazar, B. F. Keele, G. H. Learn, E. E. Giorgi, H. Li, J. M. Decker, S. Wang, J. Baalwa, M. H. Kraus, N. F. Parrish, K. S. Shaw, M. B. Guffey, K. J. Bar, K. L. Davis, C. Ochsenbauer-Jambor, J. C. Kappes, M. S. Saag, M. S. Cohen, J. Mulenga, C. A. Derdeyn, S. Allen, E. Hunter, M. Markowitz, P. Hraber, A. S. Perelson, T. Bhattacharya, B. F. Haynes, B. T. Korber, B. H. Hahn, and G. M. Shaw.** 2009. Genetic identity, biological phenotype, and evolutionary pathways of transmitted/founder viruses in acute and early HIV-1 infection. J Exp Med **206:**1273-89.

257. **Salemi, M., B. R. Burkhardt, R. R. Gray, G. Ghaffari, J. W. Sleasman, and M. M. Goodenow.** 2007. Phylodynamics of HIV-1 in Lymphoid and Non-Lymphoid Tissues Reveals a Central Role for the Thymus in Emergence of CXCR4-Using Quasispecies. PLoS ONE **2:**e950.

258. **Salminen, M. O., J. K. Carr, D. S. Burke, and F. E. McCutchan.** 1995. Identification of breakpoints in intergenotypic recombinants of HIV type 1 by bootscanning. AIDS Res Hum Retroviruses **11:**1423-5.

259. **Salzwedel, K., and E. A. Berger.** 2000. Cooperative subunit interactions within the oligomeric envelope glycoprotein of HIV-1: functional complementation of specific defects in gp120 and gp41. Proc Natl Acad Sci U S A **97:**12794-9.

260. **Sanders, R. W., M. Venturi, L. Schiffner, R. Kalyanaraman, H. Katinger, K. O. Lloyd, P. D. Kwong, and J. P. Moore.** 2002. The mannose-dependent epitope for neutralizing antibody 2G12 on human immunodeficiency virus type 1 glycoprotein gp120. J Virol **76:**7293-305.

261. **Scheid, J. F., H. Mouquet, N. Feldhahn, M. S. Seaman, K. Velinzon, J. Pietzsch, R. G. Ott, R. M. Anthony, H. Zebroski, A. Hurley, A. Phogat, B. Chakrabarti, Y. Li, M. Connors, F. Pereyra, B. D. Walker, H. Wardemann, D. Ho, R. T. Wyatt, J. R. Mascola, J. V. Ravetch, and M. C. Nussenzweig.** 2009. Broad diversity of neutralizing antibodies isolated from memory B cells in HIV-infected individuals. Nature **458:**636-40.

262. **Schnell, G., W. L. Ince, and R. Swanstrom.** 2008. Identification and recovery of minor HIV-1 variants using the heteroduplex tracking assay and biotinylated probes. Nucleic Acids Res.

263. **Schrofelbauer, B., Y. Hakata, and N. R. Landau.** 2007. HIV-1 Vpr function is mediated by interaction with the damage-specific DNA-binding protein DDB1. Proc Natl Acad Sci U S A **104:**4130-5.

264. **Scott, C. F., Jr., S. Silver, A. T. Profy, S. D. Putney, A. Langlois, K. Weinhold, and J. E. Robinson.** 1990. Human monoclonal antibody that recognizes the V3 region of human immunodeficiency virus gp120 and neutralizes the human T-lymphotropic virus type IIIMN strain. Proc Natl Acad Sci U S A **87:**8597-601.

265. **Sedaghat, A. R., J. B. Dinoso, L. Shen, C. O. Wilke, and R. F. Siliciano.** 2008. Decay dynamics of HIV-1 depend on the inhibited stages of the viral life cycle. Proc Natl Acad Sci U S A **105:**4832-7.

266. **Sen, J., A. Jacobs, H. Jiang, L. Rong, and M. Caffrey.** 2007. The disulfide loop of gp41 is critical to the furin recognition site of HIV gp160. Protein Sci **16:**1236-41.

267. **Shankarappa, R., J. B. Margolick, S. J. Gange, A. G. Rodrigo, D. Upchurch, H. Farzadegan, P. Gupta, C. R. Rinaldo, G. H. Learn, X. He, X. L. Huang, and J. I. Mullins.** 1999. Consistent viral evolutionary changes associated with the progression of human immunodeficiency virus type 1 infection. J Virol **73:**10489-502.

268. **Shapshak, P., D. M. Segal, K. A. Crandall, R. K. Fujimura, B. T. Zhang, K. Q. Xin, K. Okuda, C. K. Petito, C. Eisdorfer, and K. Goodkin.** 1999. Independent evolution of HIV type 1 in different brain regions. AIDS Res Hum Retroviruses **15:**811-20.

269. **Sheehy, A. M., N. C. Gaddis, J. D. Choi, and M. H. Malim.** 2002. Isolation of a human gene that inhibits HIV-1 infection and is suppressed by the viral Vif protein. Nature **418:**646-50.

270. **Shibata, J., K. Yoshimura, A. Honda, A. Koito, T. Murakami, and S. Matsushita.** 2007. Impact of V2 mutations on escape from a potent neutralizing anti-V3 monoclonal antibody during in vitro selection of a primary human immunodeficiency virus type 1 isolate. Journal of Virology **81:**3757-3768.

271. **Simmonds, P., P. Balfe, C. A. Ludlam, J. O. Bishop, and A. J. Brown.** 1990. Analysis of sequence diversity in hypervariable regions of the external glycoprotein of human immunodeficiency virus type 1. J Virol **64:**5840-50.

272. **Slatkin, M., and W. P. Maddison.** 1989. A cladistic measure of gene flow inferred from the phylogenies of alleles. Genetics **123:**603-13.

273. **Sonza, S., A. Maerz, N. Deacon, J. Meanger, J. Mills, and S. Crowe.** 1996. Human immunodeficiency virus type 1 replication is blocked prior to reverse transcription and integration in freshly isolated peripheral blood monocytes. J Virol **70:**3863-9.

274. **Stalmeijer, E. H., R. P. Van Rij, B. Boeser-Nunnink, J. A. Visser, M. A. Naarding, D. Schols, and H. Schuitemaker.** 2004. In vivo evolution of X4 human immunodeficiency virus type 1 variants in the natural course of infection coincides with decreasing sensitivity to CXCR4 antagonists. J Virol **78:**2722-8.

275. **Stanley, S. K., M. A. Ostrowski, J. S. Justement, K. Gantt, S. Hedayati, M. Mannix, K. Roche, D. J. Schwartzentruber, C. H. Fox, and A. S. Fauci.**

1996. Effect of immunization with a common recall antigen on viral expression in patients infected with human immunodeficiency virus type 1. N Engl J Med **334:**1222-30.

276. **Staprans, S., N. Marlowe, D. Glidden, T. Novakovic-Agopian, R. M. Grant, M. Heyes, F. Aweeka, S. Deeks, and R. W. Price.** 1999. Time course of cerebrospinal fluid responses to antiretroviral therapy: evidence for variable compartmentalization of infection. Aids **13:**1051-61.

277. **Stevenson, M., T. L. Stanwick, M. P. Dempsey, and C. A. Lamonica.** 1990. HIV-1 replication is controlled at the level of T cell activation and proviral integration. Embo J **9:**1551-60.

278. **Stiegler, G., R. Kunert, M. Purtscher, S. Wolbank, R. Voglauer, F. Steindl, and H. Katinger.** 2001. A potent cross-clade neutralizing human monoclonal antibody against a novel epitope on gp41 of human immunodeficiency virus type 1. AIDS Res Hum Retroviruses **17:**1757-65.

279. **Sun, Z., P. W. Denton, J. D. Estes, F. A. Othieno, B. L. Wei, A. K. Wege, M. W. Melkus, A. Padgett-Thomas, M. Zupancic, A. T. Haase, and J. V. Garcia.** 2007. Intrarectal transmission, systemic infection, and CD4+ T cell depletion in humanized mice infected with HIV-1. J Exp Med **204:**705-14.

280. **ter Brake, O., N. Legrand, K. J. von Eije, M. Centlivre, H. Spits, K. Weijer, B. Blom, and B. Berkhout.** 2009. Evaluation of safety and efficacy of RNAi against HIV-1 in the human immune system (Rag-2(-/-)gammac(-/-)) mouse model. Gene Ther **16:**148-53.

281. **Terpstra, F. G., B. J. Al, M. T. Roos, F. De Wolf, J. Goudsmit, P. T. Schellekens, and F. Miedema.** 1989. Longitudinal study of leukocyte functions in homosexual men seroconverted for HIV: rapid and persistent loss of B cell function after HIV infection. Eur J Immunol **19:**667-73.

282. **Tersmette, M., R. A. Gruters, F. de Wolf, R. E. de Goede, J. M. Lange, P. T. Schellekens, J. Goudsmit, H. G. Huisman, and F. Miedema.** 1989. Evidence for a role of virulent human immunodeficiency virus (HIV) variants in the pathogenesis of acquired immunodeficiency syndrome: studies on sequential HIV isolates. J Virol **63:**2118-25.

283. **Thomas, E. R., R. L. Dunfee, J. Stanton, D. Bogdan, J. Taylor, K. Kunstman, J. E. Bell, S. M. Wolinsky, and D. Gabuzda.** 2007. Macrophage entry mediated by HIV Envs from brain and lymphoid tissues is determined by the capacity to use low CD4 levels and overall efficiency of fusion. Virology **360:**105-19.

284. **Tomaras, G. D., N. L. Yates, P. Liu, L. Qin, G. G. Fouda, L. L. Chavez, A. C. Decamp, R. J. Parks, V. C. Ashley, J. T. Lucas, M. Cohen, J. Eron, C.**

B. Hicks, H. X. Liao, S. G. Self, G. Landucci, D. N. Forthal, K. J. Weinhold, B. F. Keele, B. H. Hahn, M. L. Greenberg, L. Morris, S. S. Karim, W. A. Blattner, D. C. Montefiori, G. M. Shaw, A. S. Perelson, and B. F. Haynes. 2008. Initial B-cell responses to transmitted human immunodeficiency virus type 1: virion-binding immunoglobulin M (IgM) and IgG antibodies followed by plasma anti-gp41 antibodies with ineffective control of initial viremia. J Virol **82:**12449-63.

285. **Traggiai, E., L. Chicha, L. Mazzucchelli, L. Bronz, J. C. Piffaretti, A. Lanzavecchia, and M. G. Manz.** 2004. Development of a human adaptive immune system in cord blood cell-transplanted mice. Science **304:**104-7.

286. **Trkola, A., S. E. Kuhmann, J. M. Strizki, E. Maxwell, T. Ketas, T. Morgan, P. Pugach, S. Xu, L. Wojcik, J. Tagat, A. Palani, S. Shapiro, J. W. Clader, S. McCombie, G. R. Reyes, B. M. Baroudy, and J. P. Moore.** 2002. HIV-1 escape from a small molecule, CCR5-specific entry inhibitor does not involve CXCR4 use. Proc Natl Acad Sci U S A **99:**395-400.

287. **Trkola, A., M. Purtscher, T. Muster, C. Ballaun, A. Buchacher, N. Sullivan, K. Srinivasan, J. Sodroski, J. P. Moore, and H. Katinger.** 1996. Human monoclonal antibody 2G12 defines a distinctive neutralization epitope on the gp120 glycoprotein of human immunodeficiency virus type 1. J Virol **70:**1100-8.

288. **Van Duyne, R., J. Cardenas, R. Easley, W. Wu, K. Kehn-Hall, Z. Klase, S. Mendez, C. Zeng, H. Chen, M. Saifuddin, and F. Kashanchi.** 2008. Effect of transcription peptide inhibitors on HIV-1 replication. Virology **376:**308-22.

289. **van Marle, G., M. J. Gill, D. Kolodka, L. McManus, T. Grant, and D. L. Church.** 2007. Compartmentalization of the gut viral reservoir in HIV-1 infected patients. Retrovirology **4:**87.

290. **van Rij, R. P., H. Blaak, J. A. Visser, M. Brouwer, R. Rientsma, S. Broersen, A. M. de Roda Husman, and H. Schuitemaker.** 2000. Differential coreceptor expression allows for independent evolution of non-syncytium-inducing and syncytium-inducing HIV-1. J Clin Invest **106:**1039-52.

291. **van Rij, R. P., M. Worobey, J. A. Visser, and H. Schuitemaker.** 2003. Evolution of R5 and X4 human immunodeficiency virus type 1 gag sequences in vivo: evidence for recombination. Virology **314:**451-9.

292. **van't Wout, A. B., N. A. Kootstra, G. A. Mulder-Kampinga, N. Albrecht-van Lent, H. J. Scherpbier, J. Veenstra, K. Boer, R. A. Coutinho, F. Miedema, and H. Schuitemaker.** 1994. Macrophage-tropic variants initiate human immunodeficiency virus type 1 infection after sexual, parenteral, and vertical transmission. J Clin Invest **94:**2060-7.

293. **Vancott, T. C., V. R. Polonis, L. D. Loomis, N. L. Michael, P. L. Nara, and D. L. Birx.** 1995. Differential Role of V3-Specific Antibodies in Neutralization Assays Involving Primary and Laboratory-Adapted Isolates of Hiv Type-1. Aids Research and Human Retroviruses **11:**1379-1391.

294. **Vandeyar, M. A., M. P. Weiner, C. J. Hutton, and C. A. Batt.** 1988. A simple and rapid method for the selection of oligodeoxynucleotide-directed mutants. Gene **65:**129-33.

295. **Veazey, R. S., M. DeMaria, L. V. Chalifoux, D. E. Shvetz, D. R. Pauley, H. L. Knight, M. Rosenzweig, R. P. Johnson, R. C. Desrosiers, and A. A. Lackner.** 1998. Gastrointestinal tract as a major site of CD4+ T cell depletion and viral replication in SIV infection. Science **280:**427-31.

296. **Vives, R. R., A. Imberty, Q. J. Sattentau, and H. Lortat-Jacob.** 2005. Heparan sulfate targets the HIV-1 envelope glycoprotein gp120 coreceptor binding site. J Biol Chem **280:**21353-7.

297. **Vives, R. R., H. Lortat-Jacob, and P. Fender.** 2006. Heparan sulphate proteoglycans and viral vectors : ally or foe? Curr Gene Ther **6:**35-44.

298. **Wahlberg, J., J. Albert, J. Lundeberg, A. Von Gegerfelt, K. Broliden, G. Utter, E. M. Fenyo, and M. Uhlen.** 1991. Analysis of the V3 loop in neutralization-resistant human immunodeficiency virus type 1 variants by direct solid-phase DNA sequencing. AIDS Res Hum Retroviruses **7:**983-90.

299. **Walker, L. M., S. K. Phogat, P. Y. Chan-Hui, D. Wagner, P. Phung, J. L. Goss, T. Wrin, M. D. Simek, S. Fling, J. L. Mitcham, J. K. Lehrman, F. H. Priddy, O. A. Olsen, S. M. Frey, P. W. Hammond, S. Kaminsky, T. Zamb, M. Moyle, W. C. Koff, P. Poignard, and D. R. Burton.** 2009. Broad and potent neutralizing antibodies from an African donor reveal a new HIV-1 vaccine target. Science **326:**285-9.

300. **Walter, B. L., K. Wehrly, R. Swanstrom, E. Platt, D. Kabat, and B. Chesebro.** 2005. Role of low CD4 levels in the influence of human immunodeficiency virus type 1 envelope V1 and V2 regions on entry and spread in macrophages. J Virol **79:**4828-37.

301. **Watanabe, S., K. Terashima, S. Ohta, S. Horibata, M. Yajima, Y. Shiozawa, M. Z. Dewan, Z. Yu, M. Ito, T. Morio, N. Shimizu, M. Honda, and N. Yamamoto.** 2007. Hematopoietic stem cell-engrafted NOD/SCID/IL2Rgamma null mice develop human lymphoid systems and induce long-lasting HIV-1 infection with specific humoral immune responses. Blood **109:**212-8.

302. **Wei, X., J. M. Decker, S. Wang, H. Hui, J. C. Kappes, X. Wu, J. F. Salazar-Gonzalez, M. G. Salazar, J. M. Kilby, M. S. Saag, N. L. Komarova, M. A. Nowak, B. H. Hahn, P. D. Kwong, and G. M. Shaw.** 2003. Antibody neutralization and escape by HIV-1. Nature **422:**307-12.

303. **Wei, X., S. K. Ghosh, M. E. Taylor, V. A. Johnson, E. A. Emini, P. Deutsch, J. D. Lifson, S. Bonhoeffer, M. A. Nowak, B. H. Hahn, and et al.** 1995. Viral dynamics in human immunodeficiency virus type 1 infection. Nature **373:**117-22.

304. **Wei, X., S. K. Ghosh, M. E. Taylor, V. A. Johnson, E. A. Emini, P. Deutsch, J. D. Lifson, S. Bonhoeffer, M. A. Nowak, B. H. Hahn, M. S. Saag, and G. M. Shaw.** 1995. Viral dynamics in human immunodeficiency virus type 1 infection. Nature **373:**117-22.

305. **Weiss, R. A., P. R. Clapham, R. Cheingsong-Popov, A. G. Dalgleish, C. A. Carne, I. V. Weller, and R. S. Tedder.** 1985. Neutralization of human T-lymphotropic virus type III by sera of AIDS and AIDS-risk patients. Nature **316:**69-72.

306. **Willett, B. J., K. Adema, N. Heveker, A. Brelot, L. Picard, M. Alizon, J. D. Turner, J. A. Hoxie, S. Peiper, J. C. Neil, and M. J. Hosie.** 1998. The second extracellular loop of CXCR4 determines its function as a receptor for feline immunodeficiency virus. J Virol **72:**6475-81.

307. **Willett, B. J., M. J. Hosie, J. C. Neil, J. D. Turner, and J. A. Hoxie.** 1997. Common mechanism of infection by lentiviruses. Nature **385:**587.

308. **Willett, B. J., L. Picard, M. J. Hosie, J. D. Turner, K. Adema, and P. R. Clapham.** 1997. Shared usage of the chemokine receptor CXCR4 by the feline and human immunodeficiency viruses. J Virol **71:**6407-15.

309. **Wolinsky, S. M., B. T. Korber, A. U. Neumann, M. Daniels, K. J. Kunstman, A. J. Whetsell, M. R. Furtado, Y. Cao, D. D. Ho, and J. T. Safrit.** 1996. Adaptive evolution of human immunodeficiency virus-type 1 during the natural course of infection. Science **272:**537-42.

310. **Wolk, T., and M. Schreiber.** 2006. N-Glycans in the gp120 V1/V2 domain of the HIV-1 strain NL4-3 are indispensable for viral infectivity and resistance against antibody neutralization. Med Microbiol Immunol **195:**165-72.

311. **Wong, J. K., C. C. Ignacio, F. Torriani, D. Havlir, N. J. Fitch, and D. D. Richman.** 1997. In vivo compartmentalization of human immunodeficiency virus: evidence from the examination of pol sequences from autopsy tissues. J Virol **71:**2059-71.

312. **Wrin, T., T. P. Loh, J. C. Vennari, H. Schuitemaker, and J. H. Nunberg.** 1995. Adaptation to persistent growth in the H9 cell line renders a primary isolate of human immunodeficiency virus type 1 sensitive to neutralization by vaccine sera. J Virol **69:**39-48.

313. **Wu, X. L., A. Sambor, M. C. Nason, Z. Y. Yang, L. Wu, S. Zolla-Pazner, G. J. Nabel, and J. R. Mascola.** 2008. Soluble CD4 broadens neutralization of V3-directed monoclonal antibodies and guinea pig vaccine sera against HIV-1 subtype B and C reference viruses. Virology **380:**285-295.

314. **Wyatt, R., P. D. Kwong, E. Desjardins, R. W. Sweet, J. Robinson, W. A. Hendrickson, and J. G. Sodroski.** 1998. The antigenic structure of the HIV gp120 envelope glycoprotein. Nature **393:**705-11.

315. **Wyatt, R., J. Moore, M. Accola, E. Desjardin, J. Robinson, and J. Sodroski.** 1995. Involvement of the V1/V2 variable loop structure in the exposure of human immunodeficiency virus type 1 gp120 epitopes induced by receptor binding. J Virol **69:**5723-33.

316. **Wyatt, R., and J. Sodroski.** 1998. The HIV-1 envelope glycoproteins: fusogens, antigens, and immunogens. Science **280:**1884-8.

317. **Xiang, S. H., A. Finzi, B. Pacheco, K. Alexander, W. Yuan, C. Rizzuto, C. C. Huang, P. D. Kwong, and J. Sodroski.** 2010. A V3 Loop-Dependent gp120 Element Disrupted by CD4 Binding Stabilizes the Human Immunodeficiency Virus (HIV-1) Envelope Glycoprotein Trimer. J Virol.

318. **Yi, Y., F. Shaheen, and R. G. Collman.** 2005. Preferential use of CXCR4 by R5X4 human immunodeficiency virus type 1 isolates for infection of primary lymphocytes. J Virol **79:**1480-6.

319. **Yi, Y., A. Singh, F. Shaheen, A. Louden, C. Lee, and R. G. Collman.** 2003. Contrasting use of CCR5 structural determinants by R5 and R5X4 variants within a human immunodeficiency virus type 1 primary isolate quasispecies. J Virol **77:**12057-66.

320. **Yokomaku, Y., H. Miura, H. Tomiyama, A. Kawana-Tachikawa, M. Takiguchi, A. Kojima, Y. Nagai, A. Iwamoto, Z. Matsuda, and K. Ariyoshi.** 2004. Impaired processing and presentation of cytotoxic-T-lymphocyte (CTL) epitopes are major escape mechanisms from CTL immune pressure in human immunodeficiency virus type 1 infection. J Virol **78:**1324-32.

321. **Zaitseva, M. B., S. Lee, R. L. Rabin, H. L. Tiffany, J. M. Farber, K. W. Peden, P. M. Murphy, and H. Golding.** 1998. CXCR4 and CCR5 on human thymocytes: biological function and role in HIV-1 infection. J Immunol **161:**3103-13.

322. **Zhang, H., B. Yang, R. J. Pomerantz, C. Zhang, S. C. Arunachalam, and L. Gao.** 2003. The cytidine deaminase CEM15 induces hypermutation in newly synthesized HIV-1 DNA. Nature **424:**94-8.

323. **Zhang, L., G. I. Kovalev, and L. Su.** 2007. HIV-1 infection and pathogenesis in a novel humanized mouse model. Blood **109:**2978-81.

324. **Zhang, L. Q., P. MacKenzie, A. Cleland, E. C. Holmes, A. J. Brown, and P. Simmonds.** 1993. Selection for specific sequences in the external envelope protein of human immunodeficiency virus type 1 upon primary infection. J Virol **67:**3345-56.

325. **Zhang, M., B. Gaschen, W. Blay, B. Foley, N. Haigwood, C. Kuiken, and B. Korber.** 2004. Tracking global patterns of N-linked glycosylation site variation in highly variable viral glycoproteins: HIV, SIV, and HCV envelopes and influenza hemagglutinin. Glycobiology **14:**1229-46.

326. **Zhang, Z., T. Schuler, M. Zupancic, S. Wietgrefe, K. A. Staskus, K. A. Reimann, T. A. Reinhart, M. Rogan, W. Cavert, C. J. Miller, R. S. Veazey, D. Notermans, S. Little, S. A. Danner, D. D. Richman, D. Havlir, J. Wong, H. L. Jordan, T. W. Schacker, P. Racz, K. Tenner-Racz, N. L. Letvin, S. Wolinsky, and A. T. Haase.** 1999. Sexual transmission and propagation of SIV and HIV in resting and activated CD4+ T cells. Science **286:**1353-7.

327. **Zhou, T., L. Xu, B. Dey, A. J. Hessell, D. Van Ryk, S. H. Xiang, X. Yang, M. Y. Zhang, M. B. Zwick, J. Arthos, D. R. Burton, D. S. Dimitrov, J. Sodroski, R. Wyatt, G. J. Nabel, and P. D. Kwong.** 2007. Structural definition of a conserved neutralization epitope on HIV-1 gp120. Nature **445:**732-7.

328. **Zhu, T., H. Mo, N. Wang, D. S. Nam, Y. Cao, R. A. Koup, and D. D. Ho.** 1993. Genotypic and phenotypic characterization of HIV-1 patients with primary infection. Science **261:**1179-81.

329. **Zhu, T., D. Muthui, S. Holte, D. Nickle, F. Feng, S. Brodie, Y. Hwangbo, J. I. Mullins, and L. Corey.** 2002. Evidence for human immunodeficiency virus type 1 replication in vivo in CD14(+) monocytes and its potential role as a source of virus in patients on highly active antiretroviral therapy. J Virol **76:**707-16.

330. **Zolla-Pazner, S., S. S. Cohen, C. Krachmarov, S. Wang, A. Pinter, and S. Lu.** 2008. Focusing the immune response on the V3 loop, a neutralizing epitope of the HIV-1 gp120 envelope. Virology **372:**233-46.

331. **Zwick, M. B., R. Jensen, S. Church, M. Wang, G. Stiegler, R. Kunert, H. Katinger, and D. R. Burton.** 2005. Anti-human immunodeficiency virus type 1 (HIV-1) antibodies 2F5 and 4E10 require surprisingly few crucial residues in the membrane-proximal external region of glycoprotein gp41 to neutralize HIV-1. J Virol **79:**1252-61.

332. **Zwick, M. B., A. F. Labrijn, M. Wang, C. Spenlehauer, E. O. Saphire, J. M. Binley, J. P. Moore, G. Stiegler, H. Katinger, D. R. Burton, and P. W. Parren.** 2001. Broadly neutralizing antibodies targeted to the membrane-proximal external region of human immunodeficiency virus type 1 glycoprotein gp41. J Virol **75:**10892-905.